Федеральное государственное автономное образовательное учреждение высшего образования «Уральский федеральный университет имени первого Президента России Б.Н. Ельцина»

Уральский энергетический институт

Кафедра автоматизированных электрических систем

На правах рукописи

Амир Салах Хассан Абдель Менаем

РАЗВИТИЕ МЕТОДОВ ОЦЕНКИ ПОКАЗАТЕЛЕЙ БАЛАНСОВОЙ НАДЕЖНОСТИ ЭНЕРГОСИСТЕМ С ВОЗОБНОВЛЯЕМЫМИ ИСТОЧНИКАМИ ЭНЕРГИИ

05.14.02 – Электрические станции и электроэнергетические системы

Диссертации на соискание ученой степени кандидата технических наук

Научный руководитель

доктор технических наук,

профессор, В.П. Обоскалов

Екатеринбург – 2021

Federal state autonomous educational institution of higher education

«Ural federal university named after the first president of Russia B.N. Yeltsin»

Ural power engineering institute

Department of automated electrical systems

As a manuscript

Amir Salah Hassan Abdel Menaem

IMPROVING EVALUATION METHODS OF ADEQUACY FOR RENEWABLE ENERGY INTEGRATED POWER SYSTEMS

05.14.02 – Electric power plants and systems

Dissertation for the degree of candidate of electrical engineering science

Supervisor
Doctor of technical science,
Professor, V.P. Oboskalov

Yekaterinburg – 2021

Table of contents

Introduction

Relevance of the research topic. Electric Power systems (EPSs) are undergoing a significant transformation as a result of the increasing integration of renewable energy resources, and the advent of the smart grid and its accompanying technologies. Such transformation, while it adds convenience, intelligence, and reduces environmental impacts, also adds dynamic and stochastic generations and loads that increase the systemic variability and uncertainties and so complicate the reliability assessment of EPSs. Reliability assessment has an important part in the process of adoption of EPS planning and investment [1-6]. The performance of EPS in providing adequate electric services within accepted standards to all points of consumption at any moment of time (both current and future) can be decided unacceptable or acceptable by reliability criteria [2-3, 7]. The reliability analysis approaches range from relatively simple deterministic calculations of planning reserve margins to rigorous probabilistic reliability indices [8-9].

The deterministic criterion is relatively easy to implement and interpret, but such a worst-case based deterministic approach has a main drawback in that it does not adequately reflect levels of operation risk resulted from the stochastic nature and uncertain behavior of a power system. From this perspective, probabilistic analysis methods that identify power system reliability risks needs to be investigated to better reflect the actual system behavior. This probabilistic reliability analysis incorporates the effect of uncertainties of input data on the customer service through the probabilistic evaluation of reliability indices. The probabilistic reliability indices are to identify the degree of reliability of power system through estimating the risk (probability or how likely) and the size (the expected value of frequency, duration, and magnitude) of energy deficit under a variety of scenarios. Therefore, the probabilistic methods result in effective and realistic reliability evaluation of power system. The obstacles to applying these methods are primarily computational efficiency and the lack of realistic reliability data [9]. These obstacles have been significantly overcome in recent years with the development and availability of high-

speed computation facilities and the efforts have been dedicated to collecting the components reliability data.

After the 2003 Northeast blackout, the North American Power Reliability Corporation (NERC) and Canadian Electricity Association (CEA) have been organizing with electric utilities to collect reliability data and responsible for executing the composite power system reliability studies in North America [10-12]. CEA releases reports annually on the probabilistic analysis of transmission equipment 's outage performance. Also, NERC has developed the Generation Availability Data System (GADS) and the Transmission Availability Data System (TADS) to gather outage data. In industry practice, probabilistic techniques for generation adequacy analysis have been used in nearly all regions of North America to calculate the Loss of Load Expectation (LOLE) which express the planned figure of outage hours per year. The purpose is to ensure the LOLE doesn't exceed 1 day in 10 years when all uncertainties including the forced outages of thermal generators, and renewable resources and load uncertainty are included in the simulation [13]. In Western European countries, the standard LOLE value is set at a little diverse level (3 hours per year) [14]. European Network of Electricity Transmission System Operators (ENTSO-E) annually publishes a report on the Norms, requirements, and assessment of reliability with recommendations for solving the problems of the existing methods for calculating the reliability [15]. Also, in Russia in recent years, there is an increasing interest in the problem of calculating the reliability indices. On January 1, 2019, the Preliminary National Standard of the Russian Federation was published: "304-2018: Balance reliability of power systems. Section 1. Overall regulations", which forms the conceptual apparatus in the field of calculating the balance reliability of power systems [16]. From September 1, 2019, System Operator of the Unified Energy System introduced a technical report 59012820.27.010.005-2018 which regulates methodological instructions for carrying out calculations of balance sheet reliability [17], and from March 1, 2020, a national technical standard: "GOST R 58730-2019 Unified power system and isolated power systems. Power/Energy system planning. Balance reliability calculations. Norms and requirements" was introduced.

With the continuous development of computational resources, tremendous amount of research has been done on developing probabilistic methods for power system reliability evaluation over the past several decades [18-54]. However, a trade-off between detailed modeling and computational cost is still an important issue, especially with the growing complexity, uncertainty, and dimensionality of a power system. A frequently adopted approach for the reliability indices assessment is the Monte Carlo simulation (MCS) due to its merits [18-20]. MCS does not impose restrictions on the form of the used distribution functions and can be used for composite system analysis when the system is highly nonlinear or has many uncertain variables. Moreover, a transfer function is not inevitably required. So, it can also be implemented in nondifferentiable as well as nonconvex problems. The price for its robustness is that MCS requires a great computational effort to guarantee the accuracy of the reliability indices results due to the MCS approach depends on sampling the whole state space of input variables, regardless where are the states that represent events of interest i.e. failure events of the power system meeting the required demand. Moreover, the high reliable property of power systems and the enlarged sample space with the probabilistic modeling of renewable energy resources and transmission lines outages increase more and more the MCS computational burden.

Researchers handled the MCS computational burden by adopting two research tracks: improvement of the state evaluation efficiency and the improvement of the sampling efficiency. The first research track is to provide high-performing programming patterns [21-35] for the purpose of spending less time in the state evaluation stage. The second track could be to develop more efficient sampling means [36-50] for focusing the sampling attempt in the regions of concern or approximate analytical methods [52-54] for representing the continuous random variables by a small number of the states required to be estimated. With the high reliable property of power systems, the improvement of the sampling efficiency is the best mean since the improvement of the state evaluation efficiency actually does not pay off without a good sampling algorithm. Thus, more efficient sampling techniques or approximate

analytical methods for dominating the calculation burden of the MCS method are addressed in this dissertation.

The degree of scientific elaboration of the problem. A large literature, both scientific papers and technical reports, is available about power system reliability assessment and management. Considerable studies accounted for 29% articles have been addressed the computational efficiency of the probabilistic evaluation of power system reliability [55]. Rresearch on the probabilistic reliability assessment did not stop and continue until the present time. Among Russian publications, one should especially highlight the works of such scientists as: F.L. Byk, N.I. Voropai, M.A. Dubitsky, V.Yu. Itkin, V.G. Kitushin, G.F. Kovalev, Yu.N. Kucherov, L.M. Lebedeva, N.A. Manov, V.A. Nepomniachtchi, V.P. Oboskalov, M.N. Rozanov, Yu.N. Rudenko, I.A. Ushakov, G.A. Fedotova, M.B. Cheltsov, Yu. Chukreev, M. Yu. Chukreev, V.D. Shlimovich and others. The world school of reliability is mainly represented by such researchers as: R. Allan, R. Billinton, B. Borkowska, Yi Gao, J. Endrenyi, and others. In addition, there exist research groups formed within the Institute of Electrical and Electronics Engineers (IEEE) and the International Council on Large Electrical Systems (CIGRE) and other organizations, such as NERC, ENTSO-E and the Council of European Energy Regulators (CEER). Among the organizations that participated in the comparison of methods for calculating the reliability, algorithms and programs when used as a test, the scheme developed at the Siberian Power Institute (named after L.A. Melentieva), included: Siberian Power Engineering Institute named after L.A. L. A. Melentieva (software systems Yantar, Potok); Department of Energy Cybernetics of the Academy of Sciences of Moldova (software package, Composition); Komi Scientific Center of the Ural Branch of the Russian Academy of Sciences (software package, Orion) and others [56].

The purpose of the dissertation research is to develop computationally more efficient probabilistic means than the MCS method for assessing the reliability of power systems with conserving the high computation accuracy of the MCS method.

This purpose has been declaimed to diverse degrees in the publications and the chapters on which the dissertation is based.

The objectives of the dissertation research.

- Reviewing the probabilistic approaches employed to reliability assessment of the power systems to deduce their shortcomings and so seek for an alternative approach based on developing enhancement to existing methods or a totally new method.

- Proposing probabilistic techniques with the following features: low computational time and good degree of accuracy compared with the MCS method.

- Evaluating the effectiveness of approximate analytical methods in calculating the probabilistic reliability indices.

- Developing an efficient sampling technique for focusing the sampling in the domains of interest in which loss of loads occurred to avoid the surplus time associated with the evaluation of states that make no contribution to the reliability indices.

- Studying the problem of modelling accurately based on real historical data the uncertainties of electricity demand and weather variables and representing the correlation that exists among them in a probabilistic model.

- Evaluating efficiently annual reliability indices of composite power system with renewable energy integrated (wind- solar) considering the stochastic characteristics of electricity demand and renewable energy resources.

The object of the research includes a concentrated EPS and a composite power system with limited capacities of transmission lines and concentrated EPS as separate nodes.

Scientific novelty of the dissertation research:

- The proposition of new approach based on the cross entropy-based importance sampling (CE-IS) in order to improve the sampling efficiency and convergence characteristics of the MCS method. The statistical characterization of the new approach- named ECE-IS is presented. The ECE-IS based optimization algorithm

is more efficient and robust in sampling most states that are important to the estimators of the reliability indices than other discussed methods in literature. From the reported results, the proposed method contributes to accurately evaluating the reliability indices and further enhancing the convergence of the indices in comparison with other methods. Moreover, a great speed-up was shown in terms of computation time with respect to the standard MCS method. By reducing the number of samples required for the simulation and so enabling more time to be exhausted on evaluating each sample, the proposed method paves the way for further complete model of the EPS and so obtaining highly realistic and accurate reliability indices.

- In the case of renewable energy reliability studies, a new approach combines the ECE-IS for extracting the loss of load events and the multivariate Gaussian mixture model (MGMM) for estimating the joint probability distribution of the random variables (demand and weather variables) based on real historical data to include the load and solar and wind power uncertainties and the dependence relationships among them in the reliability assessment of EPSs. The ECE-IS approach is proposed for approximating accurately the optimal ISD of the obtained MGMM and so assist IS in sampling the region of interest for the system reliability indicators (i.e., the region in which the weather variables have lower values and electricity demand has higher value). Using the ECE-IS makes the load loss events more likely to be drawn and allows us to enlarge the sample space with the probabilistic state modeling of the renewable energy conversion systems (wind turbine generators and photovoltaic arrays) and the transmission system. Based on the author's knowledge, no work considers all these RVs in the reliability assessment problem that develop more accurate estimates of the annual reliability indices.

The theoretical significance of the work lies in the development of alternative computationally efficient methods based on developing enhancement to previously methods or a wholly new method for probabilistic assessment of the reliability indices

with the purpose of striking a compromise between the detailed modelling of power system uncertainties and the computational burden of reliability indices.

The practical significance of the work. With the increasing robustness of EPSs, the occurrence of loss of load events is becoming rarer. For example, the LOLP in a real power system does not exceed 0.0001. This means that the power deficit is observed, on average, no more than 0.876 hours per year. However, sequence of rare loss of load events could lead to large blackout in a power system. Therefore, all possible combinations of rare loss of load events must be sampling efficiently. This is achieved by developing the efficient rare events simulation method (ECE-IS) for defining the approximately optimal ISD of the power system random variables making rare loss of load events more likely to be drawn. When the number of states needed to be evaluated is decreased and at the same time preserving the estimator accuracy, the efficiency of the approach will wholly computationally enhance.

The application of the proposed approach in reliability evaluation could enable to enlarge the sample space with the probabilistic modeling of more uncertainties and so matching the reality of the proposed EPS model. The impact of transmission network outages, and spatially correlated demand and renewable energy resources model, could be incorporated into the EPS model. This is accomplished by considering electricity demand and weather variables uncertainties based on real historical data. Use of real data and proper represent the uncertainties give a more realist attitude of power grid performance on the basis of actual reliability indicators and so proper reserve allocation which are dispatched according to the customers' reliability requirements and the location of renewable energy resources.

This realistic model integrated with the efficient ECE-IS method can also be included into the many problems in both operation and planning phases, such as the proper allocation of spinning reserve to allow more integration of renewable powers and improve system and nodal reliability. Using adequacy indices assessments and knowing the critical nodes during system disturbance, planners can better manage the penetration and coordination of renewable energy resources, ensuring sustainable and

reliable operation at both the system and nodal level. In the context of power system operation, operators schedule the generating units and allocate enough generation reserve amounts to ensure a lower the probability of load loss than the maximum allowed.

Research methodology. The research is carried out on the basis of the theoretical foundations of electrical engineering, probability theory and mathematical statistics. The considered methods and algorithms are tested on EPS systems. Evaluation of the effectiveness in terms of the computational efficiency and accuracy is estimated by the MCS method. Moreover, the practical applicability of the developed algorithms with respect to the reliability assessment problem is highlighted. For calculations and software implementation of the algorithms, the MATLAB software package is used. All calculations are executed on an Intel Core i5-8 G memory computer using MATLAB 2017.

The main contributions of the dissertation submitted for defense:

- The assessment of the efficiency and accuracy of the probabilistic-analytical methods and procedures with respect to the reliability evaluation problem.

- The analysis and identification of the best importance sampling strategy in estimating the optimal IS distribution of the uncertain input variables for the composite system reliability assessment problem.

- Enhancing the existing cross entropy-based importance sampling procedure to extract most the rare loss of load events in power systems;

- Integrating the ECE-IS procedure in the reliability evaluation framework that can greatly accelerate the calculation efficiency of the MCS method while not losing the accuracy. The computational efficiency and adaptability of the proposed approach are validated by the results of case studies.

- The analysis and identification of the accurate probabilistic model to handle with the historical real data complexity of the demand and weather variables for proper incorporating the random variation and chronological characteristics of electricity

demand and renewable energy resources (wind- solar) in the reliability assessment problem.

- Evaluating accurately and efficiently power system annual reliability indices with integration of a large-scale PV power stations and wind farms using the ECE-IS technique. The ECE-IS will assist IS in sampling the region of interest for the system reliability indicators (i.e., the region in which the wind farms and PV power stations have lower power generation). Moreover, it preserves the dependence structure of and renewable and load powers in the reliability evaluation procedure, thus the efficiency degradation is avoided. This ensures that the reliability indices are evaluated with an acceptable computation burden.

The author's personal contribution is the development of software for testing the effectiveness of existing and proposed statistical algorithms and methods; the proposition of new efficient simulation techniques for solving the problem of reliability assessment; studying the problem of selection of probabilistic approach which is capable of accurately modelling the uncertainties within the power system network in spite of their probability distribution and characterize the correlation among uncertainties in the power network.

The reliability of the results is validated by the results of computational tests on 5-node and IEEE-RTS 79 test schemes.

Approbation of work results were reported and discussed at 4 conferences:

- International Scientific Conference Energy Management of Municipal Facilities and Sustainable Energy Technologies (EMMFT 2018) Samara, Russia;
- Scientific Symposium on Electric Power Engineering (ELEKTROENERGETIKA 2019), Stara Lesna, Slovakia;
- 2019 IEEE 60th International Scientific Conference on Power and Electrical Engineering of Riga Technical University (RTUCON), 2019, Riga, Latvia.

- International Conference on Industrial Engineering, Applications and Manufacturing (ICIEAM 2020), Sochi, Russia.

Publications: According to the results of the work, 7 works were published and indexed in the international citation bases Scopus and Web of Science.

Dissertation structure. The dissertation consists of an introduction, 4 chapters, a conclusion, symbol list and 140 reference list. It contains 110 pages, 19 figures and 10 tables.

Chapter1 Fundamental concepts and mathematical foundation of probabilistic evaluation of power system reliability

This chapter discusses the main concepts related to power system reliability and presents the probabilistic means concerning the power system's reliability evaluation. The model of power system uncertainties is described. After that, an overview of the reliability indices is presented. Finally, the chapter formulates the statistical foundation of the MCS method and is concluded with a short discussion that outline the main deficiencies of the MCS method.

1.1. Probabilistic Approaches for Reliability Evaluation

A probabilistic analysis of power system reliability incorporates three steps: modeling of uncertainty, uncertainty expansion, and assessing the reliability indices [57-61]. Modelling of uncertainty is a mean to exemplify the state space according to the probabilistic characteristics of the renewable generation, load, and the availability of the various components in a system [58-59]. Second, the uncertainty expansion handles the impact of the input uncertainties to the customer service. By modelling the stochastic variation of uncertainties and severity associated with them, reliability indices in the third stage are calculated to quantify how reliable the system could be. The probabilistic reliability index does not only consider the probability or likelihood of incidence of uncertain events but also measures the consequence of the incidence of that event [61]. Thus, the probabilistic reliability index is estimated as the product of the probability of occurrence and the consequence of an event. Based on the measure of consequence, the reliability indices are named. The consequence can be measured in power system operation by the occurrence or magnitude or duration of loss of load faced by the users or customers of the network.

There are generally two types of probabilistic approaches for modelling the uncertainties: analytical-based methods and simulation-based methods (MCS) [58-64]. The main difference between these methods is to utilize different approaches for describing the probability density function (PDF) of power system parameters. Both approaches have advantages and disadvantages in how they model the uncertainty.

The analytical approaches analyze the PDFs using mathematical expressions such as convolution method, cumulants method, point estimate method (PEM) and unscented transformation. The analytical method in contrast to simulation method (MCS), give the same solution when recalculated. The convolution method gives highly accurate solution. However, it entails complex mathematics which obstruct its application. Approximate analytical methods such as cumulants method, PEM, and unscented transformation can act as alternatives to the MCS method and the exact analytical method (convolution method) [65]. But for their implementation it is necessary to know all the mathematical relations of the input random variables, which is not always possible. As a result, some assumptions adopted in the calculation procedure lead to calculation errors. Therefore, the MCS technique is currently still used in benchmarking the performance of approximate analytical techniques due to its accuracy [64-65].

The MCS can be generally grouped into sequential and non-sequential simulations [66-67]. The Sequential MCS method (state duration sampling) represents the uncertainties over a chronological time span to incorporate time-varying characteristics. This technique is effective in modelling the time series of renewable energy resources and electricity demand keeping the timely and spatially correlation between them. Moreover, it has the advantages of modelling any component state-duration PDF, and the ability to compute directly duration and frequency reliability indices. However, it needs significantly more computation time to reach the convergence than non-sequential MCS and maybe unfeasible for some non-sequential applications. The non-sequential MCS can be classified into the state transition sampling and state sampling. The state sampling method is extensively utilized for power system reliability evaluation since it is relatively simple and easy to implement and has a faster convergence rate [68].

Approaches to renewable energy resources modelling and reliability assessment in individual countries apply different methodologies [9-12, 14-15]. A variety of reliability evaluation and renewable generation modelling standards within different countries are illustrated in Table 1.1. The MCS is the widely used method in

practice. As shown in the table, the modelling of renewable energy resources based on climate datasets is the frequently used approach in different countries.

Table 1.1- Comparison among different countries regarding reliability evaluation approaches.

Country	Type of the assessment model	Used Reliability Indicators	Renewable generation modelling	Correlation
Great Britain	Probabilistic: Non-sequential Monte Carlo	LOLE	Detailed modelling based on climate data for the generation site.	Not considered.
France	Probabilistic: Sequential Monte Carlo	LOLE	Detailed modelling based on climate data for the generation site.	Spatial correlation of wind and PV is considered.
Belgium	Probabilistic: Analytical	LOLE P95*	RES unavailable capacity is estimated with historical data.	
Ireland	Probabilistic: Analytical	LOLE	RES unavailable capacity is estimated with historical data.	
Spain	Deterministic	Reserve margin	Take a certain percentage (5, 7, 20%) as available generation.	
Portugal	Probabilistic: Sequential Monte Carlo	Reserve margin	RES unavailable capacity is estimated with historical data.	
Netherlands	Probabilistic: Analytical approach	Reserve margin	Take a certain percentage (5, 7, 20%) as available generation.	
Pentalateral region (Central Western Europe countries)	Probabilistic: Sequential Monte Carlo	LOLE	Detailed modelling based on climate data for the generation site.	Correlation between wind, demand and PV is considered.

* LOLE P95 is a percentile 0.95 over the future states simulated.

1.2. Statistical foundations of state sampling MCS

The state sampling MCS method depends on three main steps: Sampling the state space, evaluating each state, and computing the convergence and calculating the reliability indicators. The states are randomly sampled from the PDF of the input random variables using the concept of proportionality, i.e. states are sampled proportional to their probability of occurrence. Since the MCS is a fluctuating and iterative process, the reliability indices are estimated with a confidence level. An appropriate convergence criterion is essential to ensure the accuracy of the MCS method. The coefficient of variation is mostly utilized as the stopping rule for the MCS algorithm. The MCS is described in these steps.

1.) Sampling the state space of all components and the uncertain inputs of a power system. The state sampling is implemented on both the availability of components (transmission lines, transformers, generating units, etc.) but also to the forecast uncertainty of power system variables (renewable generation, load levels, and weather states). While outages is depicted as discrete events, forecast uncertainty is represented by a continuous PDF. The states of the system can be represented by the matrix $[x_{i,j}, \forall\, i \in N; j \in n]$, N the set of simulated states and n is the set of random variables.

2.) Select a state of the power system and categorize it whether a non-loss-of-load (success) state or a loss-of-load (failure) state. The failure state is achieved if the total load is higher than the available capacity in reliability studies of concentrated EPS. While the failure state in composite power system may be based on technical limits violation or power deficit. Then, failure states are passed to the optimal power flow (OPF) algorithm. The OPF is utilized to mitigate any technical violation and to avert load curtailment so far as possible or to decrease the total load curtailment if inevitable through rescheduling of generators and load curtailments in according to the priority order.

- Once the state has been classified and the severity or consequence of failure states is computed, the estimate of reliability index $(\hat{\mathcal{R}})$ is usually represented by the coefficient of variation $\mathbb{C}v$. The reliability index $\mathcal{R}$ can be one of the power system reliability indices (LOLP- LOLE- EPNS- EENS, etc.). Besides $\mathbb{C}v$ of one or some or all reliability indices, pre-specified number of samples N can also be used as stopping criteria. Calculation of $\mathbb{C}v$ is described as (1.1) below.

$$\mathbb{C}v_k\left(\hat{\mathcal{R}}\right) = \frac{\sqrt{\mathbb{V}(\hat{\mathcal{R}})}}{\mathbb{E}\left(\hat{\mathcal{R}}\right)} \qquad (1.1)$$

  where k is the number of sampled states up to this iteration, $\mathbb{V}$ is the variance operator, and $\mathbb{E}$ is expectation operator.

3.) If the stopping criterion is satisfied ($\mathbb{C}v_k \leq$ Stopping Value or $k = N$) then stop the simulation $N = k$ and calculate the final value of the reliability indices, otherwise, return to step 2.

1.3. Modelling of power system uncertainties

The uncertainty models used vary in complexity and detail but commonly mimic the variability and stochastically of the power system factors. The modelling of power system uncertainties includes the state random sampling of component outages such as transformers, transmission lines, and generators and forecast uncertainty deviations of power system variables such as renewable generations, load levels, and weather states. While outages can be described as discrete events with likelihoods of occurrence based on historical data, forecast uncertainty is represented by a continuous random variable with corresponding PDF which can be obtained by historical data analysis or through forecasts. Integrating forecast uncertainty is to investigate the likelihood that the parameter diverges from the expected forecast value.

Transmission line model

The state space of transmission line components can be represented by either by the Bernoulli distribution (one transmission line), or by binomial distribution (a group of lines connected in parallel) [69]. In the case of Bernoulli distribution $S_l \sim \mathcal{B}r(1, q_l)$, each transmission line state S_l is either failure state or operation state depending on the transmission line failure probability or forced outage rate (FOR) q_l. In this case, the MCS method generates random numbers in the range of 0 to 1 uniformly distributed in place of sampling a distribution function. The state S of transmission line l is defined as follows:

$$S_l = \begin{cases} 0 & \text{for } r_l \leq q_l \\ 1 & \text{otherwise} \end{cases}$$

where r_l is the pseudo-random number and q_l is the FOR of transmission line l can be expressed as follows:

$$q_l = \frac{\tau\alpha}{\tau\alpha + 8760} \tag{1.2}$$

where α is the outage rate [frequency/year] and τ is the outage duration per year [h]. When S_l equals zero, the transmission line l is in the failure state. Otherwise, the S_l is equal to one. Each sample of S_l is randomly selected independently from following and previous samples.

Generation model

Fundamental for the generation model is the operating characteristics of the generating units which are utilized to model the available capacity [66,70]. The operating characteristics can be characterized as a two-state (failure or operation states) or multi-state model (operation, failure and derated states). The uncertainties of power generation depends on the probabilities of derated and failure states which is dependent on the type of generator. Since the number of generators is large, a group of same type generators (equally capacity and q). The available capacity of a group of similar generators is described by a binomial distribution for the two-state model of each generator or a multinomial distribution for the multi-state model of each generator. The two-state model is considered in the dissertation.

The available capacity of the generator group is equal to the sum of the capacity of available generators and is represented by a binomial probability mass function $\{G_g, w_g = \mathcal{B}(g; n_g, q), g = 0, \dots, n_g\}$, where n_g is the number of generators in the group, G_g is the sum of $(n_g - g)$ generation capacity. The failure probability w_g of number of generators g in a group of n_g elements can be determined by the binomial distribution:

$$\mathcal{B}(g; n_g, q) \approx C_{n_g}^g q^g (1 - q)^{n_g - g} \tag{0.31}$$

where $C_{n_g}^g = \frac{n_g!}{g!(n_g - g)!}$ is the Binomial coefficient. Figure 1.1 illustrates the binomial distribution for the g generators failure with the same capacity (50 MW) and probability of failure ($q = 5\%$) in a group including different number of generators i.e. $n_g = 5, 10, 20, 40, 80$. As $n_g \to \infty$, the binomial distribution with the expectation $\mu = q\,n_g$ and variance $\sigma^2 = q(1 - q)n_g$ is asymptotically normal distribution. According to the limit theorem of Moivre-Laplace, the binomial distribution can be replaced with a normal one if $\sigma^2 \geq 9$ [71]. Since for a real concentrated EPS (reliability zone) the number of generators is large enough, the generation system can be represented by a Gaussian distribution without a sufficiently large error. However, in order to achieve a greater accuracy of generation modeling, a group of the most powerful generators can be distinguished, described by a binomial distribution with the equivalent of the rest of the generating system to a normal distribution [71-72]. The normal distribution extends from $-\infty$ to $+\infty$, which may result in errors where there exist constraints on the values of distribution. In order to avoid extreme values outside a range of interest, a truncated normal distribution (TND) is used for the available generation variables.

Electricity demand

Uncertainties of electricity demand can be considered in a probabilistic reliability assessment by two methods. First, the chronological demand curve is converted into a multi-state distribution model. From the hourly system demand over a period (maybe a year), a clustered model is formulated for the demand based on demand levels (for example a range of 100 MW) and each system demand level has

its probability (number of hours of this demand level /8760) which is utilized as a weight parameter to obtain the annual reliability indicators [18,73]. The MCS method is executed for each demand level and reliability indices are accumulated. Second, a Gaussian distribution is used to describe the variation of total system demand [68, 74]. Usually, the total demand of an EPS, consisting of large number of demand levels, according to the Lyapunov limit theorem, is described by a normal (Gaussian) law of probability distribution, $L \sim \mathcal{N}(\mu_L, \sigma_L^2)$, where μ_L and σ_L are the mean and standard deviation, respectively.
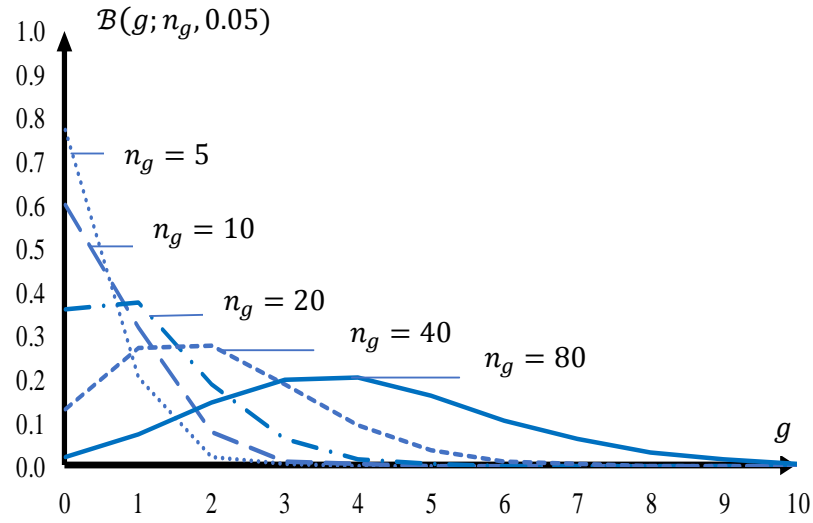
Figure 1.1- Binomial distribution for several numbers of generators in groups.

1.4. Power Flow Modeling and Optimization Framework

After system states are sampled, the system states are evaluated to select the system failure states. In CPS, if one of the subsequent two conditions is achieved for any sampled state, we can define this state as a failure state without solving the power flow model: the total load is higher than the total generation and the loading at a node is higher than the sum of the generation at that node and the capacity of the lines connected to that node. In case of power deficit states, the purpose of OPF is how to distribute the power deficit among load nodes [18, 20, 62-64, 74-80]. According to the selected criterion by which the power deficit distribution is carried out, the objective function is formed, independent variables are selected, a system of limitations and assumptions is determined [77]. A load curtailment sharing

philosophy is considered in this work. Unserved demand is shared across all the load nodes of a power system. Using weight factors in the objective function, a priority order policy is employed for nodes. The objective function is presented in a quadratic form:

$$min\left(\sum_{d=1}^{D} \pi_d PNS_d^2\right) \tag{1.4}$$

where π_d is the weight or priority of load node d and PNS_d is the amount of load curtailment or power not supplied (PNS) at each load node d.

In addition to the objective function, the power system equalities and inequalities constraints such as generation capacity limits, transmission lines capacities, and power balance equation, are essential and will strongly impact obtained reliability indices [78-85]. The power flow equations utilized for analysis is either DC or AC model. The DC power flow model is suitable for studies that need large computational burden such as security assessment and composite system reliability. As there are several procedures in the evaluation of a state, the DC power flow model has been extensively utilized in reliability assessment of power systems due to its simplicity of execution being linear model [77]. However, the DC representation cannot analyze the impact of bus voltages and reactive power on the system reliability. This simplification is acceptable, since the reliability studies mainly treat with long term power system analysis. The nodal power balance constraint can be written in the next form:

$$P_d + G_d + PNS_d - L_d = 0, \forall\, d \in D \tag{1.5}$$

In addition to (1.5), a system power balance equation is used considering the summation of line power losses in the electric network:

$$P_\Sigma + LS_\Sigma = 0 \tag{1.6}$$

Using the nodal power injection vector (P), the line power flows vector (LF) is calculated using a simplified form of DC power flows equations based on Ohm's and Kirchhoff's laws [77]:

$$LF = -[B_{br}]A^t B^{-1} P. \tag{1.7}$$

Power losses for each Monte Carlo simulation sample are calculated based on the assumption that all nodal voltages are equal to the nominal ones.

$$LS_\Sigma = \sum_{l=1}^{N_l} \frac{R_l}{V^2} LF_l^2 \qquad (1.8)$$

Power flows through transmission lines are limited by maximum transmission line capacities:

$$-LF_l^{max} \le LF_l \le LF_l^{max} \qquad (1.9)$$

The generation and curtailed load in each node are restricted by supply and demand limits:

$$0 \le G_d \le G_d^{av}, \qquad (1.10)$$

$$0 \le PNS_d \le L_d.$$

1.5. Convergence and Reliability Indices Evaluation

Once the states have been classified and the severity of failure states are computed, the reliability indices can be computed. The most significant among reliability indices are probability, mathematical expectation and variance of power or energy deficit in EPS. On their basis, other indices can be obtained, for example LOLP (Loss of Load Probability), expected power not supplied (EPNS), LOLE (Loss of Load Expectation), expected energy not supplied (EENS), etc. [9-13, 86-87]. The reliability indices can be estimated for nodes and system. System reliability indices are necessary for both planners and operators to determine the likelihood of interruption of supply, while nodal reliability indices provide information on the most important nodes during system interruption. The system LOLP and EPNS can be expressed as follows:

$$LOLP = \frac{1}{N} \sum_{i=1}^{N} I_F(x_i), \qquad (1.11)$$

$$EPNS = \frac{1}{N} \sum_{i=1}^{N} \left(\sum_{d=1}^{D} PNS_d(x_i) \right).$$

where $x_i = \{x_{i,j}, j = 1, \dots, n\}$ is the sampled state of the uncertain inputs and $I_F(x_i)$ is the failure indicator function and can be written by this formula:

$$I_F(x_i) := \begin{cases} 1 & \text{for } \sum_{d=1}^{D} PNS_d(x_i) > 0 \\ 0 & \text{for } \sum_{d=1}^{D} PNS_d(x_i) = 0 \end{cases}$$

A non-zero value of failure indicator function points out that the occurrence of load loss and a zero value points out that there is no loss of load. Similarly, the nodal LOLP and EPNS can be rewritten as follows:

$$LOLP_d = \frac{1}{N} \sum_{i=1}^{N} I_F^d(x_i), \quad \forall\, d \in D$$

$$EPNS_d = \frac{1}{N} \sum_{i=1}^{N} \left(PNS_d(x_i) \right), \forall\, d \in D$$

(1.12)

in which

$$I_F^d(x_i) := \begin{cases} 1 & \text{for } PNS_d(x_i) > 0 \\ 0 & \text{for } PNS_d(x_i) = 0 \end{cases}$$

The system LOLE and EENS can be calculated from these indices as follows:

$$LOLE = t\, LOLP,$$

$$EENS = t\, EPNS.$$

(1.13)

where t is the period of study in hours. When assessing the reliability indices is carried out annually with the hourly resolution, the period of study is equal to 8760 h.

Due to the iterative behavior of MCS method, the estimated reliability indices always come with a confidence band [88-89]. The coefficient of variation ($\mathbb{CV}$) is regarded as the measure of error for the estimators of reliability indices. A convergence criterion should be employed to halt the MCS algorithm when reaching a low level of variation in the estimated reliability indices. For example, the EPNS estimator can be calculated as follows:

$$\widehat{EPNS} = \frac{1}{K} \sum_{i=1}^{K} \left(PNS(x_i) \right)$$

$$PNS(x_i) = \sum_{d=1}^{D} PNS_d(x_i)$$

(1.14)

To know how accurate is $\hat{EPNS}$ as an estimate of $EPNS$, the coefficient of variation (expectation and variance) of the estimator are calculated as shown in (1.15). Considering the sample size is sufficiently large, the estimated value converges almost surely to the true value i.e. the estimator is unbiased as illustrated in (1.15).

$$\mathbb{E}\left[\hat{EPNS}\right] = \frac{1}{K}\sum_{i=1}^{K}\mathbb{E}[PNS(x_i)] = EPNS \tag{1.15}$$

$$\mathbb{V}\left[\hat{EPNS}\right] = \mathbb{V}\left[\frac{1}{K}\sum_{i=1}^{K}(PNS(x_i))\right] = \frac{1}{K^2}\sum_{i=1}^{K}\mathbb{V}[PNS(x_i)] = \frac{1}{K}\mathbb{V}[PNS]$$

Unfortunately, in a practical situation, we cannot actually calculate the $\mathbb{V}[PNS]$, we typically use an estimate of $\mathbb{V}[PNS]$ assuming the estimate of $\mathbb{V}[PNS]$ is unbiased. So, the variance becomes as follows:

$$\mathbb{V}\left[\hat{EPNS}\right] = \frac{1}{K(K-1)}\sum_{i=1}^{K}\left(PNS(x_i) - \hat{EPNS}\right)^2$$

Similarly, the LOLP estimator can be computed as follows:

$$\hat{LOLP} = \frac{1}{K}\sum_{i=1}^{K}I_F(x_i), \tag{1.16}$$

$$\mathbb{E}\left(\hat{LOLP}\right) = \frac{1}{K}\mathbb{E}\left[\sum_{i=1}^{K}I_F(x_i)\right] = \frac{1}{K}\sum_{i=1}^{K}\mathbb{E}[I_F(x_i)] = \frac{K}{K}\,LOLP = LOLP$$

We can use the central limit theorem to show that $\hat{LOLP}$ is normally distributed for large K with mean $LOLP$ and variance,

$$\mathbb{V}\left[\hat{LOLP}\right] = \frac{1}{K}\mathbb{V}[LOLP] = \frac{1}{K}(LOLP - LOLP^2)$$

The $\mathbb{CV}$ is given as follows:

$$\mathbb{CV}_k\left[\hat{LOLP}\right] = \frac{\sqrt{\frac{1}{K}\mathbb{V}(LOLP)}}{LOLP} = \sqrt{\frac{(1-LOLP)}{K\,LOLP}} \tag{1.17}$$

From (1.17), it can be derived the following points:

- The MCS convergence doesn't depend on the number of random variables n.
- The MCS convergence decreases with increasing the square root of the sample size, K. In other words, to decrease the variability in the LOLP estimator by a

factor of 10 requires a factor of 100 increase in the number of Monte Carlo samples.

- For high reliability power systems (small $LOLP$), the needed number of samples K become larger for getting a low level of variation and so an accurate estimate i.e. $K \cong 10^5$ for $\mathbb{CV} = 0.1$ and $LOLP = 0.001$.

Conclusion

The MCS method is suitable for composite and high-dimensional system analysis. However, it can be greatly slow as large number of samples are essential to assure the convergence of the reliability indices results. The high computational time of MCS is a significant obstacle to its application in power systems, especially with the nonlinearity of the objective function and constraints of OPF algorithm and thus necessitating the proposition of other techniques. Two approaches are adopted here. In place of the MCS, the approximate analytical methods can be utilized in the reliability evaluation problem. The assessment of their efficiency and accuracy is presented in Chapter 2. Another approach is to use variance reduction techniques (VRTs) to make the MCS method more computationally efficient The objective of VRTs is to reduce the variance of the reliability indices estimators so that the number of samples required for achieving convergence can be decreased and so, the convergence is accelerated. This is investigated in Chapter 3.

Chapter 2 Generation Reliability Evaluation using Probabilistic-Analytical Methods

Analytical methods, in contrast to simulation methods, give the same solution when re-calculated. Approximate analytical methods are discussed in this chapter in place of the exact analytical method (convolution method) due to its computational complexity disadvantage and the MCS method due to its high computational time disadvantage. The solution of approximate analytical methods is formed in the process of a certain sequence of mathematical operations. But for their implementation it is necessary to know all the mathematical relations of the input random variables, which is not always possible. As a result, some assumptions adopted in the calculation procedure lead to calculation errors. This chapter discusses the effectiveness of approximate analytical methods and procedures in determining the generation reliability in terms of the probability, mathematical expectation and standard deviation of power not supplied (LOLP-EPNS-SPNS) in a concentrated EPS (system: generation-load) and composite EPSs. Composite system analysis contains the transmission network configuration in the assessment. Compared to concentrated EPS, additional data is needed when conducting a composite reliability assessment reliability assessment, includes such as FORs and capacity limits of transmission lines.

In concentrated EPS, the mathematical basis and calculation procedures for determining the probabilistic indicators of power shortages are executed by different probabilistic analytical techniques such as convolution method, the method of combined cumulants and Gram-Charlier expansion and, the method of combined cumulants and Von Mises function. Also presented are numerical results for the probabilistic indicators of the power shortage and compared with the MCS method, in two generation cases (identical – diverse generation unit sizes).

In composite generation and transmission power system, approximate analytical methods based on a point estimate of probability distributions, are proposed and compared. The effectiveness of using the Rosenblueth and Hong schemes for

assessing the probabilistic indicators of power deficit has been determined. The first four moments can be used in representing the nature of a variable distribution as they give key information about the distribution which are mean or expectation, variance or standard deviation, skewness, and kurtosis. A modification of Hong's scheme is proposed, which consists in connecting an additional block of combination of variables. The effectiveness of the methods based on the accuracy and computation time of obtaining the solution are compared with the MCS method.

2.1. Mathematical formulation of the reliability evaluation problem in a concentrated power system

In concentrated EPS, the uncertainties of the aggregated available generating power (G^{av}) and aggregated required load (L) are considered. While, the constraints of power transmission system within concentrated EPS are not considered. Power deficit between load and generation ($PNS = L - G^{av}$) is observed at $L > G^{av}$ and is equal to zero at $L \leq G^{av}$. Usually, the total load of a concentrated EPS, consisting of an almost infinite number of electrical customers, according to the Lyapunov limit theorem, is described by a continuous normal probability distribution $L \sim \mathcal{N}(\mu_L, \sigma_L^2)$, with a known mean μ_L and variance σ_L^2. The available capacity of a group of same-type generators is usually described by a discrete binomial distribution $G^{av} \sim \mathcal{B}(n_g, q)$, where n_g is the number of generating units in the group and q is the generator probability of failure or FOR.

The sought probabilistic parameters of the power deficit (probability $\mathbb{P}_{PNS}$, mean $\mu_{PNS} = m_{PNS,1}$, and variance σ_{PNS}^2) under condition of mixed distributions i.e. the generation is a discrete random variable and is described by a probability mass function (PMF) $\{G_g, w_g = \mathcal{B}(g; n_g, q), g = 0, \ldots, n_g\}$ in which G_g is the available generation capacity at state g and the load is continuous, can be obtained as follows [71]:

$$\mathbb{P}_{PNS} = \sum_{g=0}^{n_g} w_g \big(1 - F_L(G_g)\big);$$

$$m_{PNS,1} = \sum_{g=0}^{n_g} w_g \int_{G_g}^{\infty} (x - G_g) dF_L(x);$$

$$m_{PNS,2} = \sum_{g=0}^{n_g} w_g \int_{G_g}^{\infty} (x - G_g)^2 dF_L(x);$$

$$\sigma_{PNS}^2 = m_{2,PNS} - m_{PNS}^2,$$

$$f_L(x) = \mathcal{N}(x; \mu_L, \sigma_L^2) = \frac{1}{\sqrt{\sigma_L^2 2\pi}} e^{\left(-\frac{(x-\mu_L)^2}{2\sigma_L^2}\right)}$$

(2.1)

where $f_L(x)$ and $F_L(x)$ are the distribution density and the cumulative distribution function of load, respectively, and $m_{2,PNS}$ is the second order raw moment of the power deficit. The integrals of the above expressions on the right-hand side can be written as follow [5]:

$$m_{PNS} = \sum_{g=0}^{n_g} w_g \big[(\mu_L - G_g)\big(1 - F_L(G_g)\big) + \sigma_L^2 f_L(G_g)\big];$$

$$m_{2,PNS} = \sum_{g=0}^{n_g} w_g \left\{ \big[(\mu_L - G_g)^2 + \sigma_L^2\big]\big[1 - F_L(G_g)\big] + \sigma_L^2 (\mu_L - G_g) f_L(G_g) \right\}.$$

(2.2)

As a result, with a relatively small number of generating sets, the calculation of the probabilistic indicators of the power deficit does not present any problems. In reality, a large number of different types of generators are installed in the EPS. Therefore, the PMF convolution method is used to represent the generation PMF for a number of generators groups $\big\{G_i \sim \mathcal{B}\big(n_{g\,i}, q_i\big), i = 1, \dots, N_g\big\}$, where N_g is the number of generator groups.

2.1.1 Convolution method

One of the most widely used methods for representing the PMF of the generation with a complex structure, is the PMF convolution method [5, 65, 69, 90-91]. It has advantages over other techniques. First, the PMF convolution can be used for a nonstandard PDF description. second, the PDF of the random variables sum with different PDFs can be applied in a mathematically simple manner by the convolution

of distribution functions. Finally, the probabilistic characteristics (distribution moments, semi-invariants, etc.) can be calculated quite simply with the help of PMF convolution.

Mathematically, the convolution of the PMF of several generator groups is the product of probabilities related to the possible operational conditions of the generator groups. In particular, for the convolution of a PMF of two different generators groups with available generation power $\{G_{A,i}\}$, $\{G_{B,j}\}$ and probabilities of the corresponding states $\{w_{A,i}, \sum_{i=1}^{n_A} w_{A,i} = 1\}$, $\{w_{B,j}, \sum_{j=1}^{n_B} w_{A,j} = 1\}$ given as $\{G_{A,i}, w_{A,i}, i = 0, \dots, n_A\}$, $\{G_{B,j}, w_{B,j}, j = 0, \dots, n_B\}$, the two matrices are constructed representing the equivalent PMF: $\{G_{\Sigma,ij} = G_{A,i} + G_{B,j},\ w_{\Sigma,ij} = w_{A,i} w_{B,j},\}$; $\{ i = 0, \dots, n_A,\ j = 0, \dots, n_B \}$. Algorithmically, these matrices are transformed into connected vectors. In case of representing the probabilities and available generation capacity in the vector form, the resultant matrices can be expressed as follows: $w_\Sigma = \bar{w}_A\, \bar{w}_B^T$, $G_\Sigma = \bar{G}_A \bar{e}_B^T + \bar{e}_A \bar{G}_B^T$, where $\bar{e}_A, \bar{e}_B$ − are unit vectors having the same dimension as the corresponding vectors $\bar{G}_A, \bar{G}_B$. The dimension of equal PMFs expands exponentially with the number of generators groups, and the computational burden becomes significant.

2.1.2 The method of combined cumulants and Gram-Charlier expansion

The use of cumulants and the approximation of a PDF by Gram Charlier expansion series is presented. The main objective of using the cumulant method is to replace the complicated convolution of the PDFs of input variables with a simple arithmetic process [21]. The cumulants have properties superior to moments. The additive property of cumulant (not moments) is particularly useful in power systems. By determining the cumulant of available power of generator groups, the cumulants of the load and generator groups can be easily added and so the cumulants of the PNS are computed. Then, Gram Charlier approximate series [92-94] in getting the distribution of the output variable (power deficit) from its cumulants is used by

approximating it with a normal distribution. In this case, the CDF and PDF of the normalized power deficit $\widehat{PNS} = (PNS - \mu_{PNS})/\sigma_{PNS}$ can be expressed as follows:

$$F_{\widehat{PNS}}(x) = \sum_{i=0}^{r} \frac{c_i}{i!} \Phi^{(i)}(x);$$

$$f_{\widehat{PNS}}(x) = \sum_{i=0}^{r} \frac{c_i}{i!} \varphi^{(i)}(x),$$

(2.3)

where $\Phi^{(i)}(x)$ and $\varphi^{(i)}(x)-$ i-th derivative of CDF and PDF of the standard normal distribution; r is the accepted maximum order of the Gram-Charlier series (usually $r = 4$ or 6). Coefficients of the Gram-Charlier series can be calculated from its central moments [95-97] and formulated as follows:

$$c_0 = 1; \quad c_1 = c_2 = 0; \quad c_3 = -\frac{M_3}{\sigma^3} = -\frac{\mathcal{K}_3}{\sigma^3}; \quad c_4 = \frac{M_4}{\sigma^4} - 3 = \frac{\mathcal{K}_4}{\sigma^4};$$

$$c_5 = -\frac{M_5}{\sigma^5} + 10\frac{M_3}{\sigma^3} = -\frac{\mathcal{K}_5}{\sigma^5}; \quad c_6 = \frac{M_6}{\sigma^6} - \frac{15M_4}{\sigma^4} + 30 = \frac{\mathcal{K}_6 + 10\mathcal{K}_3^2}{\sigma^6},$$

(2.1)

where $M_j, \mathcal{K}_j$ are the central moment and the cumulants of the j-th order of the variable PNS. The division of the cumulant $\mathcal{K}_j$ by σ^j is related to the normalization of PNS. Considering that $\Phi^{(1)}(x) = \varphi(x)$, the equation (2.3) can be written in this form:

$$F_{\widehat{PNS}}(x) = \Phi(x) + \sum_{i=3}^{r} \frac{c_i}{i!} \varphi^{(i-1)}(x).$$

The first six derivatives of the density of the standard normal distribution can be written as follows:

$$\varphi(x) = \frac{1}{\sqrt{2\pi}} e^{-\frac{x^2}{2}};$$

$$\varphi^{(1)}(x) = -x\varphi(x);$$

$$\varphi^{(2)}(x) = (x^2 - 1)\varphi(x);$$

$$\varphi^{(3)}(x) = (3x - x^3)\varphi(x);$$

$$\varphi^{(4)}(x) = (x^4 - 6x^2 + 3)\varphi(x);$$

$$\varphi^{(5)}(x) = -(x^5 - 10x^3 + 15x)\varphi(x);$$

$$\varphi^{(6)}(x) = (x^6 - 15x^4 + 45x^2 - 15)\varphi(x).$$

A disadvantage of the method is the need to determine cumulants of higher orders (> 4), which is difficult for most distribution functions, including the binomial distribution.

2.1.3 The method of combined cumulants and Von Mises function

The use of cumulants and the approximation of a PDF based on Von Mises function have been proposed. In this approach, the discrete and continuous distributions of input variables are addressed separately. The continuous distribution considered here is the normal distribution for describing the load. The cumulants for a discrete distribution of generation power are calculated, then, converted to moments, and after that use the Von Mises process to calculate impulses and corresponding weights. Based on the Von Mises function for generation power and continuous normal distribution of load power, the PDF and CDF of the power deficit are obtained. As proposed by Richard Von Mises [98], the equivalent PDF of the available capacity of a generator group can be considered as the weighted sum of impulses. The Von Mises function allows the definition of a discrete distribution characterized by ν impulses from the first $(2\nu - 1)$ raw moments [98]. For obtaining the equivalent impulses and their weights, the determinants of the matrices are determined from the moments in the following form:

$$D_0 = |m_0|; D_1 = \begin{vmatrix} m_0 & m_1 \\ m_1 & m_2 \end{vmatrix}; \ldots D_\nu = \begin{vmatrix} m_0 & m_1 & \ldots & m_\nu \\ m_1 & m_2 & \ldots & m_{\nu+1} \\ \ldots & \ldots & \ldots & \ldots \\ m_\nu & m_{\nu+1} & \ldots & m_{2\nu-1} \end{vmatrix}$$

The maximum order of the positive determinant determines the maximum number of impulses. In practice, the number of used impulses is not more than 5. However, in our calculations, acceptable accuracy is achieved only when the number of impulses is at least 7. Solving a group of linear equations with a matrix of coefficients similar to the structure D_ν allows determining the coefficients $\{c_i\}$ of the polynomial $\sum_{i=0}^{\nu} c_i x^i = 0$. The roots of the polynomial determine the coordinates $\{x_i\}$ of equivalent impulses. The coefficients $\{c_i\}$ are determined by the equation corresponds to

$$\begin{pmatrix} m_0 & m_1 & \ldots & m_\nu \\ m_1 & m_2 & \ldots & m_{\nu+1} \\ \ldots & \ldots & \ldots & \ldots \\ m_\nu & m_{\nu+1} & \ldots & m_{2\nu-1} \end{pmatrix} \begin{pmatrix} c_0 \\ c_1 \\ \ldots \\ c_\nu \end{pmatrix} = \begin{pmatrix} -m_{\nu+1} \\ -m_{\nu+2} \\ \ldots \\ -m_{2\nu-1} \end{pmatrix}. \tag{2.5}$$

Finally, the probabilities w_i of equivalent impulses x_i are determined from the system of equations of the raw moments

$$\begin{pmatrix} 1 & 1 & \dots & 1 \\ x_1 & x_2 & \dots & x_{\text{υ}} \\ \dots & \dots & \dots & \dots \\ x_1^{\text{υ}} & x_2^{\text{υ}} & \dots & x_{\text{υ}}^{\text{υ}} \end{pmatrix} \begin{pmatrix} w_1 \\ w_2 \\ \dots \\ w_{\text{υ}} \end{pmatrix} = \begin{pmatrix} 1 \\ m_1 \\ \dots \\ m_{\text{υ}} \end{pmatrix} \qquad (2.6)$$

The PDF of power deficit can be formulated as follows:

$$f_{PNS}(x) = \sum_{i=1}^{\text{υ}} w_i\, f_L(x - x_i) \qquad (2.7)$$

The high order raw moments needed to obtain the required number of impulses limits the von Mises's method range of applications. There are only three known distributions, where obtaining the raw moments of higher orders is not a problem. These are normal, Poisson, and Bernoulli. Mathematical expressions for the raw moments of the fourth and higher orders of other distributions have a complex structure and are given in the reference literature to a limited extent and rarely. As a rule, the sum of several probabilistic variables which are described by different PDFs with the moments or cumulants that can be calculated, form the required probabilistic variable. The high order moments of the required variable can be calculated by means of the cumulants of the elements that form the variable. More often, the considered random variable is represented as a sum of random variables with probability distributions for which raw moments or higher order cumulants can be obtained. With the known cumulants of the sum, it is possible to get the moments of higher orders of the considered RV.

The binominal PDF is usually used for describing generation a group of generators in a power system. The mathematical structure of equations used for calculating the high order raw moments of the binominal PDF is complex. The problem can be potentially alleviated by considering each generator separately. Assuming that there are only two possible operational conditions of generator (on and off), it is possible to describe the available capacity of a generator $x_i \in (0; P_{bl_i})$ by the Bernoulli distribution $x_i \sim \mathcal{B}r(1, q_i)$, where P_{bl} is the generator nominal power. The probability of the state $x_i = P_{bl_i}$ is $w_i = 1 - q_i$ (the availability

factor). The u-th order raw moment $m_{i,u}$ of the variable x_i, $i = 1, \ldots, n_g$ can be computed as follows:

$$m_{i,u} = w_i\, g_i^u.$$

where n_g is the number of generators in the group. The r-th order cumulant $\mathcal{K}_{i,r}$, $r > 1$ of the variable x_i is calculated according to the recurrent expression [92]

$$\mathcal{K}_{i,r} = m_{i,r} - \sum_{j=1}^{r-1} C_{r-1}^j m_{i,j}\, \mathcal{K}_{i,r-j}.$$

The cumulant of the capacity of generator group $x_\Sigma = \sum x_i$ can be computed as

$$\mathcal{K}_{\Sigma,r} = \sum_{i=1}^{n_g} \mathcal{K}_{i,r}.$$

Based on the obtained cumulant values, it is possible to determine the initial moments of the resulting variable x_Σ according to the recurrence relation [92]:

$$m_{\Sigma,r} = \mathcal{K}_{\Sigma,r} + \sum_{j=1}^{r-1} C_{r-1}^j m_{\Sigma,j}\, \mathcal{K}_{\Sigma,r-j}.$$

2.2 Computational results for concentrated power system

A numerical study is performed to compare the proposed procedures. A concentrated EPS with groups of generators (number, rated power (MW) and the failure probability of a generating unit) was considered: {5; 200; 0,08}; {4; 100; 0,05}; {6; 50; 0,05}] and a load described by normal distribution with mathematical expectation $\mu_L = 1000$ MW and standard deviation $\sigma_L = 100$ MW. The results of the study are summarized in Table. 2.1 and Table. 2.2, which shows a comparison of mathematical techniques for determining the probabilistic indices of a power deficit in a concentrated EPS. Table 2, to assess the specificity of one group of similar generators, the group {8; 200; 0,08}. The columns of the tables {LOLP, EPNS, SPNS} correspond to the probability, mathematical expectation and standard deviation of the power deficit, and the columns { LOLP err, EPNS err, SPNS err} correspond to the relative error of the considered mathematical method. As a basis for comparison, the method of convolution of probability series is adopted, which is considered as absolutely accurate (the first row of the table). The second and third

rows of the table correspond to the statistical test method (MCS) with 10^6 and 10^4 number of samples. Normally, with increasing the number of samples, the error decreases, but even with 10^6, the error of the mathematical expectation is nearly 2.6%. With a smaller number (10^4) of samples, the error of the method exceeds 25% as shown in Table 2.2. The negative properties of the MCS are known - to obtain acceptable accuracy, an unacceptably long computation time is required.

The cumulant combined with the Gram-Charlier series provides the results (fourth row of the table, {11.6%, -5.6%, -17.6%} (Table 1) {23.3%, 2.6%, - 14.2%} (Table 2). Here, the binomial distribution is taken as the basic one in determining the raw moments and semi-invariants. The use of the Poisson distribution as the basic one results in a considerable rise in the total error. The last method stands out significantly in terms of modeling accuracy - von Mises. The von Mises method (error {0.1%, - 0.3%, 0%} (Table 1) and {0%, 0%, 0%} (Table 2) is based on the representation of a generating system as a set of individual generators with the Bernoulli distribution. The calculated values correspond to 11 impulses. A reduction in the number of impulses to five results in a rise in the errors on average up to (2-3) %. If it is necessary to obtain accurate calculations, the method of convolution of probability series is out of competition.

Table2.2- Computational results in case of different generator groups.

Method	LOLP	LOLP err	EPNS	EPNS err	SPNS	SPNS err
Convolution	0.0020	0.0%	0.143	0.0%	4.388	0.0%
MCS-10^6	0.0020	-1.5%	0.140	-2.1%	4.315	-1.7%
MCS-10^4	0.0032	60.5%	0.226	58.6%	5.702	30.0%
Cumulant+Gram-Charlier	0.0022	11.6%	0.135	-5.6%	3.616	-17.6%
Cumulant+Von mises	0.0020	0.1%	0.142	-0.3%	4.388	0.0%

Table 2.2- Computational results in case of single generator group.

Method	LOLP	LOLP err	EPNS	EPNS err	SPNS	SPNS err
Convolution	0,0043	0,0%	0,338	0,0%	7,102	0,0%
MCS-10^6	0,0041	-3,6%	0,329	-2,6%	7,053	-0,7%
MCS-10^4	0,0034	-20,0%	0,236	-30,2%	5,244	-26,2%
Cumulant+Gram-Charlier	0,0052	23,3%	0,346	2,6%	6,097	-14,2%
Cumulant+Von mises	0,0043	0,0%	0,338	0,0%	7,102	0,0%

2.3 Mathematical formulation of the reliability evaluation problem in composite power system

A composite power system model is normally represented by a group of areas or nodes (a set of concentrated EPS) connected by transmission lines of limited capacity. The uncertainties of total available generation capacity and total required load are depicted for each concentrated EPS or node. The total load of a concentrated EPS is represented by a normal PDF, with a known mathematical expectation and variance. The normal distribution is also used for describing the aggregated load connected to each node. The available capacity of a group of similar generators is usually depicted by a binomial distribution and could be approximated by a Gaussian PDF as described in 1.3.

Due to the probabilistic nature of the load and available generation, it may turn out that the total available capacity of generation system $G_\Sigma^{av} = \sum_{d=1}^{D} G_d^{av}$ will be less than the total demand $L_\Sigma = \sum_{d=1}^{D} L_d$, $G_\Sigma^{av} < L_\Sigma$, where D is the number of system nodes. If we accept the assumption of unlimited capacity of transmission lines, the power deficit in the system can be formulated as, $PNS_\Sigma = G_\Sigma^{av} - L_\Sigma$, the positive part of which determines the reserve, and the negative part - the deficit of generating capacity. At the same time, due to, as a rule, the accepted assumption about the independence of G_Σ^{av}, L_Σ, the mathematical expectation and variance of the power deficit:

$$\mathbb{E}(PNS_\Sigma) = \mathbb{E}(G_\Sigma^{av}) - \mathbb{E}(L_\Sigma);$$
$$\mathbb{v}(PNS_\Sigma) = \mathbb{v}(G_\Sigma^{av}) + \mathbb{v}(L_\Sigma).$$

(2.8)

If we accept the assumption of a normal probabilistic distribution of power deficit, with mean and variance determined by expressions (2.8), then the probability of a power deficit in the system can be calculated through the normal distribution function:

$$\mathbb{P}(PNS_\Sigma) = F_{PNS_\Sigma}(0; \mathbb{E}(PNS_\Sigma), \mathbb{v}(PNS_\Sigma)),$$

However, in practice, there is a presence of power deficits is the result of limited capacity of transmission lines and the impossibility of delivering power from surplus node to deficient ones. As a result, the problem arises of the distribution of power deficits between the nodes through the OPF algorithm are needed as described in 1.4.

2.3.1 Point Estimate Method

The method of combined PEM and the approximation of a distribution by Gram Charlier expansion series has been considered for estimating the probabilistic indices of power deficit in composite power system. PEM concentrate the PDF of each system input into points or impulses with corresponding weights based on the knowledge of the first few moments of the variables [99], and then perform deterministic OPF calculations at each of these impulse to obtain the moments of system output. The PDF of a system output can be approximated through its raw moments by the Gram Charlier expansion series.

The essence of the PEM is to approximate the distribution function $f(x)$ of a continuous random variable by a probability series $\{x_j; w_j, \ j = 1, \dots, n_p\}$ for which the value x_j and probability w_j are determined for the points n_p (often called concentrations). In relation to the property of uncertainty, the probability w_j can be interpreted as a "weighting factor" of a point satisfying $\sum_{j=1}^{n_p} w_j = 1$. Pairs $\{x_j; w_j\}$ (often called probabilistic moments) are defined in such a way that some probabilistic criteria are satisfied as follows:

$$\sum_{j=1}^{n_p} x_j w_j = m_{x,1}; \ \sum_{j=1}^{n_p} (x_j - m_{x,1})^u w_j = M_{x,u}, u = 1,2,..,n_M. \tag{2.9}$$

where $m_{x,u}$ and $M_{x,u}$ are the u-th raw and central moment of the random variable x, respectively and n_M − is the number of moments. Here x_j is the value of the variable over which the function $h(x)$ is evaluated. The weight w_j is a factor that determines the relative importance of this estimate in the analyzed function $h(x)$. When determining the moments of the output random variable $z = h(x)$ as shown in (2.10), the PDF or CDF of the output random variables, the Gram - Charlier series is used when normalizing the variables and its moments or cumulants.

$$m_{z,u} = \int_{-\infty}^{\infty} (h(x))^u dF(x) = \sum_{j=1}^{n_p} (h(x_j))^u w_j. \tag{2.10}$$

This approach can be extended to a set of input variables $\{x_i, i = 1, \dots, n\}$, forming a multivariate probability distribution. In this case, the analyzed function depends on all

variables, $z = h(x_1, \dots x_n)$. With discreteness $\{x_i\}$, $z = h(x_{ij}, \ i = 1, \dots, n; \ j = 1, \dots, n_{p,i})$. Correspondence of weights to probabilities requires knowledge of the probabilities of joint events $\mathbb{P}(x_{1\,j_1}, \dots, x_{i\,j_i}, \dots x_{n\,j_n})$, or multivariate probability distribution, which is practically impossible to implement in real technical calculations. Here, as a rule, the assumption is made about the independence of the input variables.

There are various PEM schemes based on the number of estimation points and how the input vectors are represented [99-106]. Several PEM schemes such as Rosenblueth's PEM $(n_p)^n$ [100-101] and Hong's PEM implementations [102-103]: $(n_p \times n)$ and $(n_p \times n) + 1$, where n is the dimension of the variable being analyzed; n_p is the number of concentration points for an individual variable. The $2 \times n$ Hong PEM needs a foreknowledge of the first three moments for all the input random variables. It has large errors with increasing the number of variables. For better performance, the $2n + 1$ and $4n + 1$ schemes are suggested for including more points. The $2n + 1$ needs knowledge of all the inputs' first four moments. While the $4n + 1$ requires further knowledge of the input variable up to the 8-th moment.

2.3.1.1   Rosenblueth's PEM

To demonstrate the basic idea of Rosenblueth's PEM [100-101], consider a function $h(x)$ of one variable x, the first three central moments $M_{x,1}, M_{x,2}, M_{x,3}$ (mean, standard deviation and skewness) are known. First of all, it should be noted that on the basis of four equations (equality of three moments and equality of the sum of weights to one), two probabilistic impulses can be determined, since each impulse is characterized by two parameters (location and weight $\{x_j, w_j, j = 1,2\}$). The locations and weights of the input variable x are obtained by solving a system of nonlinear equations

$$\sum_{j=1}^{2} w_j = 1; \sum_{j=1}^{2} w_j (x_j - \mu_x)^u = M_{x,u}, u = 1, 2, 3 \tag{2.11}$$

where μ_x is the mean of the variable x. For the convenience of the mathematical representation of the central moments, the change of variables in (2.11) is performed. The coordinate of the variable point (x_j) is determined by the relative deviation ξ_j of the point from the variable mean μ_x as follows: $x_j = \mu_x + \xi_j\,\sigma_x$, where σ_x is the standard deviation of the variable x. To normalize the variables and dividing on σ_x^u and substituting by $\xi_j = (x_j - \mu_x)/\sigma_x$ and $\lambda_{x,u} = M_{x,u}/\sigma_x^u$, the equation (2.11) becomes

$$\sum_{j=1}^{2} w_j = 1; \sum_{j=1}^{2} w_j(\xi_j)^u = \lambda_{x,u}, u = 1, 2, 3 \tag{2.12}$$

where $\lambda_{x,u}$ is the standard u-th central moment. The expression (2.12) in expanded form can be written as follows:

$$\begin{cases} w_1 + w_2 = 1; \\ w_1\xi_1 + w_2\xi_1 = 0; \\ w_1\xi_1^2 + w_2\xi_2^2 = 1; \\ w_1\xi_1^3 + w_2\xi_2^3 = v_x, \end{cases}$$

where $v_x = \lambda_{x,3} = E[(x - \mu_x)^3]/\sigma_x^3$ – is the coefficient of asymmetry (skewness) of the variable x. The solution of this system of equations presented in [100] has this form

$$\xi_{x_1}, \xi_{x_2} = \frac{v_x}{2} \pm \sqrt{1 + \left(\frac{v_x}{2}\right)^2}; w_1 = \frac{1}{2}\left[1 - \frac{v_x}{2}\frac{1}{\sqrt{1 + \left(\frac{v_x}{2}\right)^2}}\right]; w_2 = 1 - w_1.$$

In the case of a standard normally (or symmetrically) distributed variable $v_x = 0$. Hence, the location $\xi_{x_1}, \xi_{x_2} = \mp 1$. Wherein: the points are $\mu_x + \sigma_x$ and $\mu_x - \sigma_x$. The weights of these points are the same $w_1 = w_2 = 1/2$.

If $h(x)$ is a function of two variables $\{x_1, x_2\}$, then the Rosenblueth procedure is to create four vectors, which are a combination of points, one from each variable, that is, it builds four input vectors so that the value of each variable is one standard deviation above or below the average value: $(\mu_{x1} + \sigma_{x1}, \mu_{x2} + \sigma_{x2})$, $(\mu_{x1} + \sigma_{x1}, \mu_{x2} - \sigma_{x2})$, $(\mu_{x1} - \sigma_{x1}, \mu_{x2} + \sigma_{x2})$ and $(\mu_{x1} - \sigma_{x1}, \mu_{x2} - \sigma_{x2})$. Since $h(x)$

represents a combination of the values of the two input variables, the weight of each vector is equal to $0{,}5^2 = 0{,}25$.

In the general case, when $h(x)$ is a function of n variables $(x_i, i = 1, \ldots, n)$, the Rosenbluth procedure chooses $N = (n_p)^n$ input vectors so that the value of each variable is one standard deviation below or above the mean, $\{\mu_{x_i} \mp \sigma_{x_i}, i = 1, \ldots, n\}$. With the same strategy for choosing the location of points for all variables, the probabilities of input vectors $(r_i = \mu_{x_1} \mp \sigma_{x_1}, \ldots, \mu_{x_i} \mp \sigma_{x_i}, \ldots, \mu_{x_n} \mp \sigma_{x_n}, i = 1, \ldots, N)$ are the same, hence the mean $h(\boldsymbol{x})$ is the average value of the functions on the set of impulses

$$h(\boldsymbol{x}) = \frac{1}{N} \sum h(r_i).$$

When solving the problem of estimating reliability indices, as a rule, the load and the available generation of the EPS are random variables. Moreover, the number of variables, even for relatively small systems, is in the hundreds. Taking into account the relations $N = (n_p)^n$, it can be argued that this method is applicable only when the number of variables is no more than 12-14. With a larger number of variables, the MCS method again becomes more efficient in terms of speed and accuracy of calculations.

2.3.1.2   Hong's PEM

Hong's method has two schemes $(n_p \times n)$ and $(n_p \times n + 1)$.

The first scheme $(n_p \times n)$ is characterized by the fact that each input vectors $r_i, i = 1, \ldots, n \times n_p$ is characterized by a deviation of only one variable $x_i, i = 1, \ldots n$. All other variables in the impulse are taken equal to their mean as follows: $r_i = \mu_{x_1}, \ldots, \mu_{x_i} + \xi_{x_{i,j}} \sigma_{x_i}, \ldots, \mu_{x_n}, j = 1, \ldots, n_p.$ Hence, the total number of evaluations is equal to $N = n \times n_p$. The coordinates of the location $\xi_{x_{i,j}}$ and the weight $w_{x_{i,j}}$ for each random variable x_i are determined by solving a system of nonlinear equations similar to (2.12) [102]:

$$\sum_{i=1}^{n}\sum_{j=1}^{n_p} w_{x_{i,j}} = 1; \quad \sum_{j=1}^{n_p} w_{x_{i,j}} \xi_{x_{i,j}}^u = \lambda_{x_i,u}, \quad \forall\, u \in n_M, i \in n \tag{2.13}$$

For one random variable ($i = 1$) and $n_p = 2$, four equations with four unknowns (coordinates and weights of the two points) are required. Solution of the system of equations (2.13) are obtained as follows:

$$\xi_{x_{i,1}}, \xi_{x_{i,2}} = \mp 1; \; w_{x_{i,1}} = w_{x_{i,2}} = 0{,}5; \; i = 1$$

In a multivariate space of variables ($x_i, i = 1, \dots, n$), the system of equations (2.13) takes this form

$$\sum_{j=1}^{n_p} w_{x_{i,j}} = 1/n; \quad \sum_{j=1}^{n_p} w_{x_{i,j}} \xi_{x_{i,j}}^u = \lambda_{x_i,u}, \quad \forall\, u \in n_M, i \in n \tag{2.14}$$

The solution of equations for each variable x_i is obtained as follows:

$$\xi_{x_{i,1}}, \xi_{x_{i,2}} = \frac{\upsilon_{x_i}}{2} \pm \sqrt{n + \left(\frac{\upsilon_{x_i}}{2}\right)^2};$$

$$w_{x_{i,1}} = \frac{1}{n}\frac{\xi_{x_{i,2}}}{(\xi_{x_{i,2}} - \xi_{x_{i,1}})}; \qquad w_{x_{i,2}} = -\frac{1}{n}\frac{\xi_{x_{i,1}}}{\left(\xi_{x_{i,2}} - \xi_{x_{i,1}}\right)}.$$

It should be noted that the coordinates or locations of the concentration points in the considered scheme depend on the number of variables n.

The second scheme. The Hong's second model ($2 \times n + 1$) is to consider one more (third) specific point - the mean of a random variable, which is equal to zero for the normalized quantities involved in calculating the central moments. From here, its location has already been determined for the third point. As a result, to determine the parameters of the points, a system of five (rather than six) equations is required - one equation for the sum of the weights and 4 to ensure the equality of the first four central moments. The advantage of the scheme is to take into account not only the third, but also the fourth (kurtosis, $k_{x_i} = \lambda_{x_i,4}$) central moments in equations (2.14). The solutions of the considered system of equations are [103]:

$$\xi_{x_{i,1}}, \xi_{x_{i,2}} = \frac{\upsilon_{x_i}}{2} \pm \sqrt{k_{x_i} - \frac{3}{4}\upsilon_{x_i}^2}; \tag{2.15}$$

$$w_{x_{i,1}} = \frac{1}{\xi_{x_{i,1}}^2 - \xi_{x_{i,1}}\xi_{x_{i,2}}}; \quad w_{x_{i,2}} = \frac{1}{\xi_{x_{i,2}}^2 - \xi_{x_{i,1}}\xi_{x_{i,2}}};$$

$$w_{x_{i,3}} = \frac{1}{n} - w_{x_{i,1}} - w_{x_{i,2}}.$$

The third concentration point is the same for all variables. Hence, there is no need to repeat many times the same calculations corresponding to the mean of the input variables. Here the weight of the point corresponding to the mean is

$$w_0 = \sum_{i=1}^{n} w_{x_{i,3}} = 1 - \sum_{i=1}^{n}\left(w_{x_{i,1}} + w_{x_{i,2}}\right) = 1 - n\left(w_{x_{i,1}} + w_{x_{i,2}}\right) = 1 - \frac{1}{\lambda_{x_i,4} - \lambda_{x_i,3}^2}.$$

Realizations of input vectors, as in the first Hong model, contain one of two points $(x_{i,j}, i = 1, \ldots, n; j = 1,2)$ of each input random variable $(x_i, i = 1, \ldots, n)$, while others variables are represented by their expected values. In addition, the last vector contains the mean of the input variables.

Scheme 2 $(2 \times n)$ +1 is considered as the linear superposition of Hong's schemes PEM $(2 \times n)$ and $(2 \times n)$ +1 [105]. The moments of the output random variable $(z = h(x))$ are defined as the average of their output moments:

$$m_{z,u} = \frac{1}{2}\{ w_0 \left(h(\mu_{x_1}, \ldots, \mu_{x_n})\right)^u + \sum_{i=1}^{n}\sum_{j=1}^{2} w_{x_{i,j}} \left(h(\mu_{x_1}, \ldots, x_{i,j}, ., \mu_{x_n})\right)^u$$

$$+ \sum_{i=1}^{n}\sum_{j=1}^{2} w_{x'_{i,j}} \left(h(\mu_{x_1}, \ldots, x'_{i,j}, ., \mu_{x_n})\right)^u \} \qquad (2.16)$$

where $x'_{i,j}$ and $x_{i,j}$ - the realization points of Hong's schemes $(2 \times n)$ and $((2 \times n) + 1)$ respectively.

Many researchers confirm that in the range of variables close to the mean, the accuracy of the 2^n Rosenblueth and $(2 \times n)$ Hong schemes are approximately the same [104]. In the area farther from the mean, which is more relevant in analyzing the reliability of systems, since rare events are of greatest interest here, one should give preference to the second Hong scheme $(2 \times n + 1)$, with $\xi_{x_1}, \xi_{x_2} = \mp\sqrt{3}$). However, even this Hong's method with probabilistic impulses at the points

$(-\sqrt{3}\sigma; 0; \sqrt{3}\sigma)$ is insufficient for analyzing the EPS reliability, since in engineering practice the load fluctuation in the $\mp2\sigma$ range is considered normally acceptable, meeting the reliability criterion. Additionally, it should be noted that the power of the most powerful generators in the EPS is comparable to the STD of generation. Hence, Hong's scheme $(2 \times n)$ implements the N-1 reliability criterion actually operating in the EPS, according to which the shutdown of any EPS element should not lead to a limitation of power consumption. As a result, when analyzing reliability, the area outside $\mp2\sigma$ or meeting the N-2 criterion and higher is of interest. This condition is partially met by the second Hong scheme for $n_p = 4$. Here, the coordinates of probabilistic impulses [103] in the $(4 \times n)$ scheme:

$$\xi_{x_1}, \xi_{x_4} = \mp\sqrt{3 + \sqrt{6}} \approx \mp2{,}33 \; ; \; \xi_{x_2}, \xi_{x_3} = \mp\sqrt{3 - \sqrt{6}} \approx \mp0{,}74; \; .$$

$$w_{x_1} = w_{x_4} = \frac{(3 - \sqrt{6})}{12} \approx 0{,}046 \; ; \; w_{x_2} = w_{x_3} = \frac{(3 + \sqrt{6})}{12} \approx 0.45 \; ;$$

In the scheme $(4 \times n + 1)$

$$\xi_{x_1}, \xi_{x_5} = \mp\sqrt{5 + \sqrt{10}} \approx \mp2{,}86; \; \xi_{x_2}, \xi_{x_4} = \mp\sqrt{5 - \sqrt{10}} \approx \mp1{,}36; \; \xi_{x_3} = 0.$$

$$w_{x_1} = w_{x_5} = (7 - 2\sqrt{10})/60 \approx 0.011; \; w_{x_2} = w_{x_4} = (7 + 2\sqrt{10})/60 \approx 0.22; \; w_{x_3} = 8/15.$$

For the problem of assessing the reliability of EPS, the areas from 2σ to 3σ are more significant. Hence, we can expect that the best option would be the superposition of the PEM $(4 \times n)$ and $(4 \times n+1)$ Hong schemes.

In the general case, 8 equations (coordinates and weights) are required to determine four impulses of an arbitrary probability distribution. As noted above, these equations are formed from the condition of equality of the first standard central moments $(0, 1, \lambda_3, \dots, \lambda_7)$. The coordinates of these impulses are the roots of the fourth degree polynomial $\xi^4 + c_3\xi^3 + c_2\xi^2 + c_1\xi + c_0 = 0$ [106]. The coefficients of the polynomial c_0, c_1, c_2, c_3 are the solution to a system of linear equations (Gram's scheme):

$$\begin{pmatrix} 0 & 1 & \lambda_3 & \lambda_4 \\ 1 & \lambda_3 & \lambda_4 & \lambda_5 \\ \lambda_3 & \lambda_4 & \lambda_5 & \lambda_6 \\ \lambda_4 & \lambda_5 & \lambda_6 & \lambda_7 \end{pmatrix} \begin{pmatrix} c_0 \\ c_1 \\ c_2 \\ c_3 \end{pmatrix} = - \begin{pmatrix} \lambda_4 \\ \lambda_5 \\ \lambda_6 \\ \lambda_7 \end{pmatrix} \tag{2.17}$$

After calculating the coordinates $\xi_1, \xi_2, \xi_3, \xi_4$ the weights are determined from the system of equations (2.14).

2.3.1.3 Modified Hong's PEM

In the problem of estimating EPS reliability, the nodal available power generations $G_1^{av}, \dots, G_D^{av}$ and loads $L_1, \dots, L_D$ are considered as independent input random variables, and their states union formulate a set of input vectors $\{r_i, i = 1, \dots, N\}$, $r_i = \{x_i, i = 1, \dots, n\}$, in which N is the number of input vectors, n is the number of input random variables $(G_d^{av}, L_d \ \forall \ d \in D)$ and D is the set of nodes. In Hong's scheme $(2 \times n + 1)$, only one nodal parameter changes - either the load or generation (criterion $N - 1$), but the power deficit is observed when two negative events are superimposed i.e. more than one nodal load and generation differ from their expected forecast value. In order to take relatively this factor into account in Hong's $2 \times n + 1$ scheme, it is proposed to introduce an additional block of analyzed vectors $\left\{ \mu_{G_d^{av}} - \xi_{G_{d,1}^{av}} \sigma_{G_d^{av}}, \right.$ $\left. \mu_{L_d} + \xi_{L_{d,2}} \sigma_{L_d}; \ \forall \ d \in D \right\}$. The weight of the vector component of this block is determined by analogy with the Rosenblueth scheme, as the probability of joint realization of two independent events $w_d = w_{G_{d,1}^{av}} w_{L_{d,2}}$.

2.4 Computational results for composite power system

In this section, based on test calculations, the applicability and efficiency of the considered PEM methods are compared in relation to the problem of assessing the reliability indices. Figure 2.1 shows a five-nodes test system. The data for the nodes and transmission lines are presented in Table 2.3. All the nodes are connected by transmission lines of the same transmission capacity but different resistance and reactance. The nodal loads and the available generating powers are independent random variables and described by normal probability distributions with a given mean and variance in Table 2.3. In terms of mean values of the generation capacity and load, the test scheme includes two in surplus, one in balance, and two deficient nodes. The

probabilistic nature of the generation and demand could potentially result in different combinations of operational states of the power system nodes.

The considered methods are compared based on the probability, expected value, and standard deviation of PNS in nodes (Nodal LOLP- EPNS- SPNS), as well as the average value and overload probability of the transmission lines. The calculations are presented in Table 2.4. The MCS with the number of statistical tests 10^4 is taken as a reference for comparing the PEM methods. With this volume of tests, the scatter of MCS results does not exceed 1.5%. The nodal loads and the available generations are considered as input variables. Hence, the number of variables (n) is 10. When comparing the methods, the relative deviation of the indicator under consideration from the corresponding indicator obtained by the MCS method is computed. To evaluate the effectiveness of the PEM schemes, the error index ϵ_i is used as shown in (2.18), which are defined as the average errors for the set of nodes and transmission lines.

$$\epsilon_i = \frac{1}{\eta}\sum_{g=1}^{\eta}\left|\frac{\beta_{i,g}^{MCS}-\beta_{i,g}^{*}}{\beta_{i,g}^{MCS}}\right| \times 100[\%], \tag{2.18}$$

where η, depending on the indicator i, is either the number of nodes or the number of transmission lines; $\beta_{i,g}^{MCS}$ $\beta_{i,g}^{*}$ − the values of the analyzed indicator i at node or transmission line g, calculated by the MCS and by the considered PEM method, respectively.

The resulting indicators can be divided into two groups: (LOLP, EPNS, and SPNS for the nodes, overload probability of the transmission lines) and (nodal power export and loading of the transmission lines). Compared to the MCS method, all the methods of PEM under consideration have a shorter calculation time. The Rosenblueth method does not outperforms all the other compared methods in terms of the speed of calculations, but it has some advantages only when calculating the indicators of nodal power deficit. This is because this method takes into account the overlap of low generation and high load events. Hong's methods $2 \times n$ and $2 \times n+1$ are practically not inferior in accuracy to the methods of Hong's $4 \times n+1$ and $2(2 \times n)+1$- both are quite accurate when assessing the indicators of the second group

and equally inaccurate when assessing the indicators of the first group. Slightly more accurate is Hong's $4 \times n+1$ method. The modified Hong's method methods $M(2 \times n)+1$, having the same performance as the other Hong's methods, makes it possible to obtain more accurate solutions for the indicators of the first group. Hence, for practical application in solving reliability evaluation problems, we can recommend Hong's methods $M(2 \times n)+1$ and $4 \times n+1$. But when analyzing the reliability, the N-1 or N-2 criterion should be considered as the basic one, but additional disturbances in the EPS are superimposed.
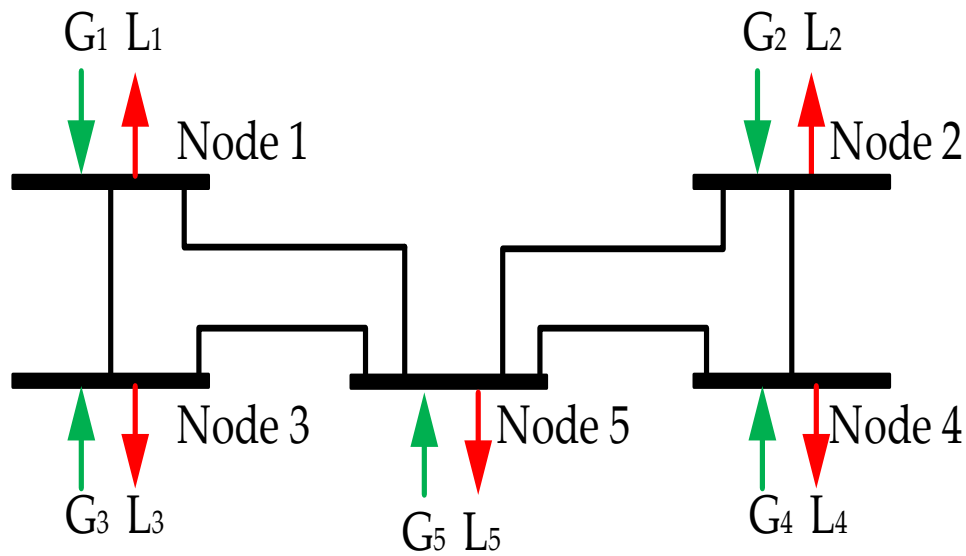

Figure 2.1- Test scheme.

Table 2.3- Test scheme data.

Transmission Lines Data					Nodes Data				
From	To	Resistance	Reactance	Capacity		Available Generation		Load (MW)	
Node	Node	(Ohm)	(Ohm)	(MW)	Node	(MW)			
1	5	10	100	500		Mean	STD	Mean	STD
1	1	1	1	1	1	1700	170	1700	170
2	2	2	2	2	2	50	5	50	5
2	3	3	3	3	3	1440	144	1440	144
3	4	4	4	4	4	1200	120	1200	120
4	5	5	5	5	5	1500	150	1500	150

Table 2.4- The PEM methods comparison with the MCS method.

Parameters	MCS	Ros-'s PEM	Hong's PEM				
		2^n	2n	2n+1	4n+1	2(2n)+1	M2n+1
Computational time, s	40	9	3.2	3.3	3.9	3.5	3.5
Deviation of Nodal EPNS, %		86.8	108.6	68.3	66.2	86.29	34.8
Deviation of Nodal SPNS, %		69.5	79.7	62.2	61	70.7	43.8
Deviation of Nodal LOLP, %		21	47.5	22.5	22.5	25.9	28.2
Average line power flow, MW	261.4	0.28%	0.13%	2.7%	2.76%	1.35%	1.18%
Deviation of line overload probability, %		41.9	74.1	50	36	45.4	13
Average Nodal export power, MW	-2.98	1%	1%	3%	3%%	7%	4%

Conclusion

In concentrated EPS, the main findings can be outlined as follows:

- The most accurate method for assessing the probabilistic parameters of the power deficit is the convolution method through separating accounting of generation and load.

- The statistical modeling method (MCS) needs a large number of tests (about 10^6) to provide an accurate solution.

- Defining the power deficit distribution function by the Gram-Charlier series gives quite large calculation errors, especially in the case of low probabilities of power deficit.

- With a large number of different types of generator groups for practical use, the von Mises method is recommended as sufficiently accurate on average and mathematically simpler.

In composite power system, the results discussion can be concluded in the following points:

- The point estimates methods are effective only when a relatively large number of events of loss of load is in the range from the minimum to maximum of the concentration points of input random variables. If the

system is extremely reliable (the loss of load events might be so rare), the loss of load events need more probabilistic impulses of the input random variables and more number of combinations among them to be investigated. Thus, the point estimates methods do not provide accurate estimates of the reliability indices.

- Rosenbluth's method is applicable only when the number of variables is no more than 12-14. With a larger number of variables, the MCS method becomes more efficient in terms of speed and accuracy of calculations.

- One principal advantage of the Hong's scheme $(n_p \times n + 1)$ is the independence of their concentration points on the number of variables.

- The Hong's scheme (2n) is the most computationally effective but is suffers from very large errors. Hong's schemes $(4 \times n + 1)$ and $(2 \times n + 1)$ give better accuracy than the 2n scheme. Hong's scheme $(4 \times n + 1)$ gives similar or slightly better performance as the $(2 \times n + 1)$ scheme, but for higher modeling accuracy, preference should be given to the (4n + 1) scheme since it gives a deeper knowledge of the input variables up to the 8th moment.

- In general, modified Hong's method M($2 \times n$) +1, having better performance than the rest of Hong's methods, by taking into account a group of combined events, provides more accurate solutions for reliability indicators describing the nodal power deficit and the overload of the transmission lines.

Chapter 3 A Framework for Reliability Evaluation through Extraction of Rare Loss of Load Events in Composite Power Systems

VRTs are presented as effective methods for accelerating the MCS computation in power system reliability assessment. VRTs are used to manage the manner each sample of the MCS method is specified to decrease the variance of the estimators of the reliability indices. By decreasing the variance, the convergence is sped-up. VRTs extract the set of states, which make a significant contribution to the evaluation of reliability indices through generating samples exploring the loss of load events and so shortening the computation time of obtaining an accurate estimate of the reliability indices. When the more reliable the power system is i.e. the smaller system failure probability (LOLP) is, the more reduction of computation time is compared with the MCS.

The name of variance reduction techniques gathers various techniques, such as subset sampling [38], importance sampling [39-41], control variates [42], antithetic variates [43], stratified sampling [44], line sampling [45-46], and directional sampling [47]. Subset simulation (SS) and importance sampling (IS) are the most substantial variance reduction approaches applied in reliability studies. SS is based on splitting the failure domain into a series of partial failure domains. This facilitates describing the probability of failure event as a product of conditional probabilities of the partial failure events. The main advantages of SS are its capability to handle complex limit-state functions (e.g., nonlinear, with possibly multiple failure regions). On the other hand, SS have some drawbacks. Firstly, the variance estimator is not directly calculated by an analytical formula as MCS and IS techniques but must be evaluated by repetition. Secondly, even if SS provides a variance reduction compared to MCS, the number of samples needed to achieve convergence is larger than that needed with other IS techniques. The objective of the IS method is to obtain the importance sampling density (ISD) in which compared with the original distribution the important region has higher occurrence likelihoods. In other words, the ISD is the density of the input variables conditional on the failure domain. The optimal selection of the ISD

can result in zero variance of the estimate of failure probability. However, in practice, sampling from the theoretically optimal ISD is not handy, because it needs knowing the failure probability and failure domain in advance. To overcome this problem, the cross-entropy technique [48-50] was applied to approximate the optimal ISD in a sequential manner. The advantage of the CE-IS approach is related to the fact that analytical updating formulas can be derived for density parameters when dealing with probability densities belonging to the natural exponential family. Another advantage concerns the fact that, similarly to the standard MCS, the estimation error is directly controlled using the estimator of the variance [48]. However, the major difficulty is to construct efficient intermediate densities used in the adaptive sampling process to approach the target optimal ISD.

This chapter primarily revise the traditional CE-IS to develop an improved version of the CE-IS named (ECE-IS) by incorporating two enhancements. The first one is developing a new updating scheme for the parameter of the intermediate density. In the proposed method, the indicator function of the intermediate failure events is defined by a smooth approximation function instead of using step function as the traditional CE-IS method. This allows exploiting all the samples from intermediate sampling levels in the density parameter updating, contrary to the traditional CE-IS method, which uses a small portion of the samples. In addition, a smooth shifting for the optimal ISD of intermediate failure events towards the target optimal ISD is achieved. This effective use of the intermediate samples leads to better estimate of the density parameter and hence to a smaller sampling error in the corresponding probability estimate. Secondly, exploiting as stopping criterion the coefficient of variation of the weights according to the smooth approximation of the optimal ISD of intermediate failure events regarding the target optimal ISD improves the robustness of the method convergence. These modifications contribute to obtaining the accurate optimal ISD of nodal generations and loads, and so, the nodal and system reliability indices are computed accurately. We primarily revise the traditional CE-IS to develop the ECE-IS and then compare the performance of the

proposed method to the traditional CE-IS and recently proposed techniques in literature such as subset simulation.

3.1. Problem formulation

The load curtailment event is defined as the inability to satisfy the loads at all nodes without violating the system operating constraints such as the limited capacity of transmission lines. Thus, the load curtailment event may result from low available generation or high required load or the limited capacity of transmission lines or union of some (or all) above. To carry out the first stage aim, the occurrence of load curtailment is verified at each sampled state of the uncertain inputs $\{x_i, i = 1, ..., N\}$, where $x_i = \{G_1^{av}, ..., G_D^{av}, L_1, ..., L_D\}$, N is the number of samples, and D is the set of nodes. Suppose the set $\mathbb{F}$ is the failure domain in the input parameter space, i.e. the domain of system failure to meet the demand. The failure domain $\mathbb{F}$ is expressed by a limit-state function $H(x_i)$ as follows: $\mathbb{F} = \{x_i: H(x_i) < 0, i = 1, ..., N\}$. The function $H(x_i)$ defines the degree of power balance of system state x_i as shown in (3.1).

$$H(x_i) = \sum_{d \in D} (G_d(x_i) - L_d(x_i)) - LS_\Sigma(x_i) \tag{3.1}$$

where LS_Σ is the summation of power losses in the system. For estimating the target failure probability (loss of load probability), the 2D-variate normal distribution of uncertain inputs is expressed by $\mathcal{N}(x; u)$, which is depicted by mean μ and covariance Σ vectors, and so $u = [\mu; \Sigma]$. To simplify the writing of equations, the vector $\{x_i, i = 1, ..., N\}$ is symbolized by x. Hence, the probability of failure can be computed by the following expression:

$$\mathbb{P}_F = \int I_F(x) \mathcal{N}(x; u) dx = \mathbb{E}_\mathcal{N}[I_F(x)], \tag{3.2}$$

in which $\mathbb{E}_g$ indicates that the expectation operator is taken with respect to the density $\mathcal{N}$ and $I_F(x)$ denotes the failure indicator function and is expressed as follows:

$$I_F(x_i) := \begin{cases} 1 \text{ for } H(x_i) < 0 \\ 0 \text{ for } H(x_i) \geq 0 \end{cases}$$

3.2. Implementation of CE-IS method

IS introduces an alternate sampling density $f(x)$, termed the ISD. A proper selection of $f(x)$ is required to represent accurately the failure domain of inputs. The probability of failure shown in (3.2) is computed regarding $f(x)$ and rewritten in the following manner:

$$\mathbb{P}_F = \int I_F(x)\,W(x)f(x)dx = \mathbb{E}_f[I_F(x)W(x)], \tag{3.3}$$

where $W(x) = \frac{\mathcal{N}(x;u)}{f(x)}$ is the likelihood ratio or importance weight function, which is expressed as a ratio of original and proposed densities. The IS estimate of $\mathbb{P}_F$ is given by:

$$\overset{\wedge}{\mathbb{P}}_F = \frac{1}{N}\sum_{i=1}^{N} I_F(x_i)W(x_i), \tag{3.4}$$

in which $\{x_i, i = 1, ..., N\}$ are identically distributed samples based on $q(x)$. To obtain the optimal selection of the ISD $f^*(x)$, the variance of $\mathbb{P}_F$ estimators have to be minimized as follows:

$$\min_f \mathbb{V}_f[I_F(x)W(x)]$$

The theoretically optimal ISD leading to zero variance is given by the following Equation:

$$f^*(x) = \frac{I_F(x)\mathcal{N}(x;u)}{\int I_F(x)\mathcal{N}(x;u)dx} = \frac{I_F(x)\mathcal{N}(x;u)}{\mathbb{P}_F}. \tag{3.5}$$

Since the optimal ISD is dependent on unknown quantities, $\mathbb{P}_F$ and $I_F(x)$, as shown in (3.5), the computation of the optimal ISD is not possible directly. The CE is used to find a near-optimal ISD for the unknown optimal ISD (the theoretically optimal ISD leading to zero variance $(f^*(x))$ through fitting a parametric density model. Typically, the density model is chosen as the same family as the original density of the input random variables (a multivariate normal probability distribution) $\mathcal{N}(x;u)$, which is depicted by mean vector μ and diagonal covariance Σ matrix, and so $u = [\mu; \Sigma]$. Hence, the density model used in the CE method is $\mathcal{N}(x;u^{IS})$ having $u^{IS} = [\mu^{IS}; \Sigma^{IS}]$ as shown in (3.6).

$$\mathcal{N}(x; u^{IS}) = \frac{1}{\sqrt{|\Sigma^{IS}|(2\pi)^n}} e^{\left(-\frac{(x-\mu^{IS})(\Sigma^{IS})^{-1}(x-\mu^{IS})^T}{2}\right)}, \tag{3.6}$$

where n is the number of variables. The parameter vector (u^{IS}) is defined through minimizing the cross entropy or KL-divergence between the unknown optimal ISD given in (3.5) and the selected probability density $\mathcal{N}(x; u^{IS})$. The cross entropy between the $f^*(x)$ and $\mathcal{N}(x; u^{IS})$ can be described as follows:

$$\begin{aligned} \mathbb{D}\big(f^*(x), \mathcal{N}(x; u^{IS})\big) &= \mathbb{E}_{f^*}\left[\ln\left(\frac{f^*(x)}{\mathcal{N}(x; u^{IS})}\right)\right] \\ &= \mathbb{E}_{f^*}\big[\ln(f^*(x))\big] - \mathbb{E}_{f^*}\big[\ln(\mathcal{N}(x; u^{IS}))\big]. \end{aligned} \tag{3.7}$$

Then, the optimization problem can be expressed in the following manner:

$$\operatorname*{argmin}_{u^{IS}} \mathbb{D}\big(f^*(x), \mathcal{N}(x; u^{IS})\big) = \operatorname*{argmax}_{u^{IS}} \mathbb{E}_{f^*}\big[\ln(\mathcal{N}(x; u^{IS}))\big]. \tag{3.8}$$

By substituting $f^*(x)$ in (3.8) with the equation (3.5), the optimization problem becomes

$$\begin{aligned} & \operatorname*{argmin}_{u^{IS}} \mathbb{D}\big(f^*(x), \mathcal{N}(x; u^{IS})\big) \\ &= \operatorname*{argmax}_{u^{IS}} \int I_F(x) W(x; u^{IS}) \mathcal{N}(x; u^{IS}) \ln(\mathcal{N}(x; u^{IS})) \, dx \\ &= \operatorname*{argmax}_{u^{IS}} \left[\frac{1}{N} \sum_{i=1}^{N} I_F(x_i) W(x_i; u^{IS}) \ln(\mathcal{N}(x_i; u^{IS}))\right], \end{aligned} \tag{3.9}$$

in which $W(x; u^{IS}) := \frac{\mathcal{N}(x; u)}{\mathcal{N}(x; u^{IS})}$.

The CE method solves this optimization problem iteratively through defining a series of intermediate densities $\{\mathcal{N}(x; u_k^{IS}), k = 1, \ldots, K\}$ in several probability spaces that gradually reach the target ISD representing well the failure region as shown in Figure 3.1. It exploits the samples from intermediate sampling levels for fitting the selected parametric density. The intermediate failure domain $\mathbb{F}_k$ and failure indicator function are defined using a threshold ζ_k as stated in (3.10). ζ_k is calculated as the θ-quantile of the sorted limit-state function values $H(x_i)$ from smallest to largest of the samples from the fitted parametric density obtained at the previous step $\mathcal{N}(x; u_{k-1}^{IS})$.

$$\mathbb{F}_k = \{x : H(x) < \zeta_k\}, \zeta_k \geq 0;$$

$$I_{F_k}(x) = \begin{cases} 1 & \text{for } H(x) < \zeta_k \\ 0 & \text{for } H(x) \geq \zeta_k \end{cases}. \tag{3.10}$$
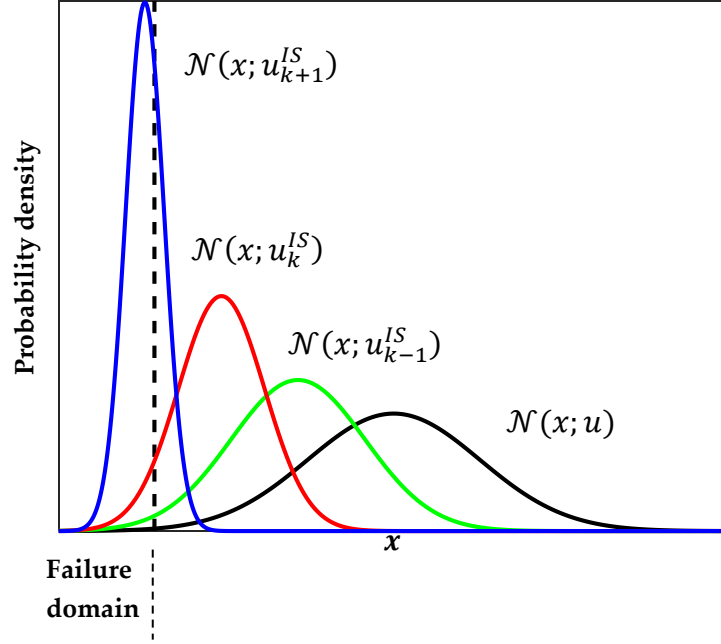

Figure 3.1. A gradual approach of the sequence of intermediate distributions to the target failure region.

Starting from an initial sampling density $\mathcal{N}(x; u_0^{IS} = u)$, the density parameter u_k^{IS} updating is executed until the threshold ζ_k becomes beyond zero. In this case, the target optimal ISD is approximated well enough by the current parametric density. In order to obtain u_k^{IS}, the optimization problem written in (3.11) is solved by taking the gradient of the function with respect to the u_k^{IS} and setting it to zero.

$$\underset{u_k^{IS}}{\operatorname{argmin}} \, \mathbb{D}\left(f_k^*(x), \mathcal{N}(x; u_k^{IS})\right) = \underset{u_k^{IS}}{\operatorname{argmax}} \left[\frac{1}{N} \sum_{i=1}^{N} I_{F_k}(x_i) W(x_i; u_{k-1}^{IS}) \ln(\mathcal{N}(x_i; u_k^{IS}))\right], \tag{3.11}$$

in which $f_k^*(x) := \frac{I_{F_k}(x)\mathcal{N}(x;u)}{\mathbb{P}_{F_k}}$ and $W(x_i; u_{k-1}^{IS}) := \frac{\mathcal{N}(x_i;u)}{\mathcal{N}(x_i;u_{k-1}^{IS})}$. The derivative at step k with respect to the parameters of $u_k^{IS} = [\mu_k^{IS}, \Sigma_k^{IS}]$, which are μ_k^{IS} and Σ_k^{IS}, are:

$$\frac{1}{N} \sum_{i=1}^{N} I_{F_k}(x_i) W(x_i; u_{k-1}^{IS})(x_i - \mu_k^{IS}) = 0$$

$$\frac{1}{N} \sum_{i=1}^{N} I_{F_k}(x_i) W(x_i; u_{k-1}^{IS}) \frac{1}{2} ((\Sigma_k^{IS})^{-2}(x_i - \mu_k^{IS})(x_i - \mu_k^{IS})^T - (\Sigma_k^{IS})^{-1}) = 0 \tag{3.12}$$

The optimal parameters at step k are derived as

$$\mu_k^{IS} = \frac{\sum_{i=1}^{N} I_{F_k}(x_i) W(x_i; u_{k-1}^{IS}) x_i}{\sum_{i=1}^{N} I_{F_k}(x_i) W(x_i; u_{k-1}^{IS})}$$

$$\Sigma_k^{IS} = \frac{\sum_{i=1}^{N} I_{F_k}(x_i) W(x_i; u_{k-1}^{IS})(x_i - \mu_k^{IS})(x_i - \mu_k^{IS})^T}{\sum_{i=1}^{N} I_{F_k}(x_i) W(x_i; u_{k-1}^{IS})} \qquad (3.13)$$

The procedure is repeated until ζ_k becomes a negative value, i.e., at least (θN) samples fall in the failure domain, where $\theta \in [0.01, 0.1]$. Thus, K is set to the current event k, and the optimal ISD is approximated quite by the density $\mathcal{N}(x; u_{K-1}^{IS})$, and the probability of failure is estimated as follows:

$$\hat{\mathbb{P}}_F = \frac{1}{N} \sum_{i=1}^{N} I_F(x_i) W(x_i; u_{K-1}^{IS}). \qquad (3.14)$$

3.3. Implementation of ECE-IS method

In the traditional CE-IM, the intermediate failure domain is identified by the intermediate failure threshold ζ_k. Because of the step indicator function $I_{F_k}(x)$, ζ_k represents only a fraction ($\theta \in [0.01, 0.1]$) of the samples of the preceding ISD $\mathcal{N}(x; u_{k-1}^{IS})$, and the other samples are neglected. In the ECE-IS, the indicator failure function of the intermediate failure events $I_{F_k}(x)$ is defined by a smooth approximation function. This allows a smooth transition for the approximately optimal ISD $q_k^*(x)$ towards the optimal ISD of the destination failure event $q^*(x)$ through exploiting all samples from the intermediate density $\mathcal{N}(x; u_{k-1}^{IS})$ in parameter u_k^{IS} updating.

The indicator failure function can be defined as follows: $I_{F_k}(x; \delta_k) = \lim_{\delta_k \to 0} \Phi\left(-\frac{H(x)}{\delta_k}\right)$, where δ_k is the control parameter of function bandwidth, and Φ is the standard normal CDF. When δ_k approaches zero, the smooth function approaches to the target step indicator function. Hence, $\delta_0 > \delta_1 > \cdots . > \delta_K > 0$ defines a decreasing series of bandwidths, as shown in Figure 3.2.

Using the smooth function of I_{F_k}, the optimization problem (3.11) becomes as follows:

$$u_k^{IS} = \operatorname*{argmax}_{u_k^{IS}} \left[\frac{1}{N} \sum_{i=1}^{N} W(x_i; u_{k-1}^{IS}, \delta_k) \ln(\mathcal{N}(x_i; u_k^{IS})) \right], \qquad (3.15)$$

in which $W(x_i; u_{k-1}^{IS}, \delta_k) := \dfrac{\Phi\left(-\frac{H(x_i)}{\delta_k}\right) \mathcal{N}(x_i; u)}{\mathcal{N}(x_i; u_{k-1}^{IS})}$. δ_k is determined such that the optimal ISD $q_k{}^*(x)$ is approximated well enough by samples drawn from $\mathcal{N}(x; u_{k-1}^{IS})$, i.e., the variance of the importance weights $W(x; u_{k-1}^{IS}, \delta_k)$ is small. This is done by minimizing the difference between the $\mathbb{CV}$ of the weights $\{W(x; u_{k-1}^{IS}, \delta_k), i = 1, \dots, N\}$ and the specified $\mathbb{CV}_{t\,arg\,et}$ at each intermediate event k, as written in (3.16).

$$\delta_k = \underset{\delta_k \in (0, \delta_{k-1})}{\operatorname{argmin}} \left| \mathbb{CV}_w - \mathbb{CV}_{t\,arg\,et} \right|. \tag{3.16}$$
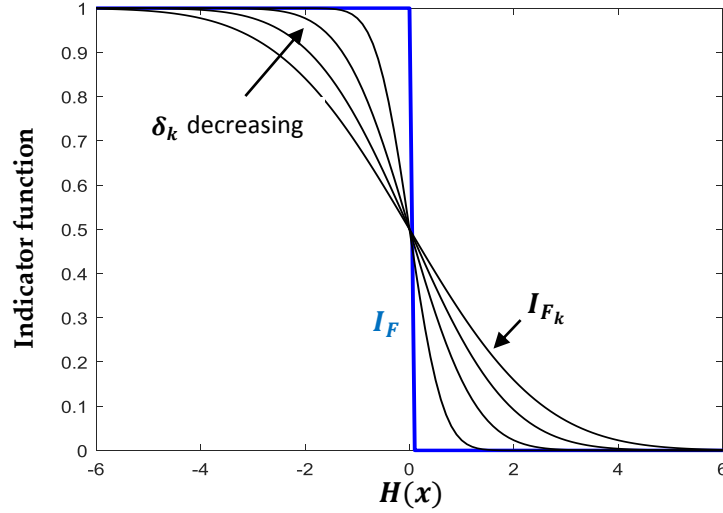

Figure 3.2. Indicator function approximation.

As shown in Algorithm 3.1, starting with $\delta_0 = \infty$ and u_0^{IS} as a nominal parameter vector, this procedure is reiterated and stopped when the $\mathbb{CV}$ of the weight calculated in (3.17) of the present smooth approximation of the optimal ISD of intermediate failure events with regard to the target optimal ISD is lower than the $\mathbb{CV}_{t\,arg\,et}$. Hence, K is set to the current event k, and the optimal ISD is approximated well enough by the density $\mathcal{N}(x; u_{K-1}^{IS})$. Utilizing the $\mathbb{CV}$ of the weights as stopping criterion instead of the parametric density $\mathcal{N}(x; u_{k-1}^{IS})$ improves the robustness of the method convergence, as will be shown in the section of results.

$$\left\{ W(x_i; \delta_k) = \frac{q^*(x_i)}{q_k{}^*(x_i)} = \frac{I_F(H(x_i))}{\Phi\left(-\frac{H(x_i)}{\delta_k}\right)}, i = 1, \dots, N \right\}. \tag{3.17}$$

The samples from the density $\mathcal{N}(x; u^{IS}_{K-1})$ will be used in the second stage as shown in Algorithm 3.1 for computing the system adequacy indices (LOLP-EPNS) for each node and system. The system LOLP and EPNS can be expressed as follows:

$$LOLP = \frac{1}{N}\sum_{i=1}^{N} I_F(x_i)W(x_i; u^{IS}_{K-1}), \qquad (3.18)$$

$$EPNS = \frac{1}{N}\sum_{i=1}^{N}\left(\sum_{d=1}^{D} PNS_d(x_i)\right)W(x_i; u^{IS}_{K-1}).$$

For nodes, the LOLP and EPNS can be rewritten as follows:

$$LOLP_d = \frac{1}{N}\sum_{i=1}^{N} I_F^d(x_i)W(x_i; u^{IS}_{K-1}) \ \forall\, d \in D \qquad (3.19)$$

$$EPNS_d = \frac{1}{N}\sum_{i=1}^{N}(PNS_d(x_i))W(x_i; u^{IS}_{K-1}) \ \forall\, d \in D,$$

in which

$$I_F^d(x_i) = \begin{cases} 1 \text{ for } PNS_d(x_i) > 0 \\ 0 \text{ for } PNS_d(x_i) = 0 \end{cases}$$

Algorithm 3.1. Procedure of reliability indices evaluation using ECE-IS

1. Set $k = 0$, $\delta_k = \infty$ and $u_k^{IS} = u$.
2. Set $k = k + 1$ and draw N samples from $\{\mathcal{N}(x_i; u^{IS}_{k-1}), i = 1,\ldots,N\}$.
3. Calculate the limit-state function $\{H(x_i), i = 1,\ldots,N\}$ and evaluate the weights $\{W(x_i; \delta_{k-1}), i = 1,\ldots,N\}$, as shown in (3.17).
4. If the $\mathbb{CV}$ of the weights is lower than $\mathbb{CV}_{target}$, go to step 8.
5. Solve the optimization problem in (3.16) to detect δ_k.
6. Estimate u_k^{IS} from solving the optimization problem in (3.15).
7. Return to step 2.
8. Set $K = k$.
9. Take the samples from $\{\mathcal{N}(x_i; u^{IS}_{K-1}), i = 1,\ldots,N\}$.
10. Select a sample and run DC-OPF algorithm to estimate the nodal and system load curtailment values.
11. Evaluate the nodal and system indicator functions $I_F^d(x_i)$ & $I_F(x_i)$ and the likelihood ratio $W(x_i; u^{IS}_{K-1})$.
12. Calculate the LOLP and EPNS indices and their coefficient of variation (convergence) for each node and system, as shown in the equations (3.18) and (3.19).
13. If the convergence of indices is acceptable or the number of samples is reached, stop the simulation, otherwise go to step 10.

First stage (steps 1–8)

Second Stage (steps 9–13)

3.4. Subset Method

The main idea of this methods is the formation of a sequence of subsets $F_1 \supset F_2 \supset \cdots \supset F_m = F$ of the state space of the system, where each subsequent subspace increases the probability of identifying a rare event and is determined on the basis of the previous one, forming a Markov chain sequence. Each subsequent subset is chosen so that the probability of the conditional event $\Pr(F_j|F_{j-1})$ would be high enough. As a result, the low probability appears to be the product of relatively high probabilities [38].

$$\mathbb{P}_F = \Pr\left(F = \bigcap_{k=1}^{K} F_k \right) = \prod_{k=1}^{K} \Pr(F_k|F_{k-1}). \tag{3.20}$$

One of the ways to form $(F_k|F_{k-1})$ is to select a given fraction p_0 of the most significant events $X_b^{k-1} = (x_1^{k-1}, x_2^{k-1}, \dots, x_j^{k-1})$, $j = p_0 N$; N–is the sample size. The significance of events is determined by the corresponding value of the criterion function $H(x)$– the smaller the value of H (x), the greater the significance. Hence the mechanism of selection of the set X_b^{k-1} follows. The sample F_{j-1} is ordered in ascending order of the criterion function. The $p_0 \cdot 100$ percentile of the function $H(x)$ is determined, which determines the set X_b^{k-1} with the volume $N_c^{k-1} = p_0 N$, and the criterion value $b_{k-1} = max(H(x), x \in X_b^{k-1})$, which is the basis for the formation of the set $F_k = \{ x: H(x) < b_{k-1}\}$. In this case, the ratio $N_c^{k-1}/N = p_0$ can be considered as the probability of the conditional event $\Pr(F_k|F_{k-1}) = p_0$.

The presented step-by-step process is characterized by a positive value $b_k > 0$ at all intermediate stages. This means that the set X_b^k contains both failure events, $H(x) < 0$, and non-failures $H(x) > 0$, that is, the nested event methodology is reduced to the analysis of the "failure" zone $x: H(x) < (b_k > 0)$, and the criterion of "failure" becomes tougher as the transition to the next stage, $b_k < b_{k-1}$. Initially, $b_1 = \infty$, which means that all states of the system belong to the analysis zone. Hence, each stage contains some non-empty set of analyzed states that satisfy the current criterion of failure. In this case, the volume of the analyzed zone is reduced from stage to stage in accordance with the selected fraction p_0 of the selection of the most significant events,

and the conditional probability of identifying "pseudo-deficient" states of the system is acceptable for the application of statistical analysis methods.

At the last stage, $b_k < 0$. This means that all events in the set with a fraction of p_0 selected according to the truncation principle are failures. But failures can also be events that did not fall into the region defined by the percentile, $b_k < H(x) < 0$. Hence, the last analyzed area should be expanded, and its probability is determined according to the relation: $\Pr(F_K|F_{K-1}) = N(H(x) < 0)/N$, where $N(H(x) < 0)$ is the number of elements of the sample of size N that satisfy the requirement $H(x) < 0$.

3.5. Results

The proposed method is tested and evaluated for the five-node test scheme, presented in Figure 2.1. The MCS method is used as a benchmarking method. The maximum number of simulation samples for MCS is 5×10^4. A coefficient of variation (convergence) of 5% for both system adequacy indices (LOLP-EPNS) is used as the stopping criterion. The rare events simulation techniques (CE-IS, SS, ECE-IS) use the following parameter values: $\theta = 0.1, \mathbb{CV}_{target} = 1.5$, maximum number of iterations $= 50$, and number of samples per iteration $= 2000$.

In Figure 3.3, the PDFs of the system limit-state function $H(x)$ are shown for different methods (CE-IS, SS, ECE-IS) and MCS. It illustrates that the proposed ECE-IS method has the largest probability of $H(x) < 0$, which is 80% in comparison with 23, 55, and 32% for MCS, CE-IS, and SS, respectively. This means that the samples extracted by the ECE-IS method are more likely to cause the load curtailment events. It represents 80% of the total sampled system states. Once the samples from the optimal distributions of nodal generations and loads are obtained, the adequacy indices (EPNS, LOLP) can be evaluated. For test purposes the EPNS, LOLP are calculated for all the nodes. The histogram in Figure 3.4 shows the computation time and the EPNS values obtained by the different methods. The computation time includes the time spent in the first stage for extracting the rare load curtailment events.
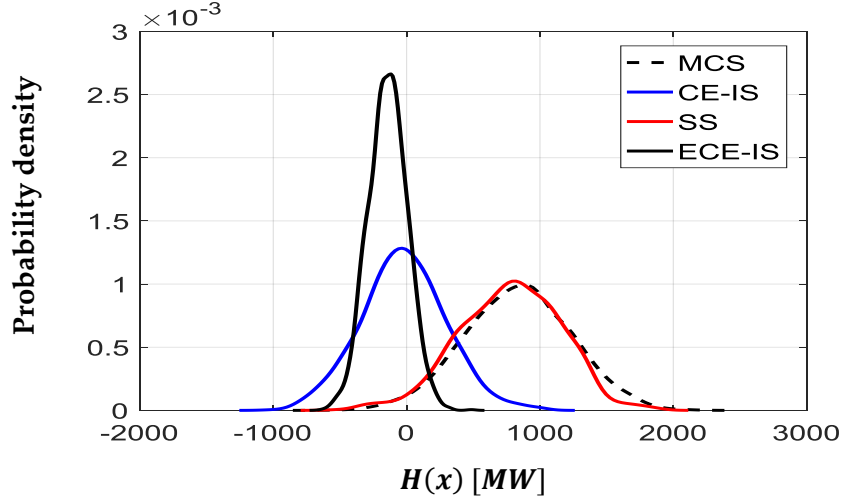
Figure 3.3. Probability density of limit-state function for different techniques.
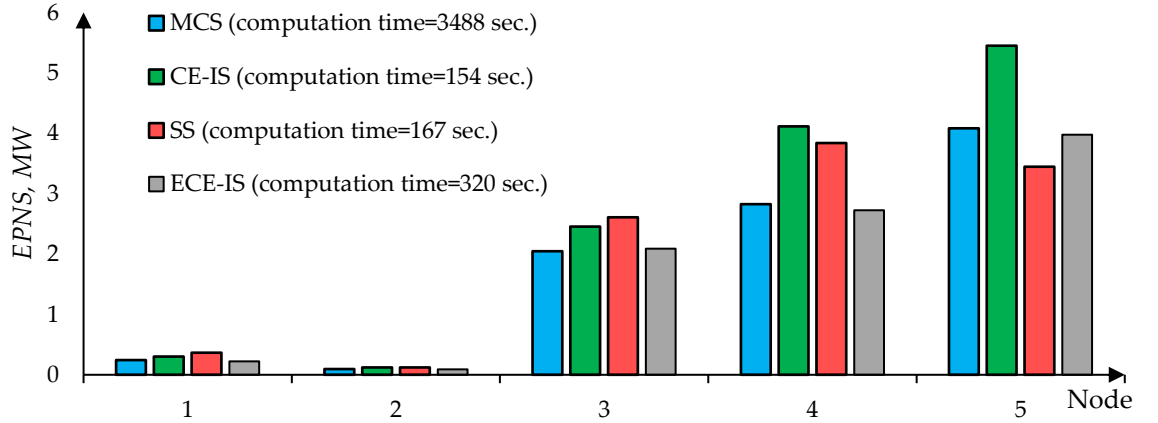

Figure 3.4. Nodal expected power not supplied.

The load curtailment sharing philosophy results in relatively small EPNS values of potentially deficient nodes 4 and 5. At the same time, the limited transmission lines capacity does not allow unlimited power supply from surplus nodes and so the greatest EPNS is at node 5. From the simulation results, it became clear that all the discussed methods significantly reduce a computation burden and the most computationally effective is the CE-IS method. It also could be seen that the method used in extracting load curtailment events could significantly affect results. Figure 3.5 shows the LOLP values for all the nodes of the test scheme. In terms of mean values, the power surplus of the node 1 is 10% higher than the transmission capacity of the connected lines. Possible power supply from node 1 is locked, and as a result, in some deficient test scheme state samples, the demand at the node is not curtailed. It can be seen from the histogram that the LOLP of node 1 is relatively small in comparison to other node values. Figures 3.6 and 3.7 show the errors of methods in comparison to the standard

MCS method. For almost all the nodes, EPNS values computed using the proposed method are accurate within range of 8%. Even though the ECE-IS method is less computationally effective than other methods, it could provide significantly more accurate results. In comparison to the traditionally used MCS approach, the proposed method is nearly eleven times faster. The smallest LOLP error values are generally also represented by the ECE-IS approach. Notice, that in the case of LOLP, even small deviations would introduce a great error, as it can be seen.
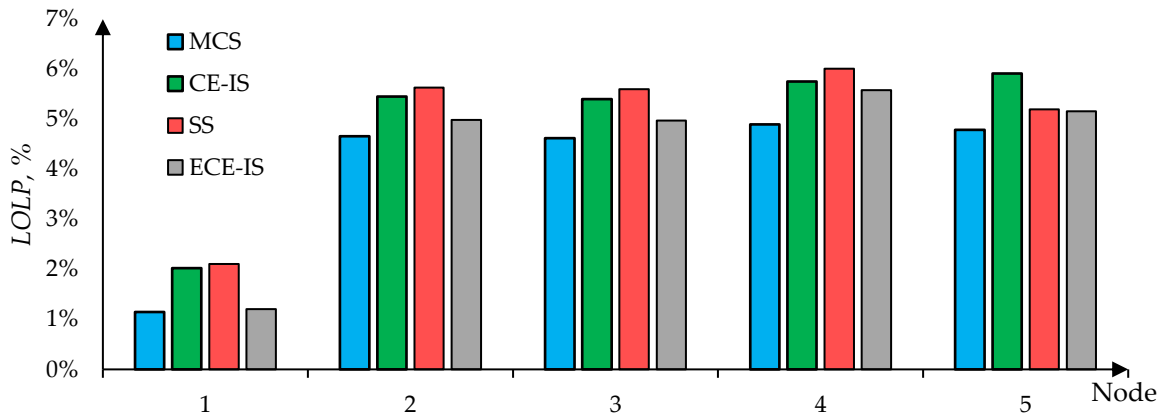

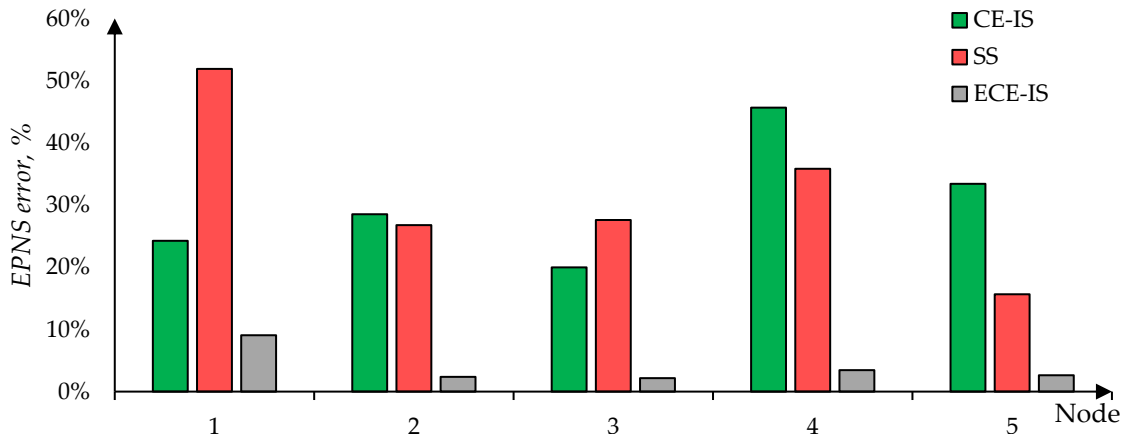Figure 3.5. Nodal loss of load probability (LOLP).

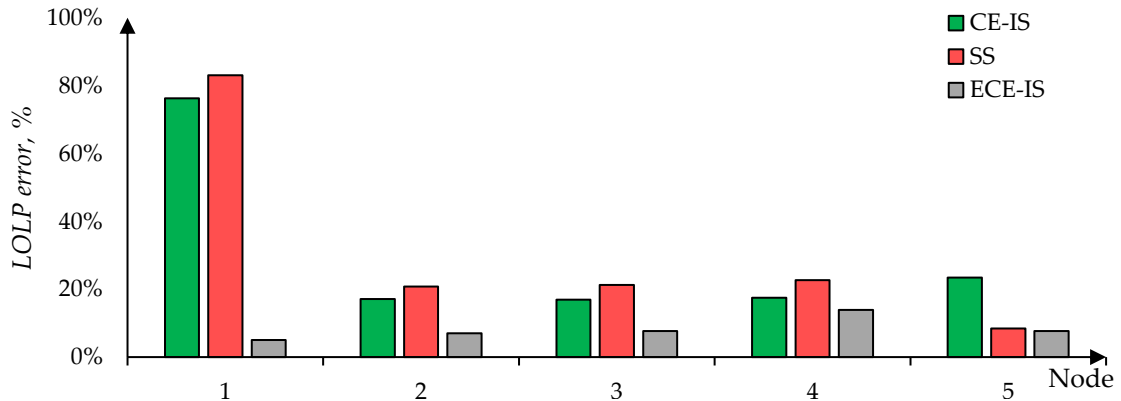Figure 3.6. EPNS error compared to the MCS approach.

Figure 3.7. LOLP error compared to the MCS approach.

3.6.   Discussion

A trade-off between the computational accuracy and computational efficiency leads to a wide number of approaches for a power system adequacy evaluation. Therefore, the comparison among methods must include the number of samples or computation time required to reach the accurate adequacy indices with acceptable convergence. In terms of the number of samples, the system LOLP and EPNS indices and their convergence using the standard MCS method and the different rare events simulation approaches are shown in Figures 3.8–3.11. For MCS, the number of samples to reach a convergence of 5% for both system LOLP and EPNS indices is 38,945 samples. The CE-IS and SS methods have the fastest convergence rate, while they do not develop accurate LOLP values. The ECE-IS has performed better, reaching a 0.0099 LOLP value with 4.7% convergence and 8.95 MW EPNS with 2.4% convergence. On the other hand, the standard MCS has achieved 0.0102 with 5% and 8.8 MW with 2.5% for LOLP and EPNS, respectively. Therefore, the ECE-IS can achieve the same accuracy of the standard MCS method for both nodal indices, as shown in Figures 3.4 and 3.5, and system indices, as shown in Figures 3.8 and 3.10. In the attitude of computational efficiency, the ECE-IS needs seven iterations for extracting 2000 samples representing the load curtailment events, and so, the total number of samples is 14,000 samples. Hence, the ECE-IS can achieve accurate results with a smaller number of samples and computation time. As shown in Figure 3.4, an 11-times speedup is achieved.
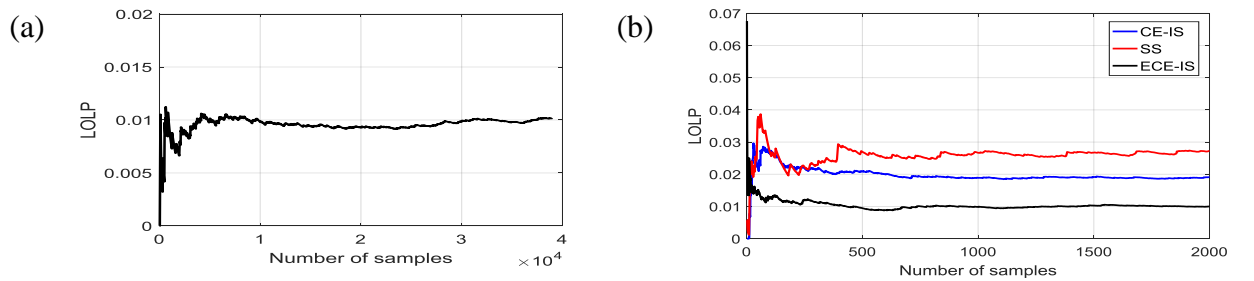

Figure 3.8 (a) System LOLP using the MCS method; (b) system LOLP using CE-IS, SS, and ECE-IS approaches.
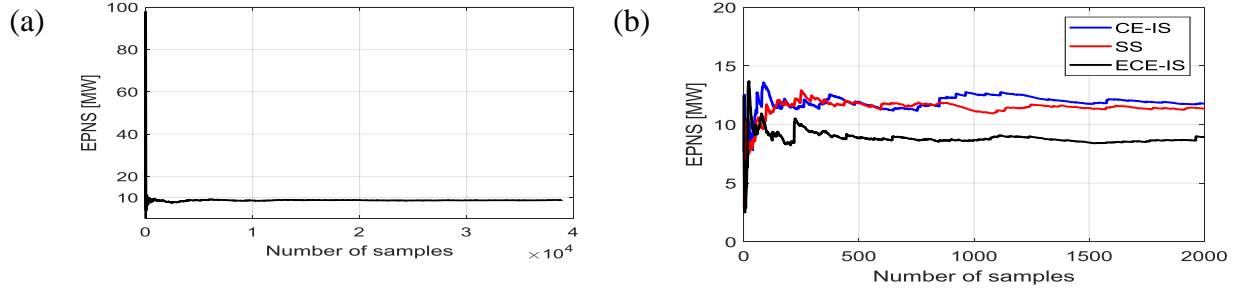
Figure 3.9 (a) System EPNS using standard MCS method; (b) system EPNS using CE-IS, SS, and ECE-IS approaches.
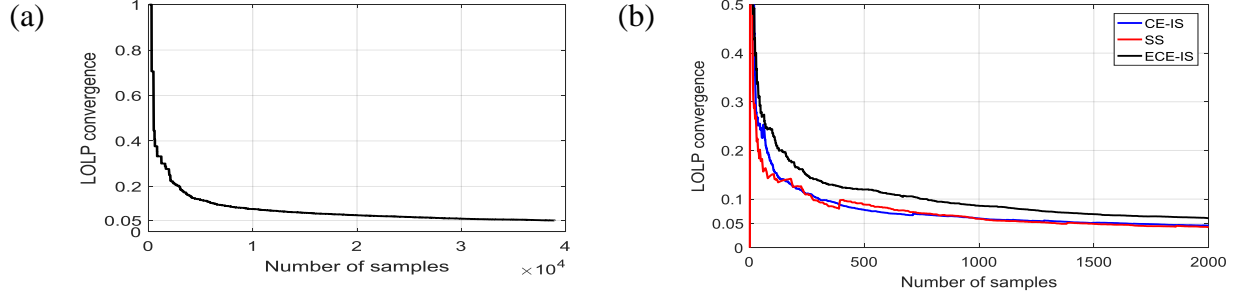
Figure 3.10 (a) System LOLP convergence using the MCS method; (b) system LOLP convergence using the CE-IS, SS, and ECE-IS approaches.
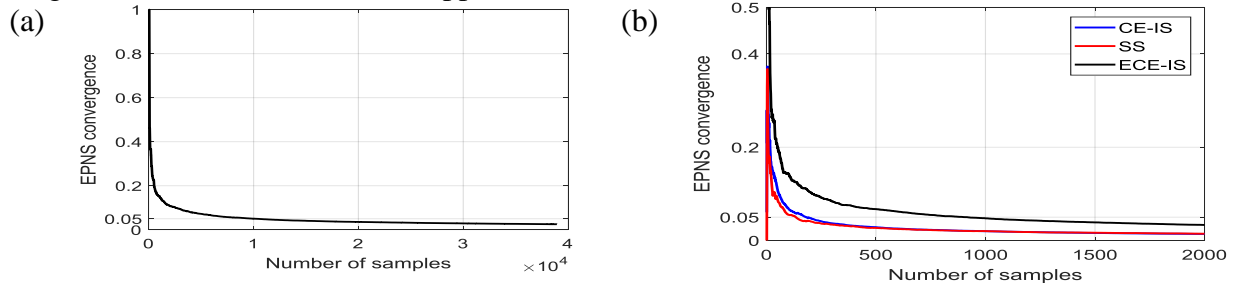
Figure 3.11 (a) System EPNS convergence using the MCS method; (b) system EPNS convergence using the CE-IS, SS, and ECE-IS approaches.

For comparing the robustness of the ECE-IS method with other rare events simulation techniques, the system LOLP, LOLP relative bias, and LOLP convergence values are illustrated in Table 3.1 for different numbers of samples per iteration. The sample analyzing times differ from each other; hence, the computation time is included in Table 3.1. Taken the LOLP value (0.0102) obtained by the standard MCS method as a reference value, the relative bias of LOLP values is computed as follows: $\frac{LOLP - LOLP(MCS)}{LOLP(MCS)}$. From the results in Table 3.1, the convergence acceleration for all methods is achieved by increasing the number of samples. However, there is a significant accuracy loss with a small number of samples for CE-IS and SS methods. However, the ECE-IS is still effective for a small number of samples. It achieves a small LOLP bias (17%) with 21% convergence at 250 number of samples.

Table 3.1- Methods comparison for different numbers of samples.

Number of Samples per Iteration	Methods	Numberof Iterations	System LOLP	Relative Bias of System LOLP	System LOLP Convergence	Time [sec]
250	CE-IS	3	0.0329	2.2	0.35	19
	SS	3	0.0613	5	0.52	21
	ECE-IS	8	0.012	0.17	0.21	43
1000	CE-IS	3	0.0219	1.14	0.055	96
	SS	3	0.041	3	0.064	85
	ECE-IS	8	0.0114	0.12	0.085	140
2000	CE-IS	3	0.0191	0.87	0.049	154
	SS	3	0.0272	1.67	0.048	167
	ECE-IS	7	0.0099	0.03	0.058	304

In order to verify the computation accuracy and efficiency of the proposed method with the dimension of the power network and the number of random variables being considered, the results of adequacy indices are presented for the IEEE-RTS 79 system shown in Figure 3.12. The system includes 24 buses and 32 generators divided among 14 generating stations totalizing 3405 MW of installed capacity. The annual system peak load is 2850 MW. The mean and standard deviation values for the loads were taken at the peak value and the $\pm 10\%$ of the peak value, respectively. A coefficient of variation (convergence) of 5% for both system adequacy indices (LOLP-EPNS) is used as the stopping criterion. For the ECE-IS and MCS methods, Table 3.2 shows the results of the system LOLP and EPNS indices, number of samples, and computation time. The computation time includes the time spent in the first stage for extracting the rare load curtailment events. The results of the ECE-IS method are 0.00121 and 0.16 MW for LOLP and EPNS, respectively. On the other hand, the standard MCS has achieved 0.00119 and 0.154 MW for LOLP and EPNS, respectively. Therefore, the ECE-IS can achieve the same accuracy of the standard MCS method for both system indices. Moreover, the ECE-IS method is considerably more efficient than the standard MCS method. The proposed method needs only a

small fraction (23%) of the samples needed by the MCS. However, in contrast to MCS, the ECE-IS method, as other techniques of rare events simulation, come along with its own set of tuning parameters, which are the target the coefficient of variation of importance weight function and the number of samples per iteration. The proper tuning of these parameters has consequences on the efficiency of the technique.
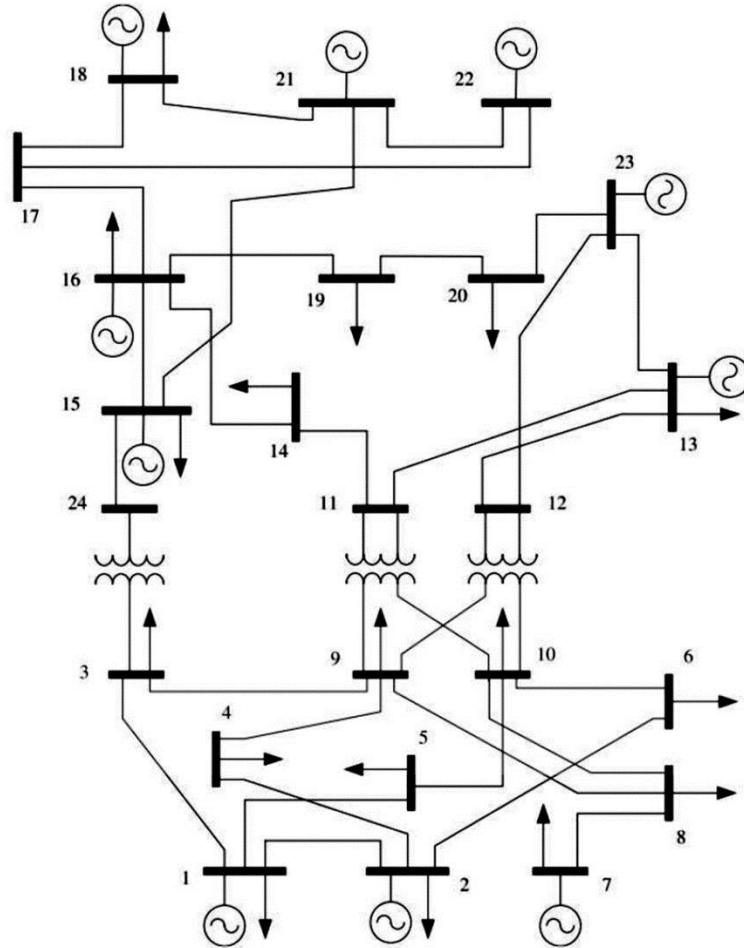
Figure 3.12- IEEE-RTS 79 system

Table 3.2- System adequacy indices for IEEE-RTS 79.

Methods	Number of Samples	System LOLP	System EPNS [MW]	Time [sec]
MCS	382000	0.00119	0.154	6220
ECE-IS	87000	0.00121	0.16	810

Conclusions

A framework of reliabilty indices evaluation has been proposed in composite generation and transmission power systems. The main purpose of the framework is to obtain accurate adequacy indices and enhance the computational efficiency of the standard MCS method. This is achieved by integrating rare events simulation methods

in the framework's first stage for identifying the approximately optimal distortion of the nodal generations and load distributions, making rare load curtailment events more likely to be drawn. As a result of the integration of the rare event simulation methods, a new approach named ECE-IS is proposed that is more efficient and robust than other methods, such as traditional CE-IS and SS in extracting the optimal distortion. From the reported results of the framework's second stage, the proposed method contributes to accurately evaluating the adequacy indices (LOLP-EPNS) and further enhancing the convergence of the indices in comparison with other methods. Moreover, a great speed-up was shown in terms of computation time with respect to the standard MCS method. The implementation of the proposed method in adequacy evaluation could allow us to use more detailed power system models, which would more accurately reflect real power system operation. The impact of different network topologies (i.e., transmission network contingencies) and chronological characteristics of power systems, such as time and spatially correlated load models, the time-dependency of renewable energy resources could be included into the power system model which will be discussed in the next chapter.

Chapter 4 Reliability Evaluation considering the Integration of Renewable Generation

Different approaches are needed to model the renewable power supplies and to evaluate their reliability contribution in power systems since the nature of these units is diverse from conventional units. The uncertainty of loads at the user part together with the uncertainty and stochasticity of renewable powers at the generation part have caused a growing challenge to the evaluation of power system reliability. Normally, demand is low during the night and increases during the day. For this reason, the solar sources display positive correlation with demand due to the natural behavior of solar radiation which is mostly strong during the day. In contrast with solar energy, wind sources offer negative correlation with demand since the wind is strong at night and declines during the daytime. Therefore, it should be noted that the dependence between renewable resources and loads conflicts the independence assumption between demand side and generation side in traditional reliability evaluation [107-108]. From a reliability perspective, there are other issues introduced into the reliability assessment including the PDFs of prime mover (wind speed, solar irradiance, and temperature), the state model of energy conversion system which is responsible for converting the wind or solar energy into electrical energy, and the correlation model among solar irradiances, wind speeds, temperature, and demand in EPSs. Moreover, with the high reliable property of power systems, assessing reliability of the EPS is more difficulty with renewable energy sources. Thus, this chapter aims to address two main issues arising from renewable energy integration, namely, how to accurately model the renewable power and electricity demand, and how to efficiently assess EPS reliability with a large-scale PV power stations and wind farms using the ECE-IS technique proposed in Chapter 3. The ECE-IS can assist IS in sampling the region of interest for the system reliability indicators (i.e., the region in which the wind farms and PV power stations have lower power generation).

Several probabilistic means have been formulated to model the renewable power in reliability assessment. They concentrate on how to represent the correlation

among the random variables. These methods can be categorized into the joint PDF estimation method and correlation matrix method. In the correlation matrix method, the correlation between random variables is defined based on the correlation matrix which is computed through the historical datasets of variables. Using Cholesky decomposition, the correlated samples are defined. This approach has been frequently utilized in literature [109–112] due to its simplicity. However, this approach assumes that the RVs are to follow a normal distribution. Unfortunately, this assumption may not be always satisfied, because wind speed and solar irradiance are not inherently represented by a normal distribution. It is essential to involve the numerous correlations among the RVs represented by any PDFs in the problem of reliability assessment.

To overcome this limitation, the Nataf transformation approach integrated with the correlation matrix method is presented in [113–114] to address the correlated variables following any PDFs. However, this approach is only efficient for linear correlation among RVs not in nonlinear correlation cases. It is identified in many works of literatures that there is a nonlinear correlation among weather and load RVs.

Recently, nonparametric, semi-parametric, and copula PDF estimations have been presented [115-121]. Copula can model the multivariate PDF by the univariate distributions and a copula function defining the dependence structure [115-117]. Selecting the most well-suited bivariate copula functions between each two random variables is the prime difficulty, especially when the dependence structure is very complicated. To handle this problem, semi-parametric or nonparametric estimation are used. The nonparametric KDE is employed to estimate according to the data the univariate PDF of wind speed [118–119] and the joint PDF of bus loads [120–121]. A semi-parametric GMM is proposed to define the multivariate distribution for wind speeds and loads [122-124]. Despite the estimation using semi-parametric or nonparametric model are effective, they need enough sample data to achieve an acceptable estimation. In addition, the approximation complexity also raises greatly with the increase of dimension [125].

Some studies [126-131] use CE-IS to conduct IS on load and renewable power RVs. In [126], a modified CE-IS method is proposed to model wind energy in the reliability evaluation procedure. The wind power generation of one wind farm was represented as multi-state model [127-129]. However, the correlation is not considered. The references [130-131] uses copula function to define the dependence between two wind power generations and utilize Weibull PDF to represent the distribution of each wind power generation. Then the CE-IS is employed to obtain the optimal ISD for each Weibull PDF without change the copula function to preserve the dependence structure. However, the dependence between wind power and loads are not considered.

All the methods in [126-131] have similar is that they employ unimodal PDFs e.g., Beta, Weibull, and Gaussian, which are not appropriate to model the sophisticated probabilistic features of load and renewable powers. Moreover, a single distribution assumption for a weather random variable may not be realistic. For example, the distribution of wind speeds at different locations may follow various types of PDFs according to their wind speed data. Second, the correlation between loads and weather random variables and the state model of energy conversion systems are ignored. It has been extensively expressed in many works of literature that the random variation of renewable powers and bus loads may show complicated dependence rather than independence or linear dependence. Therefore, the multimodal PDFs of continuous variables (wind speed, solar irradiance, temperature, and electricity demand) with complicated correlation among them based on the real data should be considered using mixture of distributions such as GMM. The actual weather and electricity demand data observed in a city located in Egypt is adopted for the uncertainty modeling of renewable and load powers. In order to estimate the annual reliability indicators efficiently and accurately of composite power system with renewable energy integrated, the ECE-IS method proposed in Chapter 3 can carry out IS on the obtained MGMM and find the IS-PDF parameters for it. Moreover, the availability state model of wind farms, PV power stations, and transmission lines are considered. The computational efficiency and adaptability of the proposed method

are validated by the results of case studies. ECE-IS preserves the dependence structure of and renewable and load powers in the reliability evaluation procedure, thus the efficiency degradation is avoided. This assures that the reliability indices are estimated with a reasonable computation burden.

4.1. Modelling of renewable power generation units

The power output of a renewable power generating units depends on two factors [107]:

- The uncertainty and variability of prime mover (wind speed- solar radiation-temperature) employed in generating the electrical power.
- The state of the wind or solar energy converter into electrical energy.

4.1.1. Wind Energy Conversion System

The role of wind energy conversion system (WECS) is to transform the wind energy into electrical energy. The model of a WECS involves three factors that affect the generation output:

- The random variation of the wind speed. It is characterized by a probabilistic model at the site being considered.
- The relation between the wind speed and WTG power output. It can be defined using the design specification of the tower and the operational factors of the WTG under the study.
- The repair and failure characteristics of the WTG. A two-state model for WTGs consists of operation and failure states is considered here.

The operation characteristics of a WTG are not the same as those of conventional generators. The generating power of a WTG is dependent on the wind speed regime which is based on the design specification of the wind turbine [132-133]. There are three wind speed values that determine the WTG power output. The WTG begin generating a power at the cut-in speed and reaching its rated power at the rated speed. The maximum speed at which the WTG will disconnect because of safety issues of wind tower and turbine is called the cut-out speed. The WTG power output $P_W(v_w)$ can be calculated as follows:

$$P_W(v_w) = \begin{cases} P_{w,rated}, & v_{w,rated} \le v_w < v_{co} \\ \dfrac{P_{w,rated}(v_w - v_{ci})}{(v_{w,rated} - v_{ci})}, & v_{ci} \le v_w < v_{w,rated} \\ 0, & otherwise \end{cases} \qquad (4.1)$$

where $P_{w,rated}$ is the rated power of wind generator and v_{ci}, $v_{w,rated}$, and v_{co} are the cut-in, the rated, and the cut-out speeds, respectively.

Given the input wind speed and WTG parameters, the WTG power output can be calculated. While the actual power output of the WTG can be defined by the WTG state. The power output is equal to zero when the WTG is in a failure state. While in operation state, the power output is set to the $P_W(v_w)$.

4.1.2. Solar Energy Conversion System

The role of solar energy conversion system is to transform solar energy into electricity. Three factors that impact the electrical power output are as follows:

- The statistical characteristic of the solar irradiance reached to the Photovoltaic (PV) cell or panel and ambient air temperature

- The number of panels connected in PV array and the electric characteristic of PV panel i.e. the relation between the power output of the PV panel and the solar irradiance and temperature.

- The failure and repair characteristic of the PV array. A two-state transition model consists of operation and failure states is considered here.

For a PV arrays comprising a large number of PV panels, the power output is the summation of the individual output of all the PV panels. The power of the PV array at maximum power point (MPP) at s_{PV} solar irradiance and T_{PV} ambient air temperature is expressed by (4.2) [134-135].

$$P_{PV}(s_{PV}, T_{PV}) = P_p(s_{STC}, T_{STC}) \frac{s_{PV}}{s_{STC}} \left(1 - \tau(T_c - T_{STC})\right) N_p N_s \qquad (4.2)$$

where $P_p(s_{STC}, T_{STC})$ is the power output of PV panel at standard test condition (STC) ($s_{STC} = 1000 \text{ W}/m^2$, $T_{STC} = 25°C$), τ is the temperature coefficient of the cell and equal to $0.04\%/°C$, and N_p, N_s are the number of panels connected in parallel and series in a PV array. T_c is the cell temperature and calculated as follows: $T_c = T_{PV} +$

$\frac{s_{PV}}{s_{NOCT}}(T_{c.NOCT} - T_{amb.NOCT})$. The nominal operating cell temperature (NOCT) measurements are ($s_{NOCT} = 800 \text{ W}/m^2$, $T_{amb.Noct} = 20°C$, $T_{c.NOCT} = 45.5°C$).

4.2. Stochastic Multivariate Dependence Modelling

To incorporate renewable energy resources in composite system reliability evaluation using simulation techniques, the first step is to construct a probabilistic model that can precisely reflect all the stochastic features, which can be followingly utilized for generating the samples. The generated samples from the probability models of the solar irradiance, wind speeds, temperature, and node/aggregated loads should be compatible with the original observations. To investigate the modeling framework, a numerical study is essential. This section presents the real data of El Gouna city located in Egypt, with latitude of 27.4025° N, and longitude of 33.6511° E. Weather data (wind speed, solar irradiance, temperature) and aggregated city demand hourly data over 2019 year is employed in this study. The datasets are based on the "Renewables. ninja" tool [136]. This tool is developed to present the weather data at any place across the globe for use in both industrial and academic settings. The techniques behind the tool are discussed in [137-138]. Figure 4.1 show the annual hourly historical data for the normalized demand and wind speed as examples. The demand power is normalized with respect to the peak value. To illustrate the bivariate data characteristics, the bivariate scatter diagrams of stochastic variables are shown in Figure 4.2. which demonstrate that the stochastic variables have highly complex and non-linear dependencies.

Three means are employed to execute the probabilistic modelling: 1) Parametric modelling (Distribution fitting approach); 2) non-parametric modelling; 3) semi-parametric modelling. The parametric modelling is based on selecting a standard PDF and then changing its parameters to accord the datasets. While, nonparametric modelling techniques such as kernel density estimation (KDE) do not depend on any standard PDFs. The model is formulated directly from the data. Finally, semi-parametric modelling includes assembling a model that has both non-parametric and parametric components. A semi-parametric probabilistic model entitled Gaussian
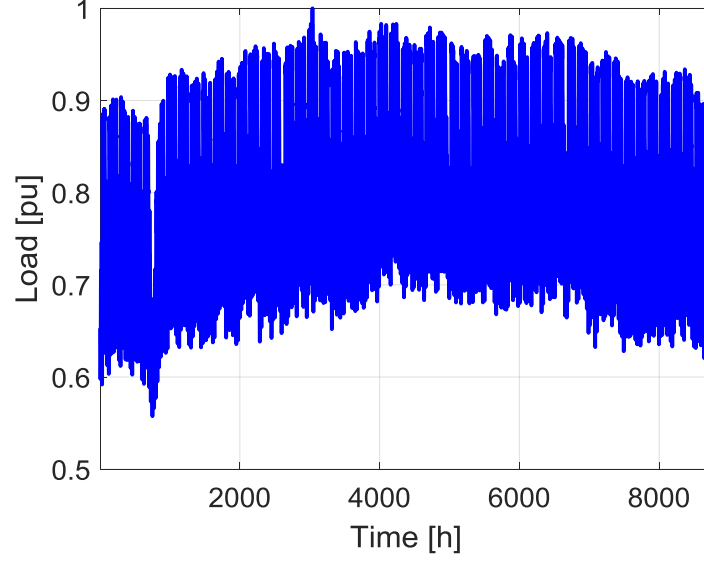
(a)
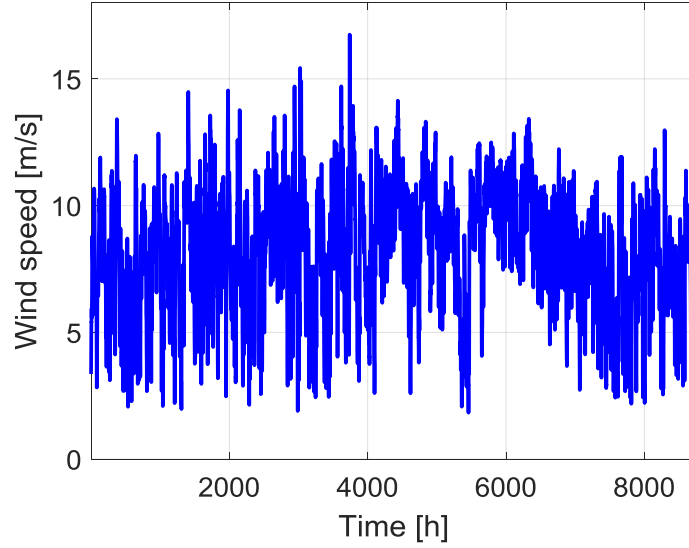
(b)

Figure 4.1. Annual hourly historical data for (a) demand; (b) wind speed.

mixture model (GMM) can represent arbitrarily complex PDFs with great flexibility. GMM is a mixture-based Gaussian clustering. It estimates the PDF by a number of Gaussian distributions having different weights. The number of components is detected by Akaike information criterion (AIC). The mean and variance parameters of each component are estimated using the Expectation-Maximum (EM) optimization or maximum likelihood estimation approach. The PDF of univariate random variable $x = \{x_i, i = 1, \dots, N\}$, where N is the number of observations can be represented by GMM as follows:

$$\mathcal{M}(x) = \sum_{c \in C} \pi_c \, \mathcal{N}(x_c; \mu_c, \sigma_c^2) \tag{4.1}$$

where π_c is the weight of component c providing that $\sum_{c \in C} \pi_c = 1$ and C is the set of components. $\mathcal{N}(x_c; \mu_c, \sigma_c^2)$ is a Normal distribution of component c in which the samples $x_c = \{x_i^c, i = 1, \dots, N\}$ belong. It can be written as follows:

$$\mathcal{N}(x_c, \mu_c, \sigma_c^2) = \frac{1}{\sqrt{\sigma_c^2 2\pi}} \, e^{\left(-\frac{(x_c - \mu_c)^2}{2\sigma_c^2}\right)}$$
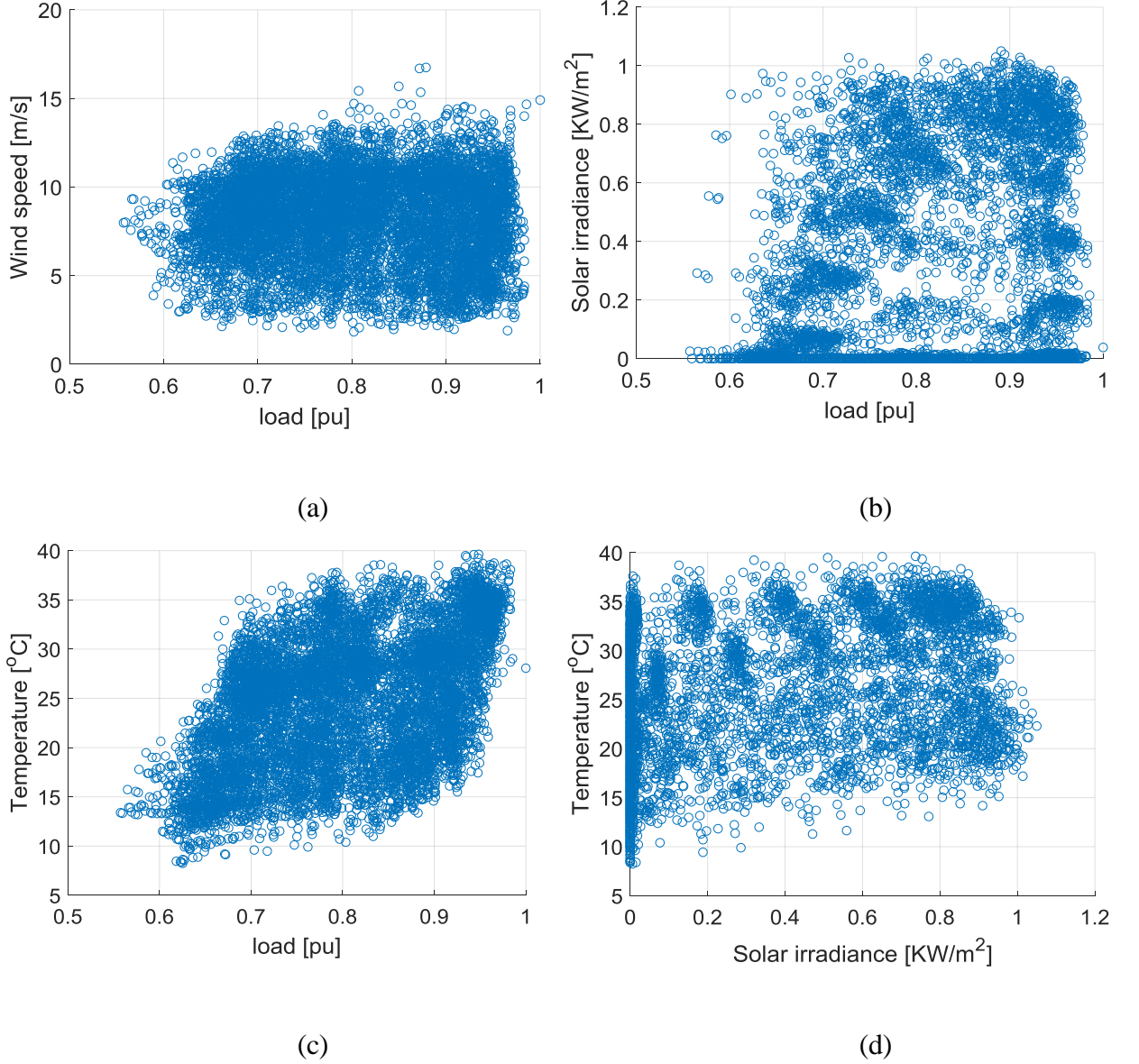
Figure 4.2. Bivariate scatter plots of historical datasets for (a) load and wind speed; (b) load and solar irradiance (c) load and temperature; (d) solar irradiance and temperature.

Fitting the historical data by different approaches: parametric, semi parametric, nonparametric is presented in Figure 4.3. We show frequency histogram (based on the original datasets) and fitted PDFs (corresponding to standard distributions, KDE, and

GMM having 5 components) of the wind speed and load. The normal and Weibull distributions are amongst the most common distribution to represent the distribution of load and wind speed in literature, respectively. Figure 4.3 shows that the normal and Weibull PDFs do not accurately represent the load and wind speed data. As it proved, the data is fitted better by the KDE and GMM distributions and doesn't follow any standard distributions.
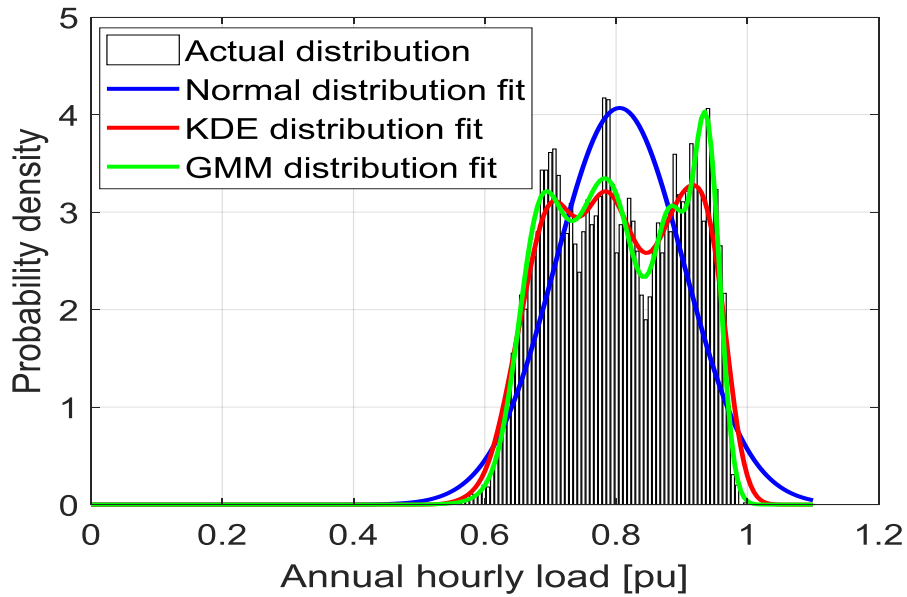
(a)
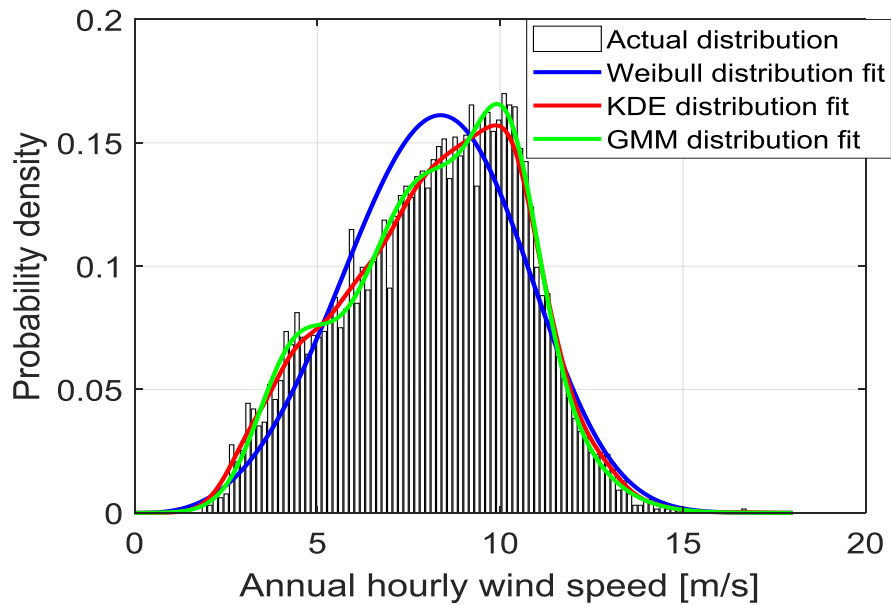
(b)

Figure 4.3. Fitting the histogram of historical data by different approaches for (a) load and (b) wind speed.

The next step is to illustrate how to model the joint PDF which involves together data on the individual PDF of stochastic inputs and on the mutual interaction between the stochastic inputs. Achieving the proper joint PDF given the univariate distributions is a complex, because there exist many joint PDFs with the same univariate distributions, following several number of correlation structures between the RVs. To obtain the multivariate joint PDF of $x = \{x_{i,j}, i = 1, .., N; j = 1, ..., n; \}$, where n is the number of correlated variables, the MGMM can be used which is expressed as follows:

$$\mathcal{M}(x) = \sum_{c \in C} \pi_c \, \mathcal{N}(x_c; \mu_c, \Sigma_c) \tag{4.2}$$

where $\mathcal{N}(x_c; \mu_c, \Sigma_c)$ is a multivariate dependent Normal distribution of component c including/involving the observations $x_c = \{x_{i,j}^c\}$.

$$\mathcal{N}(x_c, \mu_c, \Sigma_c) = \frac{1}{\sqrt{|\Sigma_c|(2\pi)^n}} \, e^{\left(-\frac{(x_c - \mu_c)\Sigma_c^{-1}(x_c - \mu_c)^T}{2}\right)}$$

The other approach for dependence modelling of stochastic variables is the method of combined univariate PDFs and the correlation matrix. It is based on two tasks: the univariate distributions modeling and the definition of correlation matrix between the random variables. To identify the dependence between pair of probability distributions, a transformation between non-normal and normal domains is required. This is carried out using the Nataf transformation technique [113-114] needing the CDF for each variable and the correlation factors between variables which is expressed by the product moment correlation. The product moment correlation is calculated from the time-series data. The variable CDF is conducted by univariate GMM and is then utilized with correlation matrix to generate correlated samples for variables. After formulating the correlation matrix in the standard normal domain, the correlated samples are generated in the standard normal domain and then are transferred to the original domain by the inverse of Nataf transformation. The Nataf transformation method and its inverse is employed to transform between the non-normal PDF variables $X = \{X_j, j = 1, ..., n\}$, where n is the number of correlated

variables and the standard normal distribution variables $Y = \{Y_j, j = 1, ..., n\}$ as follows:

$$Y = \{\Phi^{-1}[F_{X_1}(X_1)], ..., \Phi^{-1}[F_{X_n}(X_n)]\}$$
$$X = \{F_{X_1}^{-1}[\Phi(Y_1)], ..., F_{X_n}^{-1}[\Phi(Y_n)]\} \tag{4.3}$$

where Φ^{-1} is the inverse standard normal CDF and F_{X_j} is the CDF of the variable X_j. The correlated samples in the standard normal distribution is generated and returned to the original domain as shown in Figure 4.4.

To formulate the correlation matrix in the standard normal domain, there is a need to transform the correlation factor from the original field $\rho_X(X_i, X_{\acute{j}})$ to standard normal $\rho_Y(Y_i, Y_{\acute{j}})$. The $\rho_X(X_i, X_{\acute{j}})$ can be expressed as follows:

$$\rho_X(X_i, X_{\acute{j}}) = (\mathbb{E}[X_i X_{\acute{j}}] - \mu_{X_i}\mu_{X_{\acute{j}}})/\sigma_{X_i}\sigma_{X_{\acute{j}}},$$

$$\mathbb{E}[X_i X_{\acute{j}}] = \mathbb{E}[F_{X_i}^{-1}[\Phi(Y_i)]\, F_{X_{\acute{j}}}^{-1}[\Phi(Y_{\acute{j}})]] = \int_{-\infty}^{\infty}\int_{-\infty}^{\infty} F_{X_i}^{-1}[\Phi(Y_i)]\, F_{X_{\acute{j}}}^{-1}[\Phi(Y_{\acute{j}})]\, \varphi(Y_i, Y_{\acute{j}})dY_i dY_{\acute{j}}$$

The bivariate standard normal distribution of $Y = \{Y_i, Y_{\acute{j}}\}$ can be expressed as:

$$\varphi(Y_i, Y_{\acute{j}}) = \frac{1}{2\pi\sqrt{(1-\rho_Y^2)}}\, e^{-\frac{Y_i^2 - 2\rho_Y Y_i Y_{\acute{j}} + Y_{\acute{j}}^2}{2(1-\rho_Y^2)}}$$

Thus,

$$\rho_X(X_i, X_{\acute{j}}) = (\int_{-\infty}^{\infty}\int_{-\infty}^{\infty} \frac{F_{X_i}^{-1}[\Phi(Y_i)]\, F_{X_{\acute{j}}}^{-1}[\Phi(Y_{\acute{j}})]\, e^{-\frac{Y_i^2 - 2\rho_Y Y_i Y_{\acute{j}} + Y_{\acute{j}}^2}{2(1-\rho_Y^2)}}}{2\pi\sqrt{(1-\rho_Y^2)}} dY_i dY_{\acute{j}} \tag{4.4}$$
$$- \mu_{X_i}\mu_{X_{\acute{j}}})/\sigma_{X_i}\sigma_{X_{\acute{j}}}$$

It can be observed from (4.4) that the correlation coefficient ρ_X is a complex nonlinear function of the correlation coefficient ρ_Y. In order to calculate ρ_Y, a numerical search algorithm proposed in [113] is utilized to obtain the solution at any acceptable accuracy.

To illustrate the effectiveness of correlated samples generation, a comparison is made among the original datasets, uncorrelated samples, and correlated samples generated by the two approaches. The first approach is MGMM and the other (GMM ρ) is the method of combined univariate GMM and the correlation matrix in which the PDF of each variable is represented by GMM and is then employed with

the correlation matrix shown in Table 4.1 to generate the correlated samples. The correlation matrix includes all correlation factors between each pair of the solar irradiance, wind speed, temperature, and load. To generate the uncorrelated samples, the GMM is used to fit the PDF of each variable and is then used to generate samples from each PDF independently. Figure 4.5 shows the bivariate histogram of load and temperature as an example, for the original datasets, uncorrelated samples, and correlated samples by MGMM and GMM ρ. The joint probability distribution of the load and temperature obtained using the model of MGMM is compatible with those constructed from the original observations. The MGMM model is more effective than GMM ρ model even when the linear correlation between random variables exists. Thus, the chosen model is MGMM because of its principle approach of representing the distribution feature of the original joint PDF.
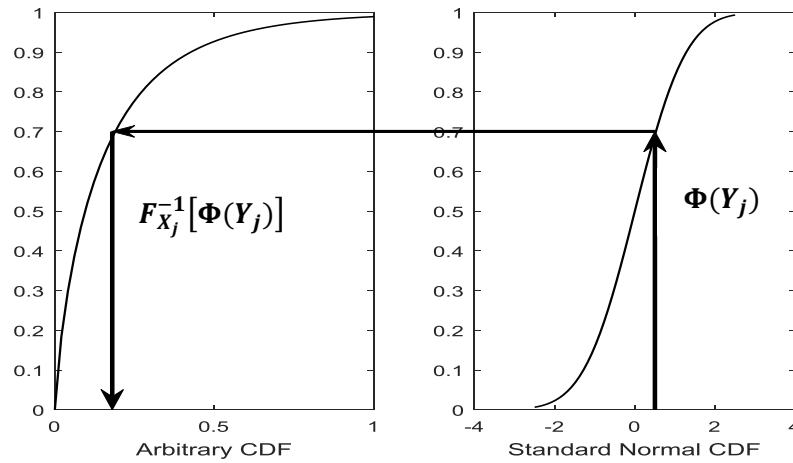
Figure 4.4. Transformation process of random values from standard normal distribution to the original arbitrary distribution.

Table 4.1- Correlation matrix

	Load	Wind speed	Solar irradiance	Temperature
Load	1	-0.0211	0.2126	0.4928
Wind speed	-0.0211	1	-0.2366	0.0328
Solar irradiance	0.2126	-0.2366	1	0.2511
Temperature	0.4928	0.0328	0.2511	1
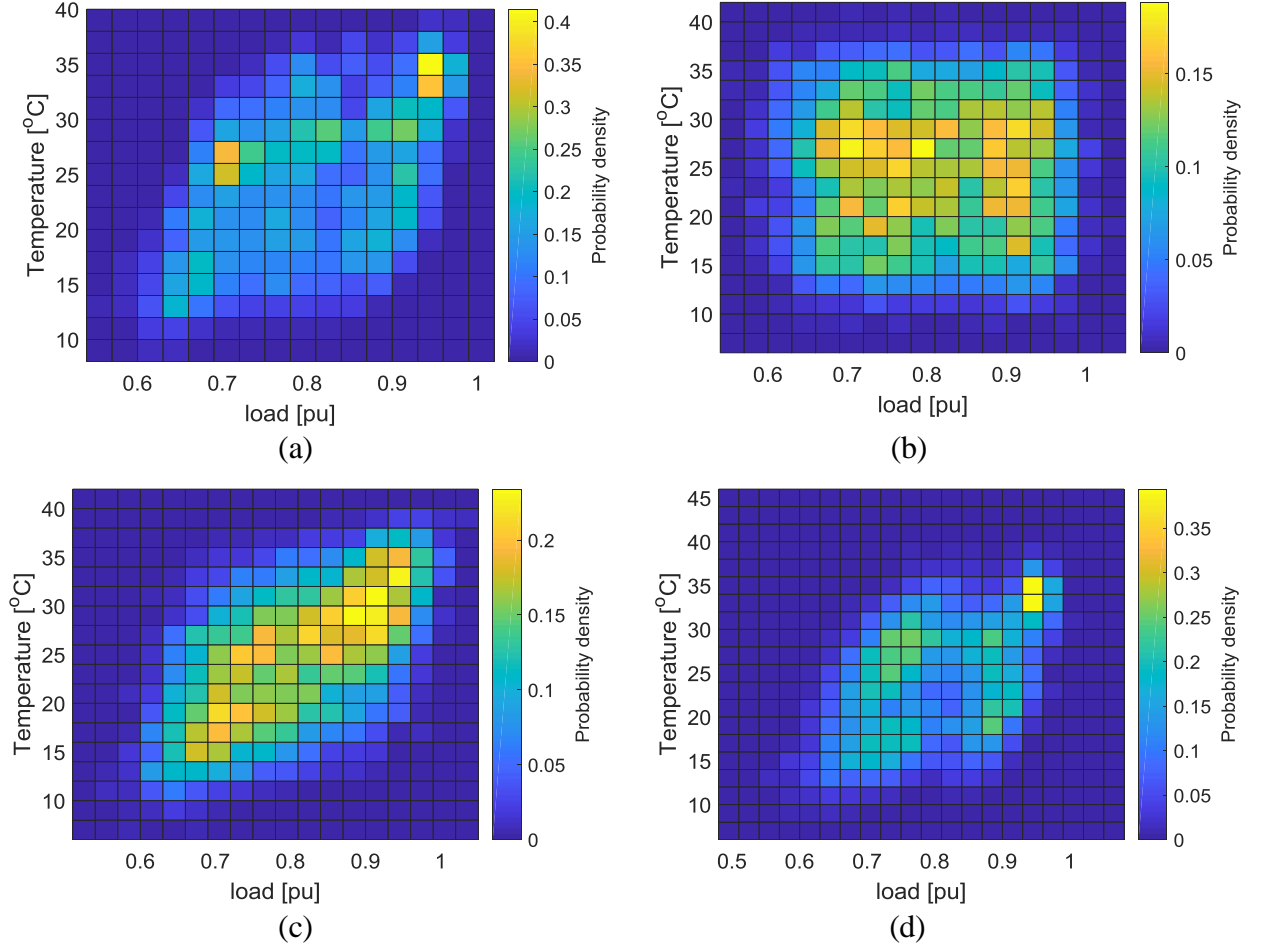
Figure 4.5. Bivariate histogram (Joint PDFs) of load and temperature for (a) original datasets; (b) uncorrelated samples using univariate GMMs; (c) correlated samples generated using GMM ρ; (d) correlated samples generated using MGMM.

4.3. Implementation of ECE-IS Method considering renewable generators

In previous chapter, The ECE-IS Method is employed to perform IS on the independent continuous variables which are the nodal available generations and required loads. The ECE-IS Method here is extended to carry out IS on dependent continuous variables and discrete variables. The random variables depicting the transmission lines states follow Bernoulli distribution having 1 or 0 denoting operation state and failure state respectively. In addition, a multivariate joint distribution (MGMM) is to represent the load, wind speed, solar irradiance, and temperature variables. Moreover, the state model of WTGs and PV arrays are considered.

A wind farm usually consists of many WTGs and therefore it is difficult to regard every WTG as an individual random variable which lead to a huge solution space of the optimal ISDs. Since the power output of a wind farm is the summation

of the output of all the available generators, we combine the 2-state models of WTGs to obtain the available state of wind farm (S_w^{av}). It is supposed that the specified wind velocity is the same for all the WTGs in the farm and WTGs are homogeneous units. For a large number of WTGs, according to the de Moivre–Laplace theorem, the available state of wind farm could be approximated by a truncated normal distribution (TND) as discussed in 1.3. Thus, based on the available state of wind farm S_w^{av}, the available power of wind farm is calculated as follows: $G_w^{av} = S_w^{av} * (P_W(v_w))$.

For a PV power station comprising a large number of PV arrays, the power output of station is the summation of the output of all the available PV arrays. As wind farm, we combine the 2-state models of PV arrays to obtain the available state of PV power station (S_{PV}^{av}). The specified solar irradiance and temperature is assumed to be the same for all the PV panels in the station and PV arrays are homogeneous units. Thus, the available state of PV station could be approximated by a TND. Based on the available state of PV station S_{PV}^{av}, the available power of PV station is computed as follows: $G_{PV}^{av} = S_{PV}^{av} * (P_{PV}(s_{PV}, T_{PV}))$.

To carry out the first stage aim (Estimation of the ISD optimal parameters), the occurrence of load curtailment is verified at each sampled state of the uncertain inputs $\{x_i, i = 1, \dots, N\}$, where

$x_i = \{G_d^{av}, S_l, L, v_w, s_{PV}, T_{PV}, S_{w.d}^{av}, S_{PV.d}^{av}\} \ \forall d \in D, l \in NT$

N is the number of samples,

L is the system power demand,

S_l is the state of transmission line l,

D is the set of nodes,

NT is the set of transmission lines,

v_w is the wind speed,

s_{PV} is the solar irradiance,

T_{PV} is the temperature,

$S_{w.d}^{av}$ is the available state of wind power station at node d, and

$S_{PV.d}^{av}$ is the available state of PV power station at node d.

The constraint of nodal power balance illustrated in chapter 2 are modified as follows:

$$P_d + G_d + G_{w.d} + G_{PV.d} + PNS_d - L_d = 0 \ \forall \ d \in D \tag{4.6}$$

The wind and solar powers constraints are added as follow:

$$0 \leq G_{w.d} \leq G_{w.d}^{av}, \ 0 \leq G_{PV.d} \leq G_{PV.d}^{av},$$

where $G_{w.d}^{av} = S_{w.d}^{av} * (P_W(v_w))$ and $G_{PV.d}^{av} = S_{PV.d}^{av} * (P_{PV}(s_{PV}, T_{PV}))$

The random variables $x_{i;U} = \{G_d^{av}, S_{w.d}^{av}, S_{PV.d}^{av}, \forall \ d \in D\}$ are expressed by individual continuous normal PDFs. To decrease the complexity of the optimal parameters computation, the independent normal distributions are expressed by a multivariate independent normal distribution $\mathcal{N}(x_{i;U}; u)$ as illustrated in 3.3, which is depicted by mean μ and diagonal covariance Σ vectors, and so the parameter $u = [\mu; \Sigma]$. The random variables $x_{i,l} = S_{i,l}, \forall \ l \in NT$ are expressed by individual discrete Bernoulli PDFs $\mathcal{B}r(x_{i,l}; q_l)$, where q_l is the FOR of line l. While the dependent variables $x_{i;E} = \{L, v_w, s_{PV}, T_{PV}\}$ are expressed as multivariate joint PDF (MGMM) $\mathcal{M}(x_{i;E}; e)$, $e = [\pi_c; \mu_c; \Sigma_c, \forall c \in C]$ to consider the correlation among variables. Therefore, the sample weight can be written by the next formula:

$$W(x_i; u^{IS}, q^{IS}, e^{IS}) := W(x_{i;U}, u^{IS}) * \prod_{l=1}^{NT} W(x_{i,l}, q_l^{IS}) * W(x_{i;E}, e^{IS})$$

$$W(x_i; u^{IS}, q^{IS}, e^{IS}) := \frac{\mathcal{N}(x_{i;U}; u)}{\mathcal{N}(x_{i;U}; u^{IS})} * \prod_{l=1}^{NT} \frac{\mathcal{B}r(x_{i,l}; q_l)}{\mathcal{B}r(x_{i,l}; q_l^{IS})} * \frac{\mathcal{M}(x_{i;E}; e)}{\mathcal{M}(x_{i;E}; e^{IS})} \tag{4.7}$$

where $x_i = \{x_{i;U}, x_{i;E}, \{x_{i,l}, \forall \ l \in NT\}\}$, $\mathcal{B}r(x_{i,l}; q_l) = (q_l)^{1-x_{i,l}}(1-q_l)^{x_{i,l}} \forall \ l \in NT$, and $u^{IS}, q^{IS} = [q_l^{IS}, \forall \ l \in NT]$, and e^{IS} are the optimal parameters of ISDs for the different distributions.

By substituting the distributions into the equation (3.11), the optimization problem becomes

$$\underset{u_k^{IS}, e_k^{IS}, o_k^{IS}}{\text{argmax}} \left[\frac{1}{N} \sum_{i=1}^{N} I_{F_k}(x_i) \, W_k(x_i; u_{k-1}^{IS}, q_{k-1}^{IS}, e_{k-1}^{IS}) \ln(\mathcal{N}(x_{i;U}; u_k^{IS}) \mathcal{M}(x_{i;E}; e_k^{IS}) \prod_{l=1}^{NT} \mathcal{B}r(x_{i,l}; q_{l_k}^{IS})) \right]$$

$$\tag{4.8}$$

in which $I_{F_k}(x_i) := \Phi\left(-\frac{H(x_i)}{\delta_k}\right)$,

$$W_k(x_i; u_{k-1}^{IS}, q_{k-1}^{IS}, e_{k-1}^{IS}) := W_k(x_i) := \frac{\mathcal{N}(x_{i;U}; u)}{\mathcal{N}(x_{i;U}; u_{k-1}^{IS})} \frac{\mathcal{M}(x_{i;E}; e)}{\mathcal{M}(x_{i;E}; e_{k-1}^{IS})} \prod_{l=1}^{NT} \frac{\mathcal{B}r(x_{i,l}; q_l)}{\mathcal{B}r(x_{i,l}; q_{l_{k-1}}^{IS})}.$$

The parameters of optimal ISD for each distribution are estimated as follows.

Multivariate independent normal distribution $\mathcal{N}\left(x_{i;U}; u^{IS}\right)$: In order to obtain u_k^{IS}, the optimization problem is solved by executing the gradient of the function relating to the u_k^{IS} and equaling it to zero.

$$\frac{1}{N}\sum_{i=1}^{N} I_{F_k}(x_i)\, W_k(x_i) \nabla_{u_k^{IS}} \ln(\mathcal{N}\left(x_{i;U}; u_k^{IS}\right)) = 0$$

The derivative at step k with respect to the parameters of $u_k^{IS} = \left[\mu_k^{IS}, \Sigma_k^{IS}\right]$, which are μ_k^{IS} and Σ_k^{IS}, are:

$$\frac{1}{N}\sum_{i=1}^{N} I_{F_k}(x_i)\, W_k(x_i)(x_{i;U} - \mu_k^{IS}) = 0$$

$$\frac{1}{N}\sum_{i=1}^{N} I_{F_k}(x_i)\, W_k(x_i) \frac{1}{2}((\Sigma_k^{IS})^{-2}(x_{i;U} - \mu_k^{IS})(x_{i;U} - \mu_k^{IS})^{T} - (\Sigma_k^{IS})^{-1}) = 0 \tag{4.8}$$

The optimal parameters at step k are derived as follows:

$$\mu_k^{IS} = \frac{\sum_{i=1}^{N} I_{F_k}(x_i)\, W_k(x_i) x_{i;U}}{\sum_{i=1}^{N} I_{F_k}(x_i)\, W_k(x_i)}$$

$$\Sigma_k^{IS} = \frac{\sum_{i=1}^{N} I_{F_k}(x_i)\, W_k(x_i)(x_{i;U} - \mu_k^{IS})(x_{i;U} - \mu_k^{IS})^{T}}{\sum_{i=1}^{N} I_{F_k}(x_i)\, W_k(x_i)} \tag{4.9}$$

Bernoulli distributions $\mathcal{B}r\left(x_{i,l}; q_l^{IS}\right)$: In order to obtain $q_{l_k}^{IS}$, the optimization function is solved by executing the gradient of the function relating to $q_{l_k}^{IS}$ and equaling it to zero. The optimal failure probability of transmission line l at step k is derived as

$$q_{l_k}^{IS} = 1 - \frac{\sum_{i=1}^{N} I_{F_k}(x_i)\, W_k(x_i)\, x_{i,l}}{\sum_{i=1}^{N} I_{F_k}(x_i)\, W_k(x_i)} \qquad \forall\, l \in NT \tag{4.10}$$

Multivariate joint PDF $\mathcal{M}\left(x_{i;E}; e^{IS}\right)$: The multivariate joint ISD can be written as follows as an original MGMM:

$$\mathcal{M}\left(x_{i;E}; e^{IS}\right) = \sum_{c=1}^{C} \pi_c^{IS}\, \mathcal{N}(x_{i;E}, \mu_c^{IS}; \Sigma_c^{IS})$$

In order to obtain e_k^{IS}, the optimization problem is solved by executing the gradient of the optimization function relating to e_k^{IS} and equaling it to zero:

$$\frac{1}{N}\sum_{i=1}^{N} I_{F_k}(x_i)\, W_k(x_i)\, \nabla_{e_k^{IS}} \ln(\mathcal{M}\left(x_{i;E}; e_k^{IS}\right)) = 0$$

The problem in case of MGMM is considered as a number of multivariate dependent normal distribution. This number is the number of components. So, the problem is solved for multivariate dependent normal distribution but the probability (weight) of sample $x_{i;E}$ belong to the component of c must be considered. The derivative at step k with respect to a component c having $e_{c,k}^{IS} = \left[\pi_{c,k}^{IS}; \mu_{c,k}^{IS}; \Sigma_{c,k}^{IS}\right]$ are as follows:

$$\frac{1}{N}\sum_{i=1}^{N} I_{F_k}(x_i)\, W_k(x_i)\, \frac{\pi_{c,k-1}\, \mathcal{N}(x_{i;E}, \mu_{c,k-1}^{IS}; \Sigma_{c,k-1}^{IS})}{\sum_{c=1}^{C} \pi_{c,k-1}\, \mathcal{N}(x_{i;E}, \mu_{c,k-1}^{IS}; \Sigma_{c,k-1}^{IS})}\, (\Sigma_{c,k}^{IS})^{-1}(x_{i;E} - \mu_{c,k}^{IS}) = 0$$

$$\frac{1}{N}\sum_{i=1}^{N} I_{F_k}(x_i)\, W_k(x_i)\, \frac{\pi_{c,k-1}\, \mathcal{N}(x_{i;E}, \mu_{c,k-1}^{IS}; \Sigma_{c,k-1}^{IS})}{\sum_{c=1}^{C} \pi_{c,k-1}\mathcal{N}(x_{i;E}, \mu_{c,k-1}^{IS}; \Sigma_{c,k-1}^{IS})}\, \frac{1}{2}\left((\Sigma_{c,k}^{IS})^{-2}(x_{i;E}\right. \tag{4.11}$$

$$\left. - \mu_{c,k}^{IS})(x_{i;E} - \mu_{c,k}^{IS})^{T} - (\Sigma_{c,k}^{IS})^{-1}\right) = 0$$

From (4.11), in addition to the sample weight $W_k(x_i)$, the weight of sample $x_{i;E}$ belonging to the distribution of component (c) $\mathcal{N}\left(x_{i;E}; \mu_{c,k-1}^{IS}; \Sigma_{c,k-1}^{IS}\right)$ is expressed by a parameter $\gamma_{c,k}\left(x_{i;E}; e_{k-1}^{IS}\right)$ as follows:

$$\gamma_{c,k}\left(x_{i;E}; e_{k-1}^{IS}\right) = \frac{\pi_{c,k-1}\, \mathcal{N}(x_{i;E}, \mu_{c,k-1}^{IS}; \Sigma_{c,k-1}^{IS})}{\sum_{c=1}^{C} \pi_{c,k-1}\, \mathcal{N}(x_{i;E}, \mu_{c,k-1}^{IS}; \Sigma_{c,k-1}^{IS})} \tag{4.12}$$

Therefore, the parameters of ISD can be expressed by the next formulas (4.13) [139].

$$\mu_{c,k}^{IS} = \frac{\sum_{i=1}^{N} I_{F_k}(x_i)\, W_k(x_i)\, \gamma_{c,k}(x_{i;E}; e_{k-1}^{IS})x_{i;E}}{\sum_{i=1}^{N} I_{F_k}(x_i)\, W_k(x_i)\, \gamma_{c,k}(x_{i;E}; e_{k-1}^{IS})}$$

$$\Sigma_{c,k}^{IS} = \frac{\sum_{i=1}^{N} I_{F_k}(x_i)\, W_k(x_i)\, \gamma_{c,k}(x_{i;E}; e_{k-1}^{IS})(x_{i;E} - \mu_{c,k}^{IS})(x_{i;E} - \mu_{c,k}^{IS})^{T}}{\sum_{i=1}^{N} I_{F_k}(x_i)\, W_k(x_i)\, \gamma_{c,k}(x_{i;E}; e_{k-1}^{IS})} \tag{4.13}$$

Finally, derivatives with respect to $\pi_{c,k}^{IS}$ using a Lagrange multiplier for the constraint $\sum_{c=1}^{C} \pi_{c,k}^{IS} = 1$ result in

$$\pi_{c,k}^{IS} = \frac{\sum_{i=1}^{N} I_{F_k}(x_i)\, W_k(x_i)\, \gamma_{c,k}(x_{i;E}; e_{k-1}^{IS})}{\sum_{i=1}^{N} I_{F_k}(x_i)\, W_k(x_i)} \tag{4.14}$$

As shown in Algorithm 3.1, starting with $\delta_0 = \infty$ and $u_0^{IS}, e_0^{IS}, q_0^{IS}$ as a nominal parameter vectors, this procedure is reiterated and δ_k is determined such that the variance of the importance weights $W(x_i; u_{k-1}^{IS}, o_{k-1}^{IS}, e_{k-1}^{IS}, \delta_k)$ as calculated in (4.15) is small. This is done by minimizing the difference between the $\mathbb{CV}$ of the weights and the specified $\mathbb{CV}_{target}$ at each intermediate event k, as written in (3.16).

$$W(x_i; u_{k-1}^{IS}, q_{k-1}^{IS}, e_{k-1}^{IS}, \delta_k)$$

$$= \Phi\left(-\frac{H(x_i)}{\delta_k}\right) \frac{\mathcal{N}(x_{i;U}; u)}{\mathcal{N}(x_{i;U}; u_{k-1}^{IS})} \frac{\mathcal{M}(x_{i;E}; e)}{\mathcal{M}(x_{i;E}; e_{k-1}^{IS})} \prod_{l=1}^{NT} \frac{\mathcal{B}r(x_{i,l}; q_l)}{\mathcal{B}r(x_{i,l}; q_{l_{k-1}}^{IS})} \tag{4.15}$$

The algorithm is stopped when the $\mathbb{CV}$ of the weight calculated in (3.17) of the present smooth approximation of the indicator function of intermediate failure events with regard to the target indicator function is lower than the $\mathbb{CV}_{t\,arg\,et}$. Hence, K is set to the current event k, and the optimal ISDs are approximated well enough by the density $\mathcal{N}(x_{i;G}; u_{K-1}^{IS}), \mathcal{M}(x_{i;E}; e_{K-1}^{IS}), and\, \mathcal{B}r(x_{i,l}; q_{l_{K-1}}^{IS}) \,\forall\, l \in NT$. The samples from these densities will be used in the second stage as shown in Algorithm 3.1 for computing the system adequacy indices (LOLE-EENS) as follows:

$$LOLE = t\frac{1}{N}\sum_{i=1}^{N} I_{F_k}(x_i)W_K(x_i), \tag{4.16}$$

$$EENS = t\frac{1}{N}\sum_{i=1}^{N}\left(\sum_{d=1}^{D} PNS_d(x_i)\right)W_K(x_i).$$

where t is the period of study in hours and here equal to 8760 h.

4.4.   Results

The proposed method is tested and evaluated for the five-node test scheme, presented in Figure 2.1. The FOR of transmission lines is set to 0.001. The standard MCS simulation method is used as a benchmarking method. The maximum number of simulation samples for MCS is 10^5. A coefficient of variation (convergence) of 5% for both annual system reliability indices (LOLE-EENS) is used as the stopping criterion.

The reliability assessment has been conducted with different renewable generation profiles. In Case I, a wind farm (16 x 3MW) has been added to the testing network at node 2 instead of the conventional generation. In Case II, we consider a solar PV power plant (48 x 1MW) at node 2 to compensate the conventional generation. In Case III, we consider both wind farm (8 x 3MW) and PV station (24 x 1MW) at node 2. Each 1 MW PV array would be divided into 16 subarrays each rated at 63.25 kW [140]. The PV panel with model number STP280-VRM-1 developed by

SUNTECH of rated power 275 W is used. The total number of panels connected in the array is 3680 connected in best available method. The repair rate and failure rate of the PV array used are 0.00381 (1/hour) and 0.000383 (1/hour) respectively [135] which lead to FOR equal to 0.09. The parameters of 3 MW WTG are as follows: the cut-in, rated and cut-out wind speeds are 3m/s, 10m/s and 25m/s respectively. The FOR of each WTG is set to 0.10 [133]. To adapt the real-life datasets on the 5-node system, the real-life datasets is scaled to match the parameters of test scheme. The electricity demand is scaled by a factor that is the peak demand of the real-life datasets divided by the aggregated load of the system. In this manner, the correlation structure between the demand and weather variables can be conserved.

To explain the significance of investigating correlation for evaluating the reliability indices, two scenarios of uncorrelated and correlated samples are considered for the three cases. To generate the uncorrelated samples, the GMM is used to fit the PDF of each variable and is then used to generate samples from each PDF independently. While the MGMM generates correlated samples of load and weather variables. Table 4.2 shows the LOLE and EENS values, the number of samples, the computation time obtained by the MCS method in case of the correlated and uncorrelated samples. The difference in results between the two scenarios (correlated-uncorrelated) indicates the importance of regarding the correlation coefficients. Correlation has a large effect on the values of reliability indices and the computational time. The convergence in case of correlated samples is higher than this of uncorrelated samples as most of samples is viable system states expressing operating conditions. Thus, the computation burden is low using correlated samples. In case I, the results of reliability indices for correlated samples are larger than those of uncorrelated because of negative correlation between wind speeds and loads i.e. the wind generation lessens with increasing the load and vice versa which leads to poor system reliability. While in case II, the positive correlation results in the solar generation follows the load and so the reliability indices are lower in case of considering the correlation than those using the uncorrelated samples. The results of case III signify that the percentage of

penetration of Wind and solar generation together should be optimized for better benefits based on minimizing the values of reliability indices.

Table 4.2 Annual reliability indices for different renewable generation profiles in case of correlated and uncorrelated scenarios.

	Correlated				Uncorrelated			
	LOLE [h/yr]	EENS [MWh/yr]	Number of samples	Time [s]	LOLE [h/yr]	EENS [MWh/yr]	Number of samples	Time [s]
Case I	81	4300	252134	5899	19.3	1870	437135	14052
Case II	76	4700	213139	4575	96	7300	618213	22458
Case III	70	10000	106032	1323	30	4312	665500	27021

The accuracy of the proposed ECS-IS method is validated through comparing its results of reliability indices with the MCS. The ECE-IS method uses the following parameter values: $\mathbb{CV}_{target} = 1.5$, maximum number of iterations = 50, and number of samples per iteration = 5000. The system EENS and LOLE are calculated by the two methods (MCS and ECE-IS) for the different cases. The reliability indices are in accordance for both methods as shown in Table 4.3. The proposed method enables effective simulation of EPSs with a large proportion of renewable power generation. Under several renewable generation profiles, the number of samples needed by the ECE-IS method to achieve the MCS accuracy is one-fifth to one-sixth compared to the MCS method. This indicates the advantage of the proposed method in considering a higher number of LOL states that allows the estimator converges quickly with a small fraction of the samples needed by the MCS without importance sampling. When comparing between the case III (less reliable) and the case I (high reliable), the efficiency gain of the proposed approach compared with the MCS method is less. The speed-up of the proposed method in case III is nearly three compared to the MCS method, while in case I, the gain is six times.

Table 4.3 Annual reliability indices obtained using the MCS and ECE-IS for different renewable generation profiles.

	MCS				ECE-IS			
	LOLE [h/yr]	EENS [MWh/yr]	Number of samples	Time [s]	LOLE [h/yr]	EENS [MWh/yr]	Number of samples	Time [s]
Case I	81	4300	252134	5899	79	4221	49000	879
Case II	76	4700	213139	4575	83	4900	38705	776
Case III	70	10000	106032	1323	65	9200	20500	486

Conclusion

The multivariate GMM is employed to consider the multimodal PDFs of continuous variables (wind speed, solar irradiance, temperature, and electricity demand) and the complicated correlation among them based on the real historical data in form of joint probability distribution. The random variation and chronological characteristics of electricity demand and weather variables for El Gouna city located in Egypt are considered. The MGMM has been provided an accurate probabilistic model to include the load, solar, and wind powers uncertainties in the reliability estimation of power systems. In order to estimate the annual reliability indicators (LOLE-EENS) efficiently and accurately of CPS with a large proportion of PV power stations and wind farms integrated, the ECE-IS method is used to carry out IS on the obtained MGMM and find the IS-PDF parameters for it. Moreover, the availability state model of wind farms, PV power stations, and transmission lines are considered. The computational efficiency and adaptability of the method of combined ECE-IS and MGMM has been confirmed by the results of case studies.

Conclusions and Recommendations

- A comprehensive review of the probabilistic approaches applied on the reliability evaluation of the power grid has accomplished.

- In a concentrated electric power system, the approximate analytical method (the method of combined cumulants and Von Mises function) has provided low computational time and good degree of accuracy compared with the Monte Carlo method. Moreover, it is mathematically simpler than the convolution method.

- In composite power system, the modified Hong's method M $(2 \times n)$ +1 has improved the computational accuracy of Hong's methods by considering a group of superimposed uncertain events (criterion $N - 2$), i.e. positive deviation of nodal load and negative deviation generation from their expected forecast value. However, in general, the point estimate methods are not recommended for the high reliability systems which is characterized by the rare occurrence of the loss of load events since the criterion $N - 2$ becomes not enough to extract these events.

- The enhanced cross entropy based on optimization algorithm has improved the sampling efficiency and convergence characteristics of the Monte Carlo method through making rare loss of load events more likely to be drawn. In addition, it is more efficient and robust than other rare events simulation methods.

- The enhanced cross entropy method has been integrated within a two-stage framework for calculating the reliability indices. From the reported results of reliability indices, the proposed method contributes to accurately evaluating the reliability indices and further enhancing the convergence of the indices in comparison with other methods. Moreover, 11-times speed-up is achieved with respect to the standard Monte Carlo method.

- The multivariate Gaussian mixture model has been employed to consider the multimodal PDFs of continuous variables (wind speed, solar irradiance, temperature, and electricity demand) and the complicated correlation among them based on the real historical data in form of joint probability distribution. The proposed model has been provided an accurate probabilistic model compared with other models to include the

load, wind, and solar power uncertainties in the reliability evaluation of electric power systems with a large-scale wind farms and PV power stations renewable integrated.

- The enhanced cross entropy method has been adopted to improve the sampling efficiency of the correlated probabilistic model of renewable energy resources and demand, and the availability state model of wind farms, photovoltaic power stations, and transmission lines outages. The method can preserve the dependence structure of renewable powers and load in the procedure of reliability assessment; thus, the reliability indices are evaluated with an acceptable computation burden.

- The computational efficiency and adaptability of the enhanced cross entropy method for assessing accurately and efficiently power system annual reliability indices in the renewable energy reliability study has been confirmed by the results of case studies. The values of the loss of load expectation and expected energy not supplied estimators agree with the Monte Carlo method. Besides, the efficiency gain of the proposed approach compared with the Monte Carlo method is nearly three to six times.

Approaches of Future Research

- Within the framework of the long-term reliability evaluation, the active power balance was considered. However, reactive power balance should be considered due to its effects on adequacy indices, especially with the high integration of renewable energy resources.

- Implementation of the enhanced cross entropy method in the reliability assessment of a real power system;

- In order to maximize the use of renewable power and reduce the CO_2 emissions, a priority should be given to the renewable generators over thermal generators in optimal power flow algorithm in case of no power deficit states.

- In the case of renewable energy reliability studies, analysis of the renewable power curtailment events because of the failure and/or capacity limits of transmission lines, demand power deficit, or the simultaneous incidence of both

these events should be examined to enable power system planners maximizing the efficiency of renewable energy utilizations.

- In smart grids with renewable penetrations, storing strategies for the renewable energy such as electric vehicle storage should be considered in the reliability assessment. However, this will increase largely the amount of computational burden.

- Implementation of the enhanced cross entropy in the sequential Monte Carlo simulation method by sequentially sampling the duration of the states should be considered for studying the reliability of smart grids in which an optimal energy management scheme is designed for the renewable generations and energy storages to improve the customers' reliability.

- Implementation of the enhanced cross entropy method in the problem of the system reserve assessment and allocation to determine the optimal location and penetration of renewable energy resources in the system.

List of Symbols

A. Abbreviations

CDF	–	Cumulative distribution function
EPS	–	Electric power system
CPS	–	Composite power system
CE-IS	–	Cross entropy-based importance sampling
ECE-IS	–	Enhanced cross entropy-based importance sampling
IS	–	Importance sampling
ISD	–	Importance sampling density
KL	–	Kullback–Leibler
PNS	–	Power not supplied
LOLE	–	Loss of load expectation
EPNS	–	Expected power not supplied
EENS	–	Expected energy not supplied
LOLP	–	Loss of load probability
SPNS	–	Standard deviation of power not supplied
MCS	–	Monte Carlo simulation
MPP	–	maximum power point
NOCT	–	nominal operating cell temperature
OPF	–	Optimal power flow
PDF	–	Probability distribution function
PMF	–	Probability mass function
PV	–	Photovoltaic
CDF	–	Cumulative distribution function
$\mathcal{R}$	–	Reliability index
Rv	–	Random variable
SS	–	Subset simulation
STC	–	standard test condition
GMM	–	Gaussian mixture model

MGMM	–	Multivariate Gaussian mixture model
TND	–	truncated normal distribution
WECS	–	Wind energy conversion system
WTG	–	Wind turbine generator
VRTs	–	Variance Reduction Techniques.

B. Notations

$C_{n_g}^g$	–	Binomial coefficient
I_F	–	Failure indicator function
$\mathbb{P}_F$	–	Failure probability
$\mathbb{V}$	–	Variance operator
$\mathbb{E}$	–	Expectation operator
$\mathbb{CV}$	–	Convergence or coefficient of variation
$\hat{\mathcal{R}}$	–	Estimator of reliability index $\mathcal{R}$
$\mathbb{D}$	–	Divergence
$\widetilde{PNS}$	–	The normalized power not supplied
ζ_k	–	A threshold intermediate level k
$\xi_{x_{i,j}}$	–	Location of concentrated point j of variable x_i
φ	–	the standard normal PDF
Φ	–	the standard normal CDF
$\mathcal{M}; \mathcal{N};$ $\mathcal{B}; \mathcal{B}r$	–	Gaussian mixture, Normal, Binomial, and Bernoulli distributions
$f; F$	–	PDF and CDF functions
δ	–	Control parameter of bandwidth of failure indicator function
ρ	–	Correlation factor
α	–	Outage rate
τ	–	Outage duration
∇	–	Gradient

C. Indices and Sets

| $\mathcal{K}$ | – | Cumulant |

m	–	Raw moment
M	–	Central moment
λ	–	Standard central moment
$i; N$	–	Index and set of samples
$j; n$	–	Index and set of random variables
$c; C$	–	Index and set of components of the GMM
$d; D$	–	Index and set of nodes
$k; K$	–	Index and set of intermediate levels
$l; NT$	–	Index and set of transmission lines
N_n	–	Number of nodes in the power system
N_m	–	Number of moments
N_l	–	Number of lines in the power system
N_g	–	Number of groups of generators in the power system
n_g	–	Number of generators in one group
N_p	–	Number of parallel panels in the photovoltaic array
N_s	–	Number of series panels in the photovoltaic array

D. Parameters

q	–	Forced outage rate of generating unit g
q_l	–	Forced outage rate of transmission line l
π_d	–	Weight factor for the load of the node d
π_c	–	Weight for the component c of the GMM
w_g	–	Failure probability of number of generators g in a group of n_g elements
A^t	–	Power system incidence matrix reduced by one row
B	–	Bus susceptance matrix
B_{br}	–	Diagonal matrix made of transmission lines susceptance
R_l	–	Transmission line resistance [Ohm]
V	–	Nominal voltage of a power system [V]

LF_l^{max}	–	Maximum power flow or transmission line l capacity
P_{bl}	–	Nominal power of generator
v_{x_i}, k_{x_i}	–	Skewness and kurtosis of variable x_i
t	–	Time

E. Variables

PNS_d	–	Power not supplied or Curtailed load at the node d
L_d	–	Load at the node d
P_d	–	Power injection at the node d
LF_l	–	Power flow of transmission line l
G_d	–	Used generation at the node d
P_Σ	–	Sum of power injections at all the nodes of the power system
LS_Σ	–	Sum of transmission lines power losses
LF	–	Power flows vector
P	–	Vector of power injections
P_{PV}	–	Power output of PV panel
P_w	–	Power output of wind turbine generator
G_d^{av}	–	Available generation at the node d
v_w	–	Wind speed
S_l	–	State of transmission line l
s_{PV}	–	Solar irradiance
S_{pv}^{av}	–	Available state of the PV power station
S_w^{av}	–	Available state of the wind farm
T	–	Temperature
$w_{x_{i,j}}$	–	Weight factor for the j concentration point of variable x_i
$W(x_i)$	–	Likelihood ratio or importance weight function of a distribution of variable x_i

References

1.   Billinton R. Reliability evaluation of power systems / R. Billinton, R.N. Allan. –New York: Springer Science+ Business Media, LLC. – 1996. – P. 534. ISBN 9788578110796.

2.   Надежность систем энергетики и их оборудования. Спр. в 4 т. / Под общей ред. Руденко Ю.Н.Т.2. Надежность электроэнергетических систем. Справочник / Под ред. Розанова М.Н. М.: Энергоатомиздат, 2000.

3.   Методические указания по проведению расчетов балансовой надежности: СТО59012820.27.010.005-2018. М.: АО "СО ЕЭС", 2018.

4.   Руденко Ю.Н. Надежность и резервирование в энергосистемах/ Ю.Н. Руденко, М.Б. Чельцов // Новосибирск: Наука.–1974.

5.   Обоскалов В. П. Надежность обеспечения баланса мощности электроэнергетических систем. – Екатеринбург: УГТУ–УПИ, 2002.

6.   Обоскалов В.П. Сравнительная эффективность методов расчета показателей балансовой надежности энергосистем / В.П. Обоскалов, Р.Т. Валиев, С.А. Гусев// Известия высших учебных заведений. Проблемы энергетики. – 2016. – № 9-10. – С. 119-125.

7.   Воропай Н.И. Надежность систем энергетики. (Сборник рекомендуемых терминов) /Н.И. Воропай. – М. : ИАЦ "Энергия," 2007. – 194 с.

8.   Okwe G.I. Adequacy analysis and security reliability evaluation of bulk power system /G.I. Okwe, K. Inyama// Journal of computer engineering. – 2013. – vol.11. – P.26-35.

9.   Review of the current status of tools and techniques for risk-based and probabilistic planning in power systems [Electronic resource] : official website – Access mode: https://e-cigre.org/publication/434-review-of-the-current-status-of-tools-and-techniques-for-risk-based-and-probabilistic-planning-in-power-systems [date of the application 01.05.2021].

10.   Reliability Standards for the Bulk Electric Systems of North America [Electronic resource]: official website – Access mode:

https://www.nerc.com/pa/Stand/Reliability%20Standards%20Complete%20Set/RSCompleteSet.pdf [date of the application 01.05.2021].

11. Probabilistic Adequacy and Measures Technical Reference Report [Electronic resource] : official website – Access mode: https://www.nerc.com/comm/PC/Probabilistic%20Assessment%20Working%20Group%20PAWG%20%20Relat/Probabilistic%20Adequacy%20and%20Measures%20Report.pdf#search=Probabilistic%20Adequacy%20and%20Measures [date of the application 01.05.2021].

12. 2016 Probabilistic Assessment [Electronic resource] : official website – Access mode: https://www.nerc.com/comm/PC/PAWG%20DL/2016ProbA_Report_Final_March.pdf#search=2016%20Probabilistic%20Assessment [date of the application 01.05.2021].

13. Чукреев Ю.Я. Сравнительный анализ вевероятностных показателей балансовой надежности и методических принципов их определения при управление развитием электроэнергетических систем /Ю.Я. Чукреев, М.Ю.Чукреев // Известия Коми научного центра УрО РАН. – 2012. – №3(11). – С. 76–81.

14. Poncela-Blanco M. Generation Adequacy Methodologies Review/ M. Poncela-Blanco, A. Spisto, N. Hrelja, F. Gianluca*// Joint Research Centre (JRC), European Union*. – 2016.

15. ENTSO-E Target Methodology for Adequacy Assessment Consultation material [Electronic resource] : official website – Access mode: https://eepublicdownloads.blob.core.windows.net/public-cdn-container/clean-documents/sdc-documents/SOAF/ENTSO-E_Target_Methodology_for_Adequacy_Assessment.pdf [date of the application 01.05.2021].

16. ПНСТ 304-2018 Единая энергетическая система и изолированно работающие энергосистемы. Балансовая надежность энергосистем. Часть 1. Общие требования [Electronic resource] : official website – Access mode: http://docs.cntd.ru/document/1200160584 [date of the application 01.05.2021].

17. Методические указания по проведению расчетов балансовой надежности : СТО 59012820.27.010.005-2018. – М. : АО «СО ЕЭС», 2018. – 25 с.

18. Чукреев Ю.Я. Модели оценки показателей балансовой надежности при управлении развитием электроэнергетических систем / Ю. Я. Чукреев, М.Ю. Чукреев. – Сыктывкар : Коми научный центр УрО РАН, 2014. – 207 с. – ISBN 978-5-89606-509-8.

19. Billinton R. Reliability assessment of electric power systems using Monte Carlo methods / R. Billinton, L. Wenyuan. – New York: Springer science + Business Media. – 1994. – 361 p. – ISBN 978-1-4899-1346-3.

20. Зоркальцев В.И. Модели оценки дефицита мощности электроэнергетических систем / В.И. Зоркальцев, Г.Ф. Ковалев, Л.М. Лебедева. – Иркутск: ИСЭМ СО РАН, 2000. – 25 с.

21. Giuntoli M. Parallel computing of sequential MonteCarlo techniques for reliable operation of Smart Grids/ M. Giuntoli, P. Pelacchi, D. Poli// International Conference on Computer as a Tool (EUROCON), Salamanca, Spain. – 2015. – P.8–11.

22. Martinez J. A parallel Monte Carlo method for optimum allocation of distributed generation/ J. Martinez, G. Guerra// *IEEE Trans. Power Syst.* 2014.– vol.*29*, – P.2926–2933.

23. Ge H. Parallel Monte Carlo simulation for reliability and cost evaluation of equipment and systems/ H. Ge, S. Asgarpoor*// Electr. Power Syst. Res.* – 2011. – vol.*81*. – P.347–356.

24. Dias J. Object oriented model for composite reliability evaluation including time varying load and wind generation/ J. Dias, *C*. Borges// 11th International Conference on Probabilistic Methods Applied to Power Systems, Singapore. –2010. – P.14–17.

25. Da Rosa M. Multi-agent systems applied to reliability assessment of power systems/ M. Da Rosa, A. Leite Da Silva, V. Miranda*// Int. J. Electr. Power Energy Syst.* –2012. –vol.3.– P.48-57.

26. Augusto da Rosa M. Agent-based Technology Applied to Power Systems Reliability/ University of Porto, Porto. – 2009.

27. Singh C. Role of artificial intelligence in the reliability evaluation of electric power systems/ C. Singh, L. Wang// Turk. J. Electr. Eng. Comput. Sci. – 2008. – vol.16. – P.189–200.

28. Leite da Silva A.M. Composite reliability assessment based on Monte Carlo simulation and artificial neural networks/ A.M. Leite da Silva, L.C. de Resende, L.A. da Fonseca Manso, V. Miranda// *IEEE Trans. Power Syst.* – 2007. – vol.90. –P.1302–1310.

29. Pindoriya N.M. Composite reliability evaluation using Monte Carlo simulation and least squares support vector classifier/ N.M. Pindoriya, P. Jirutitijaroen, D. Srinivasan, C. Singh// IEEE Trans. Power Syst. 2011. – vol.211. – P.6048–6056.

30. Urgun D. Importance Sampling Using Multilabel Radial Basis Classification for Composite Power System Reliability Evaluation/ D. Urgun, C. Singh, V. Vittal // IEEE Syst. J. –2020. –vol.294. –P.4131–4139.

31. Urgun D. A Hybrid Monte Carlo Simulation and Multi Label Classification Method for Composite System Reliability Evaluation/ D. Urgun, C. Singh*// IEEE Trans. Power Syst.* – 2019. – vol.287. –P.8535–8545.

32. Nannapaneni S. Probability-space surrogate modeling for fast multidisciplinary optimization under uncertainty/ S. Nannapaneni, S. Mahadevan//*Reliab. Eng. Syst. Saf.* –2020. – vol.106. –P.896–905.

33. Schneider F. Polynomial chaos based rational approximation in linear structural dynamics with parameter uncertainties/ F. Schneider, I. Papaioannou, M. Ehre, D. Straub// *Comput. Struct.* 2020. – *Vol.233*.

34. Kalinina A. Metamodeling for Uncertainty Quantification of a Flood Wave Model for Concrete Dam Breaks/ A. Kalinina, M. Spada, D.F. Vetsch, S. Marelli, C. Whealton, P. Burgherr, B. Sudret// *Energies.* – 2020.– *vol.13.* – *P.3685– 3691.*

35. Moustapha M. Surrogate-assisted reliability-based design optimization: A survey and a unified modular framework/ M. Moustapha, B. Sudret// Struct. Multidiscip. Optim. – 2019. – vol.60. – P.2157–2176.

36. Tomasson E. Improved importance sampling for reliability evaluation of composite power systems/ E. Tomasson, L. Soder // IEEE Trans. Power Syst. – 2017. –vol. 32. – P. 2426–2434.

37. Zhao Y. Composite Power System Reliability Evaluation Based on Enhanced Sequential Cross-Entropy Monte Carlo Simulation/ Y. Zhao, Y. Tang, W. Li, J.Y. Power// Proceedings of the IEEE Transactions on Power Systems. –2019. – vol. 34. –P. 3891–3901.

38. Hua B. Extracting rare failure events in composite system reliability evaluation via subset simulation/ B. Hua, Z. Bie, S.K. Au, W. Li, X. Wang// IEEE Trans. Power Syst. – 2015. –vol.30. – P.753–762.

39. Kroese D.P. Handbook of Monte Carlo Methods/ D.P. Kroese, T. Taimre, Z.I. Botev. –John Wiley & Sons, Inc, Hoboken, New Jersey. – 2011. – ISBN 9781118014967.

40. Billinton R. Reliability Assessment of Electric Power Systems Using Monte Carlo Methods/ R. Billinton, L. Wenyan. –Springer: New York, NY, USA. – 1994. – ISBN 9781489913487.

41. Wang Y. Adaptive sequential importance sampling technique for short-term composite power system adequacy evaluation/ Y. Wang, C. Guo, Q. Wu, S. Dong// IET Gener. Transm. Distrib.–2014.–vol.8. – P. 730–741.

42. Pereira M.V.F. Combining analytical models and monte-carlo techniques in probabilistic power system analysis/ M.V.F. Pereira, M.E.P. Maceira, G.C. Oliveira, L.M.V.G. Pinto// IEEE Trans. Power Syst. – 1992. – vol.59.141713.

43. Billinton R. Composite system adequacy assessment using sequential Monte Carlo simulation with variance reduction techniques/ R. Billinton, A. Jonnavithula// IEEE Proc. Gener. Transm. Distrib. – 1997. – vol.144. –P.1-6.

44. Zhang F. Reliability sensitivity algorithm based on stratified importance sampling method for multiple failure modes systems/ F. Zhang, Z. Lu, L. Cui, S. Song// Chin. J. Aeronaut. – 2010. – vol.23. – P.660-669.

45. Papaioannou I. Combination line sampling for structural reliability analysis/ I. Papaioannou, D. Straub// Struct. Saf. –2020. – vol.88. 102025.

46. Song J. Active learning line sampling for rare event analysis/ J. Song, P. Wei, M. Valdebenito, M. Signal// Mech. Syst. Signal. Process. 2020. – vol.147. 107113.

47. Song S. Reliability sensitivity analysis involving correlated random variables by directional sampling/ S. Song, Z. Lu, Z. Song// Proceedings of 2011 International Conference on Quality, Reliability, Risk, Maintenance, and Safety Engineering, Xi'an, China. –2011.

48. González-Fernández R.A. Composite systems reliability evaluation based on Monte Carlo simulation and cross-entropy methods/ R.A. González-Fernández, A.M. Leite Da Silva, L.C. Resende, M.T. Schilling// IEEE Trans. Power Syst. – 2013. – vol.28. – P.4598–4606.

49. Cao Q.D. Cross-entropy based importance sampling for stochastic simulation models/ Q.D. Cao, Y. Choe// Reliab. Eng. Syst. Saf. – 2019. – vol.191.

50. Abdel Menaem A. An efficient framework for adequacy evaluation through extraction of rare load curtailment events in composite power systems/ A. Abdel Menaem, R. Valiev, V.P. Oboskalov, T.S. Hassan, H. Rezk, M. Ibrahim // Mathematics. –2021. –vol.8. – P.1-21 – https://doi.org/10.3390/math8112021; https://www.researchgate.net/publication/345805054_An_Efficient_Framework_for_Adequacy_Evaluation_through_Extraction_of_Rare_Load_Curtailment_Events_in_Composite_Power_Systems.

51. Huang J. An Efficient Probabilistic Assessment Method for Electricity Market Risk Management/ J. Huang, Y. Xue, Z. Y. Dong, K. P. Wong// IEEE Transactions on Power Systems– 2012. – vol. 27. – P.1485-1493.

52. Руденко Ю.Н. Надежность систем энергетики /Ю.Н. Руденко, И.А. Ушаков. – Новосибирск: Наука, 1989. – 328 с. – ISBN 5-02-028747-4.

53. Oboskalov V. Mathematical methods for probabilistic estimation of power shortage in concentrated electric power systems/ V. Oboskalov, A. Abdel Menaem, R. Valiev, A. Mahnitko, R. Varfolomejeva// Proceedings of the 10th International Scientific Symposium on Electrical Power Engineering, Elektroenergetika. –2019. – P. 128–132.

54. Обоскалов В.П. Определение показателей балансовой надежности оэс методами точечной оценки/ В.П. Обоскалов, А. Абдель Менаем// Изв. Ран. Энергетика. – 2020. –№ 6. –С. 40–53.

55. Abunima, H. A Systematic Review of Reliability Studies on Composite Power Systems: A Coherent Taxonomy Motivations, Open Challenges, Recommendations, and New Research Directions/ H. Abunima, J. Teh, C. Lai, H. Jabir// Energies. – 2018. – vol.11, 2417.

56. Ковалев Г.Ф. Сопоставительный анализ результатов исследований надежности ЭЭС, выполненный с помощью разных программ // Методические вопросы исследования надежности больших систем энергетики. Выпуск 41/ СЭИ СО АН СССР. – Иркутск, 1991. – С. 53-59.

57. Athraa A. Computational techniques for assessing the reliability and sustainability of electrical power systems: A review/ A. Athraa, N. Abdul Wahab, I. Aris, J. Jasni, A. Abdalla// Renewable and Sustainable Energy Reviews. –2017. – vol.80. –P.1175-1186.

58. Mortez A. A comprehensive review on uncertainty modeling techniques in power system studies / A. Mortez, A. Hajebrahimi, M. Fotuhi-Firuzabad // Renewable and Sustainable energy reviews. – 2016. – vol.57. – P.1077-1089.

59. Zakaria A. Uncertainty models for stochastic optimization in renewable energy applications/ A. Zakaria, F. Ismail, M.S. Hossain, M.A. Hannan// Renewable Energy. –2020. –vol.145. –P.1543-1571.

60. Talari S. Stochastic modelling of renewable energy sources from operators' point-of-view: A survey/ S. Talari, M. Shafie-khah, G. Osório, J. Aghaei,

J. Catalão// Renewable and Sustainable Energy Reviews. –2018. –vol.81. –P.1953-1965.

61. Heylen E. Review and classification of reliability indicators for power systems with a high share of renewable energy sources/ E. Heylen, G. Deconinck, D. Hertem// Renewable and Sustainable Energy Reviews. –2018. – vol.97. – P. 554-568.

62. Чукреев Ю.Я. Модели обеспечения надежности электроэнергетических систем/ Ю.Я. Чукреев. – Сыктывкар: Коми НЦ УрО РАН. – 1995. –176 с.

63. Зоркальцев В.И. Минимизация дефицита мощности в ЭЭС с учетом потерь мощности в линиях электропередачи/ В.И. Зоркальцев, Г.Ф. Ковалев, Л.М. Лебедева, С.М. Пержабинский // Электричество. –2010. –№ 9.

64. Ковалев Г.Ф. Надежность систем электроэнергетики. Новосибирск: Сибирская/ Г.Ф. Ковалев, Л.М. Лебедева // изд. фирма "Наука" Академиздатцентра "Наука". –2015.

65. Волков Г.А. Оптимизация надежности электроэнергетических систем. М.: Наука. – 1986.

66. Almutari A. Probabilistic generating capacity adequacy evaluation: Research roadmap /A. Almutari, M.H. Ahmed, M.M.A. Salama // Electric power system research. – 2015. – vol. 129. – P.83-93.

67. Соболь И.М. Метод Монте-Карло. М.: Наука. – 1968. – 64 с.

68. Руденко Ю.Н. Надежность и резервирование в энергосистемах /Ю.Н. Руденко, М.Б. Чельцов. – Новосибирск: Наука. – 1974. – 264 с.

69. Обоскалов В.П. Применение вероятностно-статистических методов и теории графов в электроэнергетике: уч. Пособие/ В.П. Обоскалов, С.Е. Кокин, И.Л. Кирпикова. – Екатеринбург: УрФУ, 2016.

70. Billinton. R. A comparison of three fundamentally different methods for generating capacity reliability evaluation /R. Billinton, L.Goel// Electric power system research. – 1994. – vol. 29 – P.1-8.

71. Обоскалов В.П. Резервы мощности в электроэнергетических системах/ В.П. Обоскалов. – Свердловск: УПИ. – 1989. – 92 с.

72. Непомнящий В.А. Учет надежности при проектировании энергосистем/В.А. Непомнящий. – М.: Энергия. – 1978. – 200 с.

73. Обоскалов В.П. Влияние конфигурации графика нагрузки на показатели балансовой надежности ЭЭС / В.П. Обоскалов, Р.Т. Валиев, И.Л. Кирпикова, С.А. Дехтяр // Электроэнергетика глазами молодёжи Научные труды IV международной научно-технической конференции/ Южно-Российский государственный политехнический университет имени М.И. Платова. – Новочеркасск, 2013. – С. 75-78.

74. Чукреев Ю.Я. Модели обеспечения надежности электроэнергетических систем/ Ю.Я. Чукреев. – Сыктывкар: Коми НЦ УрО РАН. – 1995. –176 с.

75. Зоркальцев В.И. Модели оценки дефицита мощности электроэнергетической системы / В.И. Зоркальцев, С.М. Пержабинский // Сибирский журнал индустриальной математики. – 2012. – №1 (49). – С. 34-43.

76. Дубицкий М.А. Выбор и использование резервов генерирующей мощности в электроэнергетических системах / М.А. Дубицкий, Ю.Н. Руденко, М.Б. Чельцов. – М.: Энергоматиздат. – 1988. – 272 с.

77. Обоскалов В.П. Алгоритмические аспекты расчета вероятностных показателей дефицита мощности в задаче балансовой надежности ОЭС/ В.П. Обоскалов // Изв. РАН. Энергетика. – 2020.– № 2. С. 59–74.

78. Зоркальцев В.И. Минимизация дефицита мощности в ЭЭС с учетом потерь мощности в линиях электропередачи / В.И. Зоркальцев, Г.Ф. Ковалев, Л.М. Лебедева, С.М. Пержабинский // Электричество. – 2010. – №9. – С. 56-60.

79. Зоркальцев В.И. Модели оценки дефицита мощности электроэнергетической системы / В.И. Зоркальцев, С.М. Пержабинский // Сибирский журнал индустриальной математики. – 2012. – №1 (49). – С. 34-43.

80. Обоскалов В.П. Вероятностно-аналитический метод расчета показателей балансовой надежности ОЭС / В.П. Обоскалов, Р.Т. Валиев / Известия Российской академии наук. Энергетика. – 2019. – №1. – С. 37-49.

81. Манусов В.З. Вероятностные задачи в электроэнергетике / В.З. Манусов. – Новосибирск: НЭТИ. – 1981. – 119 с.

82. Borkouska B. Probabilitic load flow/ B. Borkowska// IEEE Transactions on Power Apparatus and Systems. – 1974. – vol. 93 – P.752-759.

83. Allan R.N. Evaluations methods and accuracy in probabilistic load flow solutions / R.N Allan, A.M. Late da Silva, R.C. Burchett // IEEE Transactions on Power Apparatus and Systems. – 1981. – vol. 100. – P.2539-2546.

84. Leite da Siva A.M. Probabilistic load flow considering dependence between input nodal powers / A.M. Leite da Siva, V.L. Arienti, R.N Allan // IEEE Transactions on Power Apparatus and Systems. – 1984. – vol.6. – P. 67-68.

85. Schilling M. Th. Bibliography on power system probabilistic analysis (1962-1988) / M.Th. Schilling, A.M. Leite da Silva, R. Billinton, M.A. El-Kafy // IEEE Transactions on Power Systems. – 1990. – vol. 5. – P. 1-11.

86. Биллинтон Р. Оценка надежности электроэнергетических систем: Пер. с англ./ Р.Биллинтов, Р. Аллан. – М.: Энергоатомиздат. – 1988. – 288с.

87. Обоскалов В.П. Структурная Надежность Электроэнергетических Систем / В.П. Обоскалов. – Екатеринбург: УрФУ. – 2012. – 194 с.

88. Abdel Menaem A. Comparing Three Methods for Solving Probabilistic Multi-Area Load Shedding Distribution / A. Abdel Menaem, V.P. Oboskalov// International Conference on Industrial Engineering, Applications and Manufacturing (ICIEAM 2020). –19-22 May 2020.

89. Rubino G. Rare Event Simulation using Monte Carlo Methods/ G. Rubino, B. Tuffin– John Wiley & Sons, Inc, Hoboken, New Jersey. – 2009. – ISBN: 9780470772690.

90. Маркович И.М. Режимы энергетических систем. – М.: Энергия. – 1969.

91. Обоскалов В.П. Оценка вероятностных параметров дефицита мощности в концентрированной ЭЭС/ В.П. Обоскалов, А. Абдель Менаем, А.В. Кирпиков// Известия Российской академии наук. Энергетика. –2019. – vol.4. – стр. 16-26.

92. Kendall M. Kendall's Advance Theory Statistic – New York: Oxford Univ. –1987.

93. Cramer H. Numerical Methods of Statistics. – Princeton: N.Y. Princeton Univ. Press. – 1946.

94. Tian W. Cumulant based probabilistic power systems simulation using Laguerre polynomials/ W. Tian, D. Sutanto, Y. Lee, H. Quthred// IEEE Trans. Energy converts. – 1989. – vol.4. – P. 567-574.

95. Bloom J. Representing the production cost curve of a power system using the method of moments/ J. Bloom //. IEEE Trans Power Syst.– 1992. – vol.7 – P.1370-1377.

96. Schellenberg A. Cumulant-based probabilistic optimal power flow (P-OPF) with Gaussian and gamma distributions/A. Schellenberg, W. Rosehart, J. Aguado// IEEE Trans Power Syst. – 2005. – vol.20. – P. 773-781

97. Zhao Y Uncertainty analysis for bulk power systems reliability evaluation using Taylor series and nonparametric probability density estimation/ Y. Zhao, F. Fan, J. Wang, K. Xie// Int J Electr Power Energy Syst. – 2015. – vol. 64. – P.804-814.

98. Mises V. Mathematical Theory of Probability and Statistics. – N.Y. Academic. – 1964.

99. Verbic G. Probabilistic optimal power flow in electricity markets based on a two-point estimate method / G. Verbic, A. Canizares // IEEE Trans Power Syst – 2006. – vol.21. – P.1883-1893

100. Rosenblueth E. Point estimates for probability moments/ E. Rosenblueth // Proc. Natl. Acad. Sci. – 1975. – vol. 72. – P. 3812–3814.

101. Rosenblueth E. Two-point estimates in probability/ E. Rosenblueth// Appl. Math. Model. – 1981. – vol. 5. – P. 329–335.

102. Hong H. An efficient point estimate method for probabilistic analysis/ H. Hong// Reliab. Eng. Syst. Saf. – 1998. – vol. 59.– P. 261–267.

103. Hong H. Point-estimate moment-based reliability analysis/ H. Hong// Civil Engineering Systems. – 1996. –vol. 13. –P. 281–294.

104. Christian J. The point-estimate method with large numbers of variables/ J. Christian, G. Baecher// International journal for numerical and analytical methods in geomechanics. –2002. –vol. 26. – P. 1515–1529.

105. Delgado C. Point estimate method for probabilistic load flow of an unbalanced power distribution system with correlated wind and solar sources/ C. Delgado, J. Dominguez-Navarro// Electrical Power and Energy Systems. – 2014. – vol. 61. – P. 267–278.

106. Morales J. Point Estimate Schemes to Solve the Probabilistic Power Flow/ J. Morales, J. Perez-Ruiz// IEEE Transactions on Power Systems. –2007. – vol. 22. – P. 1594–1601.

107. Abdel Menaem A. Integration of renewable sources into microgrid considering operational and planning uncertainties/ A. Abdel Menaem, V.P. Oboskalov // Advances in Intelligent Systems and Computing. 2020. – vol.972. – P. 225-241.

108. Tomasson E. Impact of High Levels of Variable Renewable Energy on Power System Generation Adequacy/ KTH Royal Institute of Technology School of Electrical Engineering and Computer Science, Stockholm, Sweden. – 2020.

109. Li W. Effect of bus load uncertainty and correlation in composite system adequacy evaluation/ W. Li, R. Billinton// IEEE Trans Power Syst. – 1991– vol.6. –P.1522–1529.

110. Li X. Transmission line overload risk assessment for power systems with wind and load-power generation correlation/ X. Li, X. Zhang, L. Wu, P. Lu, S. Zhang// IEEE Trans Smart Grid– 2017. – vol. 6. –P.1233–1242.

111. Miranda M. Spatially correlated wind speed modeling for generation adequacy studies in the UK/ M. Miranda, R. Dunn// Proc. IEEE Power Eng. Soc. Gen. Meeting– 2007.

112. Zhang S. Adequacy evaluation of wind farm integration in power generation and transmission systems/ S. Zhang, G. Li, M. Zhou // Proc. Int. Conf. Sustain. Power Gener. Supply – 2009. – P. 1–7.

113. Qin Z. Generation system reliability evaluation incorporating correlations of wind speeds with different distributions/ Z. Qin, W. Li, X. Xiong// IEEE Trans Power Syst. – 2013. –vol.28.– P.551–558.

114. Qin Z. Incorporating multiple correlations among wind speeds, photovoltaic powers and bus loads in composite system reliability evaluation/ Z. Qin, W. Li, X. Xiong// Appl Energy– 2013. –vol.110. –P.285–294.

115. Papaefthymiou G. Using copulas for modeling stochastic correlation in power system uncertainty analysis/ G. Papaefthymiou, D Kurowicka// IEEE Trans. Power Syst. –2009. – vol. 24. –P. 40–49.

116. Wang N. An efficient approach to power system uncertainty analysis with high-dimensional dependencies/ N. Wang, C. Kang, M. Miao, R. Shi, Q. Xia, // IEEE Trans. Power Syst. –2018. – vol. 33. –P. 2984–2994.

117. Li Y. Modelling wind speed correlation in system reliability assessment using copulas/ Y. Li, W. Li, K. Xie // IET Renew. Power Gener. –2012.–vol. 6. – P.392–399.

118. Qin Z. Estimating wind speed probability distribution using kernel density method/ Z. Qin, W. Li, X. Xiong// Electr Power Syst Res.–2011.–vol.81.– P.2139–2146.

119. Xu X. Estimating wind speed probability distribution by diffusion-based kernel density method/ X. Xu, Z. Yan, S. Xu // Electr Power Syst Res. – 2015.– vol.121. – P.28–37.

120. Yuan Z. Load modeling utilizing nonparametric and multi-variate kernel density estimation in bulk power system reliability evaluation/ Z. Yuan, X. Zhang, J. Zhou // Proceedings of the CSEE–2009.– vol. 29. – P. 27–33.

121. Yuan Z. Nonparametric disaggregation load model in power system reliability evaluation incorporating the additive correlation/ Z. Yuan, F. Fan, J.

Yang, S. Li, J. Wang, L. Geng // Proceedings of the CSEE–2015.– vol. 35– P. 6039–6047.

122. Singh R. Statistical Representation of Distribution System Loads Using Gaussian Mixture Model/ R. Singh, B. C. Pal, R. A. Jabr// IEEE Transactions on Power Systems–2010.– vol. 25. –P. 29-37.

123. Ge F. Parameter estimation of a Gaussian mixture model for wind power forecast error by Riemann L-BFGS optimization/ F. Ge, Y. Ju, Z. Qi// IEEE Access –2018. – vol. 6.– P. 38892-38899.

124. Ke D. A novel probabilistic optimal power flow model with uncertain wind power generation described by customized Gaussian mixture model/ D. Ke, C. Y. Chung, Y. Sun// IEEE Transactions on Sustainable Energy –2016. – vol. 7. – P. 200-212.

125. Nagler T. Evading the curse of dimensionality in nonparametric density estimation with simplified vine copulas/ T. Nagler, C. Czado// Journal of Multivariate Analysis –2016. – vol.151. – P.69–89.

126. Lucarelli G. Three approaches to use Cross-Entropy in reliability evaluation of composite system with high penetration wind energy/ G. Lucarelli, C. Yan, Z. Bie, C. Wang, T. Ding, F. Xiong// *2016 IEEE PES Asia-Pacific Power and Energy Engineering Conference (APPEEC)* –2016. – P. 227-231.

127. Gonz´alez-Fern´andez R. Reliability assessment of time-dependent systems via sequential cross-entropy Monte Carlo simulation/ R. Gonz´alez-Fern´andez, A. Silva// IEEE Trans. Power Syst. –2011. – vol. 26. – P. 2381–2389.

128. Silva A. Probabilistic assessment of spinning reserve via cross-entropy method considering renewable sources and transmission restrictions/ A. Silva, J. Castro, R. Billinton // IEEE Transactions on Power Systems –2018. –vol. 33. – P. 4574-4582.

129. Da Silva A. Composite reliability evaluation with renewable sources based on quasi-sequential Monte Carlo and cross entropy methods/ A. Da Silva, R. Gonz´alez-Fern´andez, S. Fl´avio, L. Manso// Int. Conf. Probabilistic Methods Appl. Power Syst. –2014. –P. 1–6.

130. Tomasson E. Generation adequacy analysis of multi-area power systems with a high share of wind power/ E. Tomasson, L. Soder // IEEE Trans. Power Syst. –2017. – vol. 33. – P. 3854–3862.

131. Ansari O. A hybrid framework for short-term risk assessment of wind-integrated composite power systems/ O. Ansari, C. Y. Chung// IEEE Transactions on Power Systems–2019. – vol. 34. – P. 2334-2344.

132. Sulaeman S. A wind farm reliability model considering both wind variability and turbine forced outages/ S. Sulaeman, M. Benidris, J. Mitra //IEEE Transactions on Sustainable Energy–2017. – vol. 8. – P. 629-637.

133. Abdel Menaem A. Optimal Integration of Renewable Power into Distribution Network based Probabilistic Bus Voltage-Feeder Current Uncertainty Analysis / A. Abdel Menaem, V.P. Oboskalov, M. Anatolijs, R. Varfolomejeva // 60th International Scientific Conference on Power and Electrical Engineering of Riga Technical University, Riga, Latvia. – 2019.

134. Riffonneau Y. Optimal Power Flow Management for Grid Connected PV Systems With Batteries/ Y. Riffonneau, S. Bacha, F. Barruel and S. Ploix// *IEEE Transactions on Sustainable Energy* –2011. – vol. 2. – P. 309-320.

135. Stember L. A Methodology for Photovoltaic System Reliability & Economic Analysis/ L. Stember, W. Huss, M. Bridgman// IEEE Transactions on Reliability –2009. – vol. 31. – P. 296-303.

136. Renewables Ninja. [Electronic resource] : official website – Access mode: https://www.renewables.ninja/ [date of the application 01.05.2021].

137. Pfenninger S. Long-term patterns of European PV output using 30 years of validated hourly reanalysis and satellite data/ S. Pfenninger, I. Staffell // Energy –2016. – vol.114. – P.1251–1265.

138. Staffell I. Using bias-corrected reanalysis to simulate current and future wind power output/ I. Staffell, S. Pfenninger// Energy –2016. – vol.114. – P.1224-1239.

139. Kurtz N. Cross-entropy-based adaptive importance sampling using Gaussian mixture/ N. Kurtz, J. Song //Structural Safety –2013. – vol.42. – P. 35-44.

140. Abbood A. Modeling and simulation of 1 MW grid connected photovoltaic system in Karbala city/ A. Abbood, M.A. Salih, A.Y. Mohammed// Int. J. Energy Environ. – 2018. – vol.9. – P. 153-168.